

Design of a System for the Creation of Biaxially Aligned Fibrin Microthread Scaffolds for Cardiac Regeneration

A Major Qualifying Project Report
Submitted to the Faculty
Of
Worcester Polytechnic Institute
in partial fulfillment of the requirements for the
Degree of Bachelor Science

By

Kara McCluskey

Laura Pumphrey

Gabriela Romero

Aubrie Vannasse

April 30th, 2015

Advisors: Professor George Pins, Megan O'Brien

Table of Contents

Table of Contents	i
Authorship.....	iv
Acknowledgements.....	vi
Abstract.....	vii
Table of Figures	viii
Table of Tables	xi
1 Introduction	1
2 Literature Review	4
2.1 Myocardial Infarction	4
2.1.1 Current Treatment Strategies	4
2.1.2 Limitations of Current Strategies.....	5
2.2 Myocardial Architecture	6
2.3 Design Parameters to Mimic Mechanical Properties of the Heart.....	8
2.4 Scaffolds for Tissue Regeneration	9
2.4.1 Electrospun Fiber Network	10
2.4.2 Hydrogels.....	11
2.4.3 Hydrophilic Polysaccharides	12
2.4.4 Collagen and Gelatin.....	13
2.4.5 Composites.....	14
2.4.6 Fibrin and Fibrin Microthreads.....	15
3 Project Strategy.....	20
3.1 Initial Client Statement	20
3.2 Initial Needs, Wants & Constraints	21
3.3 Initial Objectives.....	23
3.4 Final Needs, Wants & Constraints.....	25
3.5 Final Objectives	27
3.6 Revised Client Statement.....	32
4 Device Design.....	34
4.1 Functions and Specifications	34
4.2 Conceptual Design Phase.....	36
4.2.1 Brainstormed Design Elements.....	37
4.2.2 Evaluation of Design Elements.....	38

Gathering Threads	38
Aligning Threads	44
Anchoring Threads	49
Frame to Support Aligned Threads	54
4.2.3 Quantitative Assessment of Design Elements	58
4.3 Development & Verification of Final Design.....	61
4.3.1 Gathering Threads – Box Remover	62
4.3.2 Aligning Threads – Grooved Device	64
4.3.3 Anchoring Threads – Suction Element	69
4.3.4 Providing a Supportive Frame – Washer & Peg	71
4.3.5 Final Modifications, Adjustments & Design Verification.....	72
4.3.6 Complete Design of Production System	82
5 Device Validation & Results	86
5.1 Comparison of Fabrication Processes.....	87
5.2 Quantitative Testing.....	89
5.2.1 Alignment and Spacing Validation.....	90
5.2.2 Ball Burst Testing	99
6 Discussion of Results.....	119
6.1 Alignment & Spacing	119
6.1.1 Limitations of Alignment & Spacing Results.....	120
6.2 Ball Burst Testing	120
6.3 Impact Analysis	122
6.3.1 Economics.....	122
6.3.2 Environmental Impact.....	123
6.3.3 Societal Influence.....	123
6.3.4 Political Ramifications.....	124
6.3.5 Ethical Concern.....	124
6.3.6 Health and Safety Issue.....	125
6.3.7 Manufacturability.....	125
6.3.8 Sustainability.....	126
7 Final Design and Validation	127
7.1 System Validation.....	128
7.1.1 Transferable Frame: Adhesive Framing Mechanism and Vellum Frame.....	129
7.1.2 Composite Frame: Gel Casting.....	131

8	Conclusions and Recommendations	134
8.1	Recommendations.....	134
	References.....	139
	Appendix A - Metrics Rubric	143
	Appendix B – Decision Matrices	148
	Appendix C – Automated Composite Scaffold Production	152
	Appendix D – Alignment Testing Method Validation Procedure	156
	Appendix E – Alignment Testing Protocol.....	158
	Appendix F – Ball Burst Testing Method Validation Procedure.....	160
	Appendix G - Ball Burst Compression Testing Procedure.....	161

Authorship

1	Introduction.....	McCluskey, Pumphrey, Romero, Vannasse
2	Literature Review.....	McCluskey, Pumphrey, Romero, Vannasse
2.1	Myocardial Infarction.....	McCluskey
2.2	Myocardial Architecture.....	Pumphrey, Romero
2.3	Design Parameters to Mimic Mechanical Properties of the Heart.....	Romero
2.4	Scaffolds for Tissue Regeneration.....	Pumphrey, Romero, Vannasse
2.4.1	Electrospun Fiber Network.....	Pumphrey
2.4.2	Hydrogels.....	Vannasse
2.4.3	Hydrophilic Polysaccharides.....	Vannasse
2.4.4	Collagen and Gelatin.....	Pumphrey
2.4.5	Composites.....	Pumphrey
2.4.6	Fibrin and Fibrin Microthreads.....	Pumphrey, Romero
3	Project Strategy.....	McCluskey, Pumphrey, Romero, Vannasse
3.1	Initial Client Statement.....	McCluskey
3.2	Initial Needs, Wants & Constraints.....	McCluskey
3.3	Initial Objectives.....	Pumphrey
3.4	Final Needs, Wants & Constraints.....	Vannasse
3.5	Final Objectives.....	Romero, Vannasse
3.6	Revised Client Statement.....	McCluskey
4	Device Design.....	McCluskey, Pumphrey, Romero, Vannasse
4.1	Functions and Specifications.....	McCluskey
4.2	Conceptual Design Phase.....	McCluskey, Romero
4.2.1	Brainstormed Design Elements.....	McCluskey
4.2.2	Evaluation of Design Elements.....	Romero
4.2.3	Quantitative Assessment of Design Elements.....	Romero
4.3	Development & Verification of Final Design.....	McCluskey, Pumphrey, Romero, Vannasse
4.3.1	Gathering Threads – Box Remover.....	McCluskey
4.3.2	Aligning Threads – Grooved Device.....	McCluskey
4.3.3	Anchoring Threads – Suction Element.....	McCluskey
4.3.4	Providing a Supportive Frame – Washer & Peg.....	Pumphrey, Romero
4.3.5	Final Modifications, Adjustments & Design Verification.....	McCluskey, Pumphrey, Romero, Vannasse
4.3.6	Complete Design of Production System.....	Pumphrey
5	Device Validation & Results.....	McCluskey, Pumphrey, Romero
5.1	Comparison of Fabrication Processes.....	Pumphrey

5.2	Quantitative Testing	McCluskey, Romero
5.2.1	Alignment and Spacing Validation	Romero
5.2.2	Ball Burst Testing	McCluskey
6	Discussion of Results	McCluskey, Pumphrey, Romero
6.1	Alignment & Spacing	Romero
6.2	Ball Burst Testing	McCluskey
6.3	Impact Analysis	Pumphrey
7	Final Design and Validation	Vannasse
8	Conclusions and Recommendations	Romero, Vannasse
	Appendix A - Metrics Rubric.....	Romero
	Appendix B – Decision Matrices	Romero
	Appendix C - Automated Composite Scaffold Production	Pumphrey
	Appendix D - Alignment Testing Method Validation Procedure	Romero
	Appendix E - Alignment Testing Protocol	Romero
	Appendix F – Ball Burst Testing Method Validation Procedure	McCluskey
	Appendix G - Ball Burst Compression Testing Procedure	McCluskey

Acknowledgements

We would like to thank and acknowledge the guidance and support of Professor George Pins and Megan O'Brien. Additionally, we would like to acknowledge the patient efforts of Thomas Partington in helping us create our device and to thank Professor Kristen Billiar for assisting us in our mechanical testing efforts. We would also like thank the following people for their contributions:

Lisa Wall

Professor Raymond Page

Professor Zoë Reidinger

Laura Hanlan

Abstract

Using the previously researched fibrin microthreads, we developed a novel system to reproducibly construct biaxially aligned fibrin microthread composite scaffolds with customizable planar sheet orientation to mimic the anisotropic alignment of native myocardial tissue to facilitate the regeneration of cardiac tissue. This system includes a grooved suction device to reproducibly align microthreads, a transfer frame to facilitate transfer between surfaces and a final composite scaffold formation frame. To validate the system, samples were first generated using our novel system and compared to manually organized thread controls. Composites were formed by the incorporation of a fibrin hydrogel with the aligned microthreads. To demonstrate the reproducibility of the scaffold production, we measured the alignment and spacing of the fibrin microthreads and the maximum load each scaffold could sustain. In measuring the thread alignment and spacing, a statistically significant difference ($p=0.035$) in thread spacing was found between the manually fabricated scaffolds and those created using the automated system. Results from mechanical testing showed a difference in the variance of loads sustained by the manual and automated scaffolds, with a standard deviation of 1.222N for the manual scaffolds and a standard deviation of 0.5300N for the automated scaffolds, suggesting the automated system is superior to the manual method in consistency. However, there was not a statistically significant difference ($p=0.244$) in the variances of maximum load sustained between scaffolds fabricated with the manual method and those with the automated system. Overall, these findings demonstrated the ability of the new systems to reproducibly fabricate biaxially aligned fibrin microthread composite scaffolds with more consistent properties than the current manual method.

Table of Figures

Figure 1: Transplantation Mortality (Lund et al., 2013).....	6
Figure 2: Orientation of Fibers in the Myocardium (Wei-Ning et al., 2012).	7
Figure 3: Structural Layers of the Myocardium (Severs et al., 2008).	7
Figure 4: Fiber tractography of porcine heart (blue -60°, red +60°) (Froeling et al., 2014).....	8
Figure 5: Laminated Composites (A) Assembly of layered composite. (B-D) The effect change in orientation of fibers has on cell alignment (Yang et al., 2011).....	15
Figure 6: Hierarchy of Primary and Secondary Objectives in Ranking Order	32
Figure 7: Spool Storage	39
Figure 8: Box remover from a (A) top view and (B) cross sectional view.....	40
Figure 9: Rolling Grabber from a (A) top view and (B) cross sectional view.....	41
Figure 10: Lint Roller	42
Figure 11: Shaker.....	43
Figure 12: Threaded Rod	44
Figure 13: Hinge Mechanism.....	45
Figure 14: Clips on a Rail (top view).....	46
Figure 15: Grooved Device.....	47
Figure 16: Funnel.....	48
Figure 17: Pot Holder Maker	49
Figure 18: Suction Mechanism	50
Figure 19: Saran Wrap.....	51
Figure 20: PDMS Sandwich from side view	52
Figure 21: Clips from side view.....	53
Figure 22: Washer and Peg with (A) top view of aligned threads in peg, (B) side view of aligned threads, (C) top view of washer and (D) top view of washer with two layers of threads.....	54
Figure 23: PDMS Frame, top view	55
Figure 24: Square Platform.....	56
Figure 25: Loom Platform	57
Figure 26: CAD Model of Box Remover	62
Figure 27: CAD of Extrusion Alignment Frame	63
Figure 28: CAD of Sliding Pyramid Grooved Device.....	64
Figure 29: Folding Pyramid Grooved Device Sketch (Step 1).....	65
Figure 30: Sliding Pyramid Grooved Device Sketch (Step 2).....	65
Figure 31: Close-up of Aligned Threads Using Sliding Pyramid.....	66
Figure 32: Sliding Pyramid Grooved Device Sketch (Step 3).....	66
Figure 33: Segmented Portion of Sliding Pyramid Grooved Device.....	67
Figure 34: Grooved Device (Flat Platform).....	67
Figure 35: Grooved Device (Mesh Screen Element).....	68
Figure 36: Laboratory Shaker Plate (http://orbitalshakers.net/products/helix-150-150bl).....	69
Figure 37: Suction element	70
Figure 38: Suction element with grooved platform	70
Figure 39: Pegs/clamps and aligned threads in (A) top view and (B) side view	71
Figure 40: Washer and Peg Design.....	72
Figure 41: Automated Machine	73

Figure 42: Frame for the coextrusion fibrin microthreads with red arrows pointing to anchors for ends of fibrin microthreads.	73
Figure 43: Preliminary Suction Box Prototype (3 grooves)	75
Figure 44: Final Suction Box Prototype (21 grooves)	76
Figure 45: Suction Box Plate at 2x Magnification.....	76
Figure 46: Steps for Use of the Adhesive Framing Mechanism.....	77
Figure 47: Adhesive Framing Mechanism Process with Alignment and Fibrin Thread Removal	78
Figure 48: Steps to adhering threads to vellum paper frames for gel casting.....	79
Figure 49: Part 1 of the framing system, compared to the slide	80
Figure 50: Series of images showing (1) black acetal plastic, (2) the PDMS wells	81
Figure 51: Examples of well dividers used by the past project groups to create the PDMS wells for the client (Lifetechnologies).....	81
Figure 52: Suction box with zoomed in grooved platform	83
Figure 53: Suction box with secured threads in grooved platform.....	83
Figure 54: Microthreads adhered to vellum frame	84
Figure 55: Frame for addition of fibrin gel	84
Figure 56: Final composite scaffold, with fibrin gel (red) and fibrin microthreads (yellow).....	85
Figure 57: Thread handling for manual and automated processes by forceps, scissors and tape.	88
Figure 58: Pictures of aligned fibers for validation of space measuring method (Ayres, 2008)..	91
Figure 59: Results of validation testing of spacing method compared to FFT method.	92
Figure 60: Frames used for scaffold alignment analysis	93
Figure 61: Method for measuring spacing between threads	94
Figure 62: (A) Thread separation in manual scaffold (n=1). (B) Thread separation in automated scaffold (n=1).....	95
Figure 63: (A) Thread separation in manual scaffolds (n=22) (B) Thread separation in automated scaffolds (n=16)	97
Figure 64: Average thread separation for (n=38)	98
Figure 65: Average thread separation between users for (n=38).....	99
Figure 66: Ball Burst Testing Fixture (Washington University School of Medicine in St. Louis)	100
Figure 67: Ball Burst Testing Set-Up	101
Figure 68: Burst to Failure of Moist Paper	102
Figure 69: Ball Burst Load vs. Extension of Moist Paper	103
Figure 70: Cut-to-Size Sample.....	105
Figure 71: Load vs. Extension of Batch #1 Concentrated Samples (Fridge (blue) vs. Room (red))	106
Figure 72: Load vs. Extension of Batch #2 Regular Samples (Fridge (blue) vs. Room (magenta))	107
Figure 73: Load vs. Extension of Concentrated (red) & Regular (blue) Samples from both Batches.....	108
Figure 74: Failure of Batch #1 (Left) vs. Batch #2 (Right)	109
Figure 75: Load vs. Extension of Batch #1 (blue) and Batch #2 (green) (Concentrated Samples)	109
Figure 76: Frame width and inner diameter measurements prior to testing.	111
Figure 77: Scaffold between nylon washer prior to testing	112
Figure 78: Ball Burst Compression Testing Set-Up	113

Figure 79: Load vs. Extension of both manual and automated samples (n=20 each)	115
Figure 80: Maximum load values and data distributions for both manual (n=20) and automated samples (n=20).....	116
Figure 81: Width and Framer Inner Diameter Distributions for both sample types.....	117
Figure 82: Schematic and pictures of automated system developed	128
Figure 83: Suction Box with rubber gasket	129
Figure 84: Suction box with zoomed in grooved platform.....	129
Figure 85: Adhesive Framing Mechanism.....	130
Figure 86: Picture of Adhesive Framing Mechanism	130
Figure 87: Vellum frame addition to the Adhesive Framing Mechanism	131
Figure 88: Picture of vellum frame process.....	131
Figure 89: Frame for addition of fibrin gel.....	132
Figure 90: Picture of scaffolds in Composite Frame	132
Figure 91: Final composite scaffold, with fibrin gel (red) and fibrin microthreads (yellow).....	132
Figure 92: Aligned fibrin threads separated by distance 'd'	135
Figure 93: Angle manipulation diagram	136
Figure 94: Suction box with tape on either side of grooves (indicated by arrows).	152
Figure 95: Dyed microthreads within four grooves of the suction box.	153
Figure 96: Tape placed on top of threads to secure in alignment.	153
Figure 97: Removal of threads from aligned grooves.	153
Figure 98: Transfer of aligned threads to transfer paper.....	154
Figure 99: Threads pulled in tension on transfer paper.	154
Figure 100: Two vellum frames positioned under aligned threads.....	154
Figure 101: Addition of silicone glue to vellum frame and aligned threads.	154
Figure 102: Composite mold with three scaffolds.....	155

Table of Tables

Table 1: Pros & Cons of Different Scaffold Materials	19
Table 2: Initial Needs & Wants	21
Table 3: Project Constraints.....	22
Table 4: Design Team Pairwise Comparison of Objectives	23
Table 5: Client Pairwise Comparison of Objectives.....	24
Table 6: Ranked Objectives Primary Objectives	25
Table 7: Needs, Wants, and Constraints for Primary Stakeholders	26
Table 8: Final Objectives and Corresponding Second Objectives.....	27
Table 9: Final Pairwise Comparison Chair for Ranked Final Objectives.....	28
Table 10: Functions and Sub-Functions	35
Table 11: Parameters and Specifications	36
Table 12: Initial Brainstorm of Design Elements	37
Table 13: Pros & Cons of Spool Storage	39
Table 14: Pros & Cons of Box Remover (Thread Scooper)	40
Table 15: Pros & Cons of Rolling Grabber	42
Table 16: Pros & Cons of Lint Roller.....	42
Table 17: Pros & Cons of Shaker	43
Table 18: Pros & Cons of Threaded Rod.....	44
Table 19: Pros & Cons of Hinge Mechanism	45
Table 20: Pros & Cons of Clips on a Rail.....	46
Table 21: Pros & Cons of Grooved Device	47
Table 22: Pros & Cons of Funnel	48
Table 23: Pros & Cons of Pot Holder Maker.....	49
Table 24: Pros & Cons of Suction Mechanism.....	51
Table 25: Pros & Cons of Saran Wrap.....	51
Table 26: Pros & Cons of PDMS Sandwich.....	52
Table 27: Pros & Cons of Clips	53
Table 28: Pros & Cons of Glue/Tape.....	53
Table 29: Pros & Cons of Washer and Peg.....	55
Table 30: Pros & Cons of PDMS Frame	55
Table 31: Pros & Cons of Square Platform	56
Table 32: Pros & Cons of Loom Platform	57
Table 33: Decision Matrix Template	59
Table 34: Results from Decision Matrix.....	60
Table 35: Final Top Scores	61
Table 36: Primary Objectives, Testing Methods and Significance of Data.....	87
Table 37: Difficulties observed from manual and automated processes	88
Table 38: Spacing method calculations used to validate alignment	91
Table 39: Validation of Testing Method Test Groups	104
Table 40: Summary of Ball Burst Testing Results	118
Table 41: Gap calculation depending on the angle (θ)	136

1 Introduction

As the leading cause of mortality in the United States, heart disease is responsible for one in four deaths per year (Murphy et al., 2012). In particular, a myocardial infarction (MI) blocks arterial blood flow to the myocardial tissues leading to irreversible damage. The resulting scar tissue negatively impacts the heart function, and can lead to end stage heart failure. Current treatment methods such as the use of a ventricular assist device (VAD) or administration of anti-thrombolytic agents aim to target infarct symptoms, but do not heal the damaged tissue. Therefore, the current gold standard of treatment is a heart transplant (Xin et al., 2013). While a transplant is an effective treatment for myocardial infarction, currently there are over 4,000 people on the waiting list for a donor heart in the United States alone, a number far exceeding the amount of organs available (U.S. Department of Health and Human Services, 2014). Those who do receive a transplant have a 69% 5-year survival rate due to a variety of post-transplant complications, including hypertension, renal dysfunction, cardiac allograft vasculopathy (CAV), acute rejection, infection, among others (Christman et al., 2004). Therefore, there is a need for a regenerative therapy to facilitate myocardium repair for regained function.

Tissue engineering and biomaterial research involving the use of biomaterial scaffolds, growth factors and cellular transplantation are being explored as an option for myocardial repair (Christman et al., 2004). The myocardium contains layers of myofibers that vary in orientation across the ventricular wall, which are essential in heart function, but pose a particular challenge for guided tissue repair (Wei-Ning et al., 2012).

In Professor Pins's lab, fibrin is being explored as a biomaterial for use in tissue regeneration applications. Fibrin is a protein that exists in the body to create provisional matrices to facilitate wound healing. Fibrin microthreads have demonstrated the ability to facilitate

directional cell guidance to promote aligned fiber regeneration in other tissues such as skeletal muscle and anterior cruciate ligament (Cornwell, 2007). These microthreads have the potential to mimic the anisotropic alignment of the myocardium to facilitate the repair of the oriented fiber matrix. By creating a composite scaffold of fibrin microthreads within a fibrin gel, it allows for the mechanical properties of the microthreads to be combined with a matrix for biological delivery. These properties allow for the scaffold to guide tissue regeneration of the myocardial fiber alignment.

The goal of this project was to design and develop a novel system to reproducibly construct biaxially aligned 1cm^2 fibrin microthread composite scaffolds with 20-75 microthreads and customizable planar sheet orientation between 0° and 90° to mimic the anisotropic alignment of native myocardial tissue to facilitate the aligned fiber regeneration of cardiac tissue.

The designed system simplifies and streamlines the construction of multi-layered microthread scaffolds. The current manual method, involves extensive physical handling of the microthreads, resulting in inconsistent alignment and spacing that is not reproducible between users. This new system increases the consistency and precision of thread alignment and spacing to provide a superior fabrication system to the current manual method that allows for reproducibly between users. Included in the system is a grooved suction device to reproducibly align microthreads, a transfer frame to facilitate secured movement between surfaces and a final composite that is formed by the addition of a fibrin hydrogel to the aligned fibrin microthreads.

To validate the system's ability to create scaffolds that mimic the fiber alignment of native myocardium, the team compared scaffolds generated using the novel system against those made manually to determine which method was superior in reproducible scaffold construction. To measure for reproducibility of the two different scaffold production methods, the design team

measured the alignment and spacing of the fibrin microthreads and the maximum load each composite scaffold could sustain. With measuring the thread alignment and spacing, the team found a statistical significance ($p=0.035$) in the threads spacing when comparing the manual scaffolds to the automated scaffolds. Additionally, mechanical testing showed a difference in the variance of loads sustained between the manual and automated scaffolds with standard deviations of 1.222N and 0.5300N respectively. This suggests that the automated scaffold has a more consistency with the loads sustained than the manual scaffolds. In proving the reproducibility of scaffold production using the automated system, the team demonstrated the superiority of their system for the creation of scaffolds to mimic the fiber alignment of native myocardial tissue.

Future work with these aligned fibrin composites will include the addition of cardiomyocytes, creation of multiple layers with varying alignment and application to other aligned tissues. By seeding the scaffold with cardiomyocytes, the results would demonstrate how the high alignment of the microthreads could impact the behavior of the cells with the intention of creating functional scaffolds. The addition of multiple scaffold layers in varying alignment would aim to mimic the multiple fiber alignments found in the myocardium. Lastly, while this system is currently being used for the development of scaffold for cardiac regeneration, it can be applied in the future to other highly aligned tissues for regeneration after disease or injury.

The following sections of this document present a literature review of the current status of cardiac regeneration techniques, followed by the project approach, design alternatives, and the analysis performed in order to prove the effectiveness of composite fibrin scaffolds.

2 Literature Review

2.1 Myocardial Infarction

In the human body, the heart is the organ responsible for circulating blood to provide the rest of the body with vital oxygen and nutrients. In the United States, nearly one million people experience heart attacks every year and only about half of them survive (National Institutes of Health, 2014). A heart attack, or myocardial infarction, occurs when there is a restriction of blood flow to a particular section of the heart. This lack of blood flow, referred to as ischemia, can result in myocardial necrosis. Although the time between restriction of flow and cell death varies, models from animal studies suggest that cell death (infarction) can begin in as little as 20 minutes with complete necrosis occurring after 2 to 4 hours (Thygesen et al., 2012). Because of the small window of time between myocardial ischemia and infarction, it is crucial that the infarction is treated as soon as possible to reduce the extent of cellular death and resulting non-functional scar tissue.

2.1.1 Current Treatment Strategies

Currently, there are several different treatment strategies for myocardial infarctions. These include: administration of cardiac drugs, angioplasty, cardiac bypass surgery, ventricular assist device (VAD) and full cardiac transplant. Cardiac medications, specifically anticoagulants and antiplatelet agents, help to remove existing blood clots and reduce the risk of additional formations in the blood vessels. If more extensive intervention is needed, a non-invasive procedure called an angioplasty can be performed to help widen the blockage and allow for restored blood flow (Zijlstra, 2001). In cases where this isn't successful, a cardiac bypass surgery can be performed to surgically reroute the flow of blood around the blocked artery (Hlatky et al., 2009). A patient with reduced cardiac function can be put on a VAD, which is a mechanical

pump that helps the ventricles pump blood to the rest of the body (National Institutes of Health, 2014). Lastly, in cases where these treatments above are inadequate due to excessive tissue damage, a full cardiac transplant can be performed (Lund et al., 2013).

2.1.2 Limitations of Current Strategies

Out of the four strategies discussed above, only one has the ability to successfully ‘treat’ a myocardial infarction. While cardiac medications, angioplasty, and cardiac bypass surgery are effective strategies for preventing a myocardial infarction from occurring again in the future, they cannot reverse the cellular death that has already occurred. VADs can make up for the lost function as a result of the damaged tissue, but come with a variety of risks such as blood clots, infection or even stroke (Givertz, 2011) and a survival rate of only 1-2 years (Miller et al., 2011). For these reasons, a full cardiac transplant is currently the only strategy for treatment cellular death and loss of function. As of now, there are over 4,000 people on the waiting list for a heart in the U.S. (U.S. Department of Health and Human Services, 2014) and there is an inadequate amount of donor hearts available to fulfill this need. Even if a person is able to receive a heart, there are a variety of complications that can occur within the first several years after transplantation. Figure 1 shows a distribution of the various contributors to transplant mortality in adult recipients around the world from 1994 to June 2012.

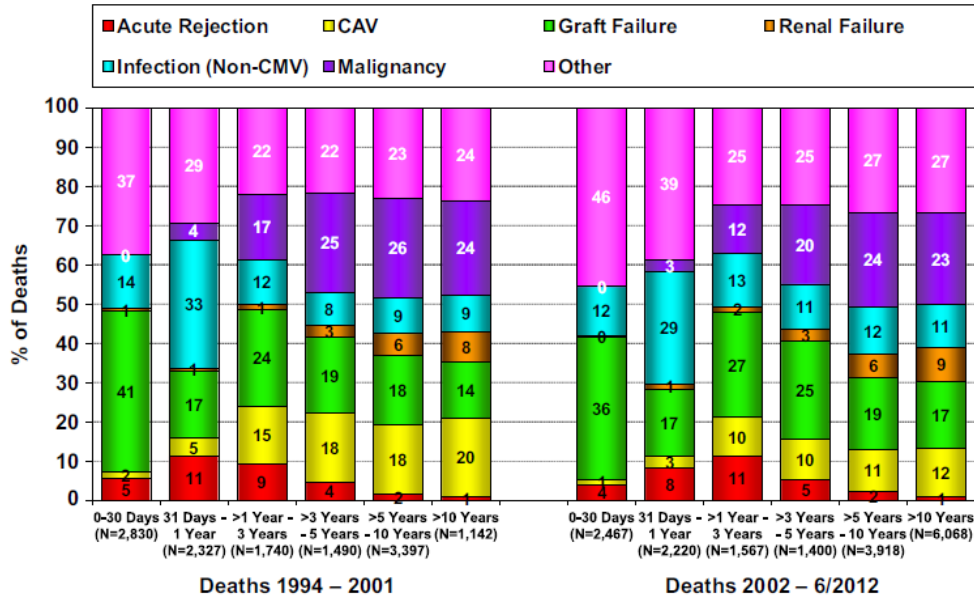


Figure 1: Transplantation Mortality (Lund et al., 2013)

In the first year, infection and graft failure (low cardiac output) are the leading causes of death in transplant patients. Over the next 3+ years, malignancy and cardiac allograft vasculopathy (vessel wall thickening) become more prevalent.

All of the treatment methods above mainly aim to target infarct symptoms, but do not actually heal the damaged tissue. Therefore, there is a need to develop a therapy for myocardial infarction that mimics the structure of the myocardial muscle and allows for regained cardiac function.

2.2 Myocardial Architecture

The structural design of the myocardium is not a uniform continuum. It is a composite of discrete cell layers consisting of myofibers (Nielsen et al., 1991). The ventricular myocardium consists of a band of myofibers that vary in orientation across the ventricular wall (Smaill et al., 2004). It has been demonstrated that the fiber angles vary by up to 180° in animal hearts. The fiber angle at each layer of the myocardium is estimated to change progressively from 80° ± 7° at the endocardium, to 30° ± 13° at the midwall of the heart, and to -40° ± 10° at the epicardium, with a

0° alignment at the circumference of the heart (Wei-Ning et al., 2012). Figure 2 depicts the multiple fiber orientations of the myocardium in porcine specimens depending on the wall thickness.

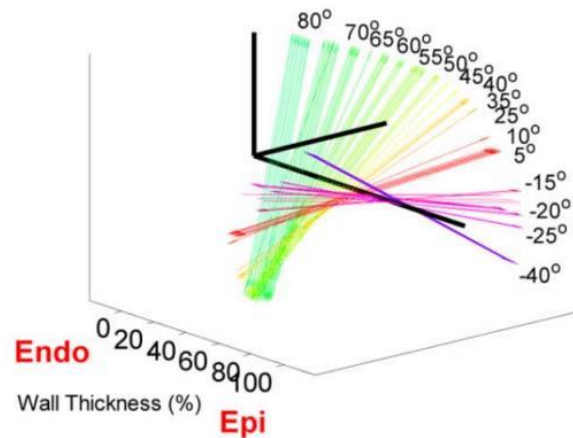


Figure 2: Orientation of Fibers in the Myocardium (Wei-Ning et al., 2012).

The ventricular myocardium is structurally orthotropic, with myocytes arranged in layers that are typically four cells thick (Smaill et al., 2004). These myocytes are oriented in parallel and define the fiber direction. Myocardial layers coincide with the planes where the maximum systolic shear is found (Arts et al., 2001). Adjacent layers are separated by cleavage planes that present radial orientation in the heart apex. A simplified image of the structural layers of the myocardium is shown in Figure 3:

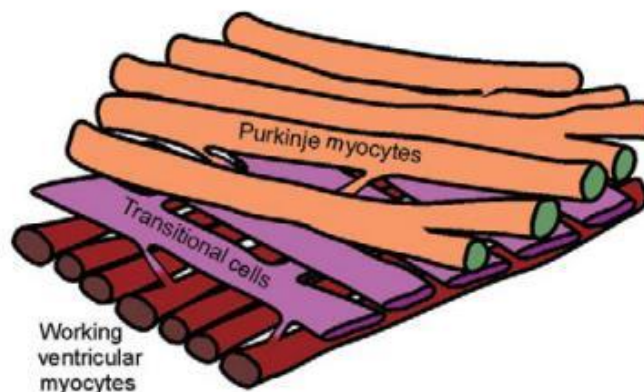


Figure 3: Structural Layers of the Myocardium (Severs et al., 2008).

Each layer in this area of the myocardium contains different types of cells. In addition, due to the fiber structure of the myocardium, each layer can induce different shear waves according to the direction of the fibers (Wei-Ning et al., 2012). Developments with diffusion imaging has allowed for the fiber tractography of the heart to demonstrate this varied fiber orientation. This allows for insight into the mechanical and electrical function in both the function and dysfunction myocardial tissue (Froeling et al., 2014). An ex vivo porcine heart showing fiber tracts of different local helix angles is shown in Figure 4:

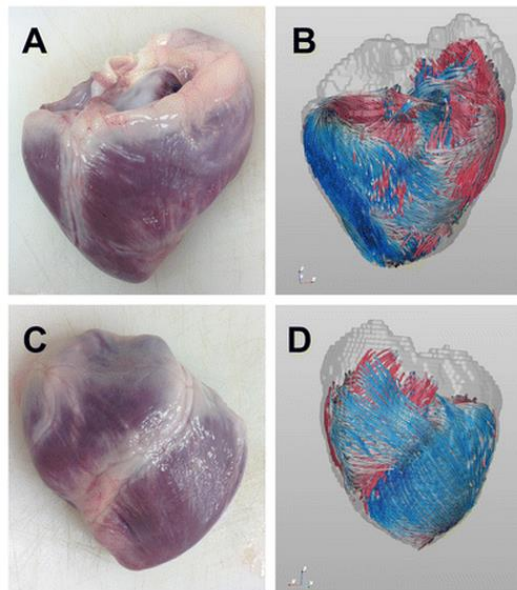


Figure 4: Fiber tractography of porcine heart (blue -60° , red $+60^\circ$) (Froeling et al., 2014)

In the following section, important mechanical and structural parameters for designing scaffolds to mimic the heart are explained. These will be considered when evaluating the scaffolds created through this study.

2.3 Design Parameters to Mimic Mechanical Properties of the Heart

Due to the complexity of the heart, when designing scaffolds for regeneration, it is important to consider several mechanical characteristics. For instance, the myocardium doesn't behave similarly to its neighboring tissue. Different from the epicardium, the myocardium is less

isotropic at low biaxial strains (Costa et al., 2001). Additionally, the myocardial stiffness is considered to be an essential myocardial diastolic property independent of the loading conditions (Chen et al., 2008; Watanabe et al., 2006). Mechanically the myocardial tissue must have a stiffness of 10-20 kPa at the beginning of the diastole and 200-500 kPa at the end of diastole. However, during contraction, the myocardial stiffness tends to be 1.5 to 3 times stiffer in the fiber direction than the cross-fiber direction (Costa et al., 2001). Furthermore, myocardial fibers are organized into laminated branches. This suggests that myocardium may be locally orthotropic having distinct cross-fiber stiffness within its planes (Legrice et al., 2001), making the heart even more complicated to precisely quantify its stiffness.

Several attempts to mimic the myocardial structure have been developed. One in particular involves the fabrication of scaffolds with seeded cells that aim to target damaged myocardial areas. An overview of these efforts is shown in the following section.

2.4 Scaffolds for Tissue Regeneration

The behavior of a cell is largely dependent on biological factors, chemical markers, mechanical properties and the structure of the surrounding environment. The manipulation of these variables allows for controlling the phenotype of the cell. Biomimetic scaffolds have been explored to match the extracellular matrix and drive tissue regeneration (Chan et al., 2008). The purpose of tissue engineered scaffolds can be described as a predefining frame where tissue regeneration is needed, enabling temporary functional replacement of the tissue as it supports regeneration by allowing infiltration of cells, proteins and/or genes (Hollister et al., 2002).

In order to obtain a bioengineered scaffold, the following properties should be considered: architecture, biocompatibility, cyto- and tissue compatibility, and mechanical properties of native tissue. The architecture of the scaffold needs to provide cells a structure that allows for proper

integration, metabolic transport, and dispersion of nutrients (Chan et al., 2008). Lastly, the scaffold must have the appropriate mechanical properties that provide stability and facilitate tissue regeneration.

Unfortunately, some of the design requirements mentioned above can conflict with one another and may require optimization between multiple characteristics. For example, the scaffold may sacrifice its mechanical strength in order to achieve better morphology (Hollister et al., 2002). The scaffold fabrication process must be optimized so that these properties can be manipulated and allow the scaffold to meet all design requirements.

Following myocardial infarction, the cardiac extracellular matrix undergoes dynamic alterations of its chemical and mechanical properties that regulate the inflammatory and reparative responses (Dobaczewski et al., 2010). The complex provisional fibrinogen matrix is then replaced by dense collagen scar tissue, which can impair function of the myocardial tissue. These extensive biological cues and actions of the extracellular matrix have provided challenges for the development of scaffolds for cardiac tissue regeneration therapies. The following sections explore various methods that have been explored to attempt to mimic and enhance the natural tissue regeneration.

2.4.1 Electrospun Fiber Network

Electrospinning has provided a method to create nano- to macro-scale fibrous networks of synthetic or natural materials. This creates a topography that can then mimic the extracellular matrix with a high porosity and surface area-to volume ratio, which may improve the cellular interactions. The electrospun fiber membrane has been used for many biomedical applications including scaffolds for tissue regeneration, medical implants, wound healing, and drug delivery (Zong et al., 2005).

Electrospun polymer fibers as a scaffold material can provide mechanical strength similar to that of native tissue and can be customized to many desired mechanical properties, structural characteristics and compositions (Bosworth et al., 2013; Coburn et al., 2011). Alterations in these properties will result in changes in the cell alignment and behavior due to the instructive signals provided by the material. Zong *et al.* determined certain processing techniques that allow for the alignment of fibers that mimic the native tissue ECM (Zong et al., 2005). The team cultured cardiomyocytes on poly(lactic-co-glycolic acid) (PLGA) non-woven electrospun fiber scaffolds and found that the fiber architecture promoted isotropic or anisotropic growth depending on the orientation of the fibers. Therefore, it was proven that the structure and function for tissue engineered cardiac tissue can be directed through the change in chemistry and topography of the surface.

Some limitations with electrospun fiber scaffolds are found with its structure. The pores are often too small for cellular infiltration and depending on the fabrication technique the scaffold will be a 2D structure, which causes there to be limited cell infiltration (Coburn et al., 2011). Instead the cells will proliferate essentially on the surface of a rough planar sheet. Therefore, they are more commonly being explored as a layer in a laminate scaffold with other materials where they provide mechanical strength.

2.4.2 Hydrogels

Hydrogels are three-dimensional insoluble hydrophilic polymer networks. These have the ability to absorb large volumes of water, making them a sound method for mimicking soft tissue structures and increasing the biocompatibility of the material (Shapiro et al., 2013). They allow for hydration, but also for cell adherence, proliferation, and differentiation. Hydrogel materials provide an environment for cells to thrive and for biological agents to be immersed evenly

through the material (Bosworth et al., 2013; Sapir et al., 2011). Hydrogels have weak mechanical properties, and do not possess the mechanical strength for load bearing applications, but can be used in defects and promote regeneration in a minimally invasive manner (Shapiro et al., 2013). The common types of hydrogels that are used for biomedical engineered scaffold applications are gelatin, collagen, and most commonly, native collagen.

In the extracellular matrix, the common molecules of connective tissue are type I collagen, decorin and glycosaminoglycans, with collagen being the most abundant element (Pins et al., 1997). Collagen has a high biocompatibility because it is a naturally occurring material compared to synthetic materials (Glowacki et al., 2008). Therefore, collagen can be used both in a native form as well as a more denatured gelatin depending on the intended function. Type I collagen is most commonly used due to its ability to entrap cells directly as it is reconstituted into a gel, its biocompatibility, and fibrous and cohesive nature. Some of the disadvantages of using collagen for a scaffold material are that collagen can cause suppression of cell proliferation and protein synthesis as well as no inherent rigidity.

2.4.3 Hydrophilic Polysaccharides

Hydrophilic polysaccharides are a biomaterial that plays a critical role in modulating the activities of signaling molecules (Ma et al., 2006). These materials help in mediating certain intercellular signaling and to control local biological activity. The advantage of hydrophilic polysaccharides over other biomaterials is that they are biodegradable, hydrophilic, and relatively low cost, which shows that these have many features that are desirable for a numerous applications.

An example of this material type is alginate, derived from brown sea algae. This linear polymer contains various acids, including β -L guluronic and α -D mannuronic. Alginate is

soluble in liquids at room temperature but forms a gel when in the presence of cations such as calcium. The material is spongy and is easy to manipulate, allowing it to have efficient penetration of cells into the matrix itself. Unfortunately, this material lacks the intricate three dimensional structure used in tissue engineering, which is ideal for uniform cell distribution and good diffusion of nutrients (Mohan, 2005).

Current uses of this material include an injection targeting damaged myocardium. Alginates, which can be used in the form of a cross-linked hydrogel, have similar mechanical properties to those of the myocardial extracellular matrix. Injecting alginate to the heart, could substitute for damaged extracellular matrix and aid with myocardial infarctions and reduce or reverse the tissue remodeling (Domb et al., 2011).

2.4.4 Collagen and Gelatin

Collagen is the most common type of material in the connective tissues of the body and is a major component of the extra cellular matrix (ECM). Currently, Zimmermann et al. and Kofidis et al. are researching ways to incorporate cell-seeded collagen scaffolds into myocardial tissue regeneration strategies (Kofidis et al., 2002; Kofidis et al., 2003; Zimmermann et al., 2004). Incorporating these types of scaffolds has been found to limit the ventricular remodeling and improve function that is normally deteriorated following myocardial infarction. The incorporation of growth factors and other biological cues within these collagen matrices is being explored despite questions surrounding some of the contents approval for use in humans (Silvestri et al., 2013).

Gelatin, known as denatured collagen, is being researched in the form of foam and cell seeded and unseeded sponges. Sakai et al. have found that gelatin sponges dissolve after 12 weeks following implantation and allow for the ingrowth of fibrous tissue with the degradation

of the patches (Sakai et al., 2001). A disadvantage of the foam, known as Gelfoam, which is supplied through Upjohn, Ontario, Canada, is its limited mechanical strength in withstanding cyclic stresses. To improve this, Miyagi et al. have experimented with a poly(ϵ -caprolactone) (PCL) spray-coated substrate (Miyagi et al., 2010).

2.4.5 Composites

The strategy of a composite scaffold is the combination of two different polymers, which are often blends of natural and/or synthetic materials. This composite provides both the biocompatibility from natural polymers and the mechanical strength of the synthetic polymer. Recently, the combination of natural materials such as collagen or gelatin have been explored in combination with artificial polymers such as poly(L-lactic acid)-*co*-poly(ϵ -caprolactone) and poly(lactic acid)-*co*-(glycolic acid) (PGLA). Studies conducted by Grover et al. found that any blends containing collagen type I, insoluble elastin or gelatin formed a scaffold with the desired mechanical strength, degradation kinetics and structure necessary for effective cardiac tissue regeneration (Grover et al., 2012b; Grover et al., 2012a). Additionally, composites with conductive properties have been explored due to their ability to allow for electrical signal transmission and tissue contraction such as Polyaniline (PANi), polypyrrole (PPy) and carbon nanofibers (CNF), as this electrical signal is needed to create the contractile tissue within the heart.

Recent research efforts have developed laminated composites that combine an electrospun fibrous network for mechanical strength and a hydrogel to aid in cellular infiltration (Bosworth et al., 2013). Laminated composites are an arrangement of alternating layers of hydrogel and electrospun fibers that allow for cell adherence and proliferation within the hydrogel layer and structural cues to aid cell alignment provided by the electrospun fibers. Yang

et al. showed that there is a clear connection between cell alignment and the orientation of the fibers, as shown in Figure 5 below (Yang et al., 2011).

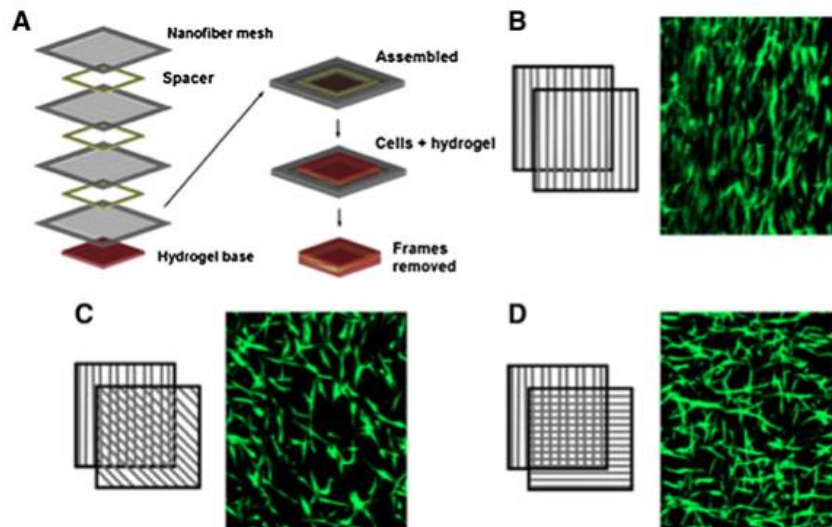


Figure 5: Laminated Composites (A) Assembly of layered composite. (B-D) The effect change in orientation of fibers has on cell alignment (Yang et al., 2011).

This can be applied to tissues such as the myocardium, because it contains different alignments of the tissue and varying mechanical properties between layers. While the structure and composition of these scaffolds is still being developed, it has already shown to better mimic the native tissue when compared to each component individually.

2.4.6 Fibrin and Fibrin Microthreads

Fibrin used as a scaffold has the potential to deliver cells in wounded tissue. For instance, the provisional extracellular matrix formed when a tissue is wounded is composed mainly by fibronectin and fibrinogen, two components that contribute to tissue formation and cytokines release (Stroncek et al., 2008). Fibrin has already gained Food and Drug Administration (FDA) approval for human use (Silvestri et al., 2013). The idea of using fibrin microthreads as a tool for cell delivery allows for growth, migration and differentiation of cells in addition to biocompatibility (Cornwell & Pins, 2007).

Depending on the concentration of fibrinogen and thrombin, the density, mechanical strength, and conformation of the resulting fibrin matrix can be altered (Silvestri et al., 2013). It often has the ability to be used as a gel injection into the damaged myocardium, which has been found to allow for limited regeneration. As a gel, fibrin's mechanical properties are much lower than that of native tissues and cannot withstand cyclic stresses. To overcome this, recent studies have looked to combine fibrin with a more mechanically strong synthetic polymer that can aid with cell delivery (Lisi et al., 2012).

Fibrin microthreads are coextruded from fibrinogen and thrombin solutions at a speed of 4.25 mm/min to a HEPES buffer bath at pH of 7.4 at room temperature (Cornwell & Pins, 2007). These threads are then air-dried and stretched between 150-200% of their original length to optimize their tensile properties. Threads have relatively smooth surfaces with small topographies that display similar properties to those of fibrin, offering a stable supporting platform that facilitates cell delivery and alignment (Proulx et al., 2011). Additionally, fibrin microthreads have the potential for reducing fibrosis and facilitating the remodeling of large muscle injuries (Page et al., 2011). Fibrin microthreads can stabilize and regenerate a wound more effectively than thicker hydrogels due to their ability to deliver cells deeper in the tissue. Some studies even suggest that microthreads might mitigate the need to accomplish vascularization to promote cell survival, something that fibrin hydrogels do not offer. Fibrin microthreads can be used as a matrix to anchor cells during delivery since they promote longitudinal growth and cell alignment (Page et al., 2011).

Current research shows microthreads being used as a bundle to seed human mesenchymal stem cells (hMSCs) and then transplanted into wounds. Cell-seeded sutures made from fibrin microthreads are shown to present a higher percentage of hMSCs delivered than IM injection (Guyette et al., 2013). Additionally, it has been shown that in the presence of fibroblast growth

factor-2 (FGF-2), cell growth and alignment in fibrin microthreads increased significantly (Cornwell & Pins, 2010). FGF-2 is a naturally occurring molecule that promotes different signals for each type of cell, and in this case it was able to enhance the proliferation of fibroblasts.

Furthermore, fibrin microthreads are a mechanically robust thread material proven to show high tensile strength approaching 4.5 MPa. Although alone these do not attain sufficient tensile properties for high load bearing situations such as ligament tissue regeneration (Cornwell, 2007), fibrin microthreads can be manipulated by tuning the mechanical properties through processing techniques, chemical treatments and/or UV crosslinking. With an intermediate dry step in the fabrication process, the threads were found to have an increased strength compared to threads without an intermediate step (Grasman et al., 2014). Chemical crosslinking of threads allows for stronger and stiffer threads than those uncrosslinked (Grasman, Page, Dominko, & Pins, 2012).

Since fibrin microthreads have been used previously in cardiac applications, further studies must be conducted in order to analyze their capability to mimic the myocardium structure. If successful, a multi-layered scaffold based on fibrin microthreads will be created.

Below is a summary of the different types of scaffold materials and the pros and cons of the application of each:

Scaffold Material	Pros	Cons	Reference
<i>Electrospun Fiber Network</i>	<ul style="list-style-type: none"> - High surface area to volume ratio - Customizable mechanical strength, structure and composition - Customizable orientation of fibers 	<ul style="list-style-type: none"> - Limited infiltration due to small pore size - Largely 2D structure 	(Bosworth et al., 2013) (Coburn et al., 2011) (Zong et al., 2005)
<i>Hydrogels</i>	<ul style="list-style-type: none"> - Mimics soft tissue characteristics - Allows for cell adherence, proliferation, differentiation 	<ul style="list-style-type: none"> - Weak mechanical properties 	(Bosworth et al., 2013) (Glowacki et al., 2008) (Pins et al., 1997) (Sapir et al., 2011) (Shapiro et al., 2013)

	<ul style="list-style-type: none"> - Provides a 3D environment - Can be made from native material 		
<i>Hydrophilic Polysaccharides</i>	<ul style="list-style-type: none"> - Biodegradable - Hydrophilic - Low cost - Easy to manipulate - Efficient penetration of cells - Injectable 	<ul style="list-style-type: none"> - Lacks 3D structure with uniform cell distribution and profusion of nutrients 	<p>(Domb et al., 2011) (Ma et al., 2006) (Mohan, 2005)</p>
<i>Collagen and Gelatin</i>	<ul style="list-style-type: none"> - Major component found in ECM - Can be used as sponge or foam - Allow for ingrowth of fibrous tissue 	<ul style="list-style-type: none"> - Low mechanical strength 	<p>(Kofidis et al., 2002) (Kofidis et al., 2003) (Miyagi et al., 2010) (Sakai et al., 2001) (Silvestri et al., 2013) (Zimmermann et al., 2004)</p>
<i>Composites</i>	<ul style="list-style-type: none"> - Combines biocompatibility and mechanical strength - Customizable degradation kinetics - Potential for electrical signal transmission and tissue contraction - Layers allowing for cellular infiltration - Facilitate cell alignment 	<ul style="list-style-type: none"> - Components of combinations are still under development - Synthetic components can cause inflammatory response 	<p>(Bosworth et al., 2013) (Grover et al., 2012a) (Grover et al., 2012b) (Yang et al., 2011)</p>
<i>Fibrin</i>	<ul style="list-style-type: none"> - Approved by FDA for human use - Biocompatible - Allow for growth, migration and differentiation - Customizable density, mechanical strength and confirmation 	<ul style="list-style-type: none"> - Limited regeneration as a gel injection - Low mechanical properties as a gel 	<p>(Cornwell & Pins, 2007) (Cornwell & Pins, 2010) (Grasman et al., 2012) (Grasman et al., 2014) (Guyette et al., 2013) (Lisi et al., 2012) (Page et al., 2011) (Proulx et al., 2011) (Silvestri et al., 2013) (Stroncek & Reichert, 2008)</p>

<p style="text-align: center;"><i>Fibrin Microthreads</i></p>	<ul style="list-style-type: none"> - Efficient cell delivery mechanism - Reduces fibrosis - Promote migration, proliferation and alignment of cells - Tunable mechanical and structural properties - Customizable orientation of longitudinal axis 	<ul style="list-style-type: none"> - Difficult to form scaffold - Low production rate 	
---	---	---	--

Table 1: Pros & Cons of Different Scaffold Materials

The following sections of the document will present more in-depth details regarding the project approach.

3 Project Strategy

3.1 Initial Client Statement

The challenge posed to the design team was to develop a system to fabricate a fibrin-based scaffold for the construction of a multi-layered tissue construct. To determine a strategy for developing this scaffold, the design team examined the wants and needs of the client as described in the initial client statement. The initial client statement presented to the team was to:

“Design, develop, and characterize an automated system to create a bi-axially aligned fibrin-based scaffold that will facilitate the construction of a multilayered tissue construct.”

The current method to fabricate an aligned fibrin scaffold is the manual placement of individual threads. The design team was challenged to develop an automated system to align fibrin microthreads into planar sheets. These sheets would then be manipulated so that these could be stacked on top of one another to create a multi-layered tissue constructs. Through further discussion with the client, it was established that the myocardium would be the tissue of focus for the scope of the project. From here, the design team was able to develop a list of objectives based on the wants, needs, and constraints of the client that would help to develop a project strategy.

Through interviews and discussions with the client, the design team determined a set of objectives and constraints. These initial project objectives helped the team understand the direction of the project and its overall desired outcomes. However, these objectives would need further clarification as the design team moved through the design process.

Through determining the primary stakeholders and more critically examining their needs, wants and constraints, the design team was able to give detail to the final objectives and classify

them into primary and secondary objectives. By doing this, the design team was able to establish a clear definition of the project strategy and design processes.

Primary Stakeholders

After reading literature and reviewing the design process, the team found that they needed to identify the specific stakeholders involved before beginning the design process. The three stakeholders for the design project were the design team, the client, and the user. The role of the team was to design a system to be used by the client and user. After identifying these stakeholders, the design team interviewed the client and user to make a list of needs, wants & constraints, as well as to develop objectives.

3.2 Initial Needs, Wants & Constraints

After examining the client statement from the primary stakeholders as well as reviewing the literature, we established a set of needs and wants shown below in Table 2 that must be met by the design.

Needs	Wants
<ul style="list-style-type: none"> • Automated system • Biocompatible • Able to support cell culture • Easy to use 	<ul style="list-style-type: none"> • Reproducible • Biaxially aligned • Transferable

Table 2: Initial Needs & Wants

From these needs and wants the team was able to develop the project’s initial objectives. After meeting with the client, the advisor, and consulting related literature, the design team established a set of objectives for the project.

After meeting with the client, the advisor, and consulting related literature, the design team established a set of constraints for the project. These constraints were divided into two categories, biological and technical. The list of constraints is outlined below in Table 3.

<i>Constraints</i>		<i>Description</i>
Biological	Biocompatible	<ul style="list-style-type: none"> - Safe for user - Able to be implanted successfully
	Biodegradable	<ul style="list-style-type: none"> - Made of non-reactive materials - Nearly bioinert - No acidic byproducts
Technical	Limited Time	<ul style="list-style-type: none"> - One academic year
	Cost	<ul style="list-style-type: none"> - Money allowance for supplies (total budget = \$624)

Table 3: Project Constraints

Biological Constraints

The biological response of the design is a constraint that was extremely important for the the design team to take into consideration. The system created by the team needed to be able to produce a biocompatible scaffold, meaning that it would need to have the ability to adapt to the host tissue into which it would be implanted. In the context of the project, this would mean that the scaffold material must not induce a foreign body response. At the same time, the scaffold material must also not exhibit cytotoxicity, thus maintaining the ability to support cardiomyocytes seeding. It must additionally be able to be successfully implanted into the body, and have a controlled degradation rate to allow for tissue regeneration.

In addition to controlling the rate of degradation, a bioinert material would need to be selected whose degradation products would not elicit an immune response. Currently, there are only materials that are *nearly* bioinert. These materials, however, exhibit very minimal interaction with native tissue *in vivo*. If not bioinert or *nearly* bioinert, during degradation a material can produce acidic byproducts, which may increase the degradation rates of the material and can cause a negative immune response in the body. For these reasons, both of these biological constraints must be met in order to have a successful scaffold.

Technical Constraints

The technical limitations of the project pertain to the overall design process. As the team examines the timeline for the creation of the system, the team is limited to one academic year in order to complete the project. The monetary constraint of the design is due to a limited budget of \$624 that the design team will utilize to purchase supplies as well as cover lab fees. These two constraints limit the extent of the overall design and outcome of the project. The team was determined to meet all of the constraints and complete the project successfully.

3.3 Initial Objectives

To begin the design process, the team met with the client to observe the current scaffold fabrication process. From this meeting and continued review of current literature, the design team was able to develop the first set of primary objectives. These objectives were based on the client’s initial wants and needs for the system. The team was able to come up with five initial primary objectives: *reproducible*, *able to support viable cell culture for 7 days*, *able to be manipulated*, and *easy to use*. A pairwise comparison chart (PCC) of these primary objectives was developed and the team (Table 4) and client (Table 5) separately ranked each objective in order to determine their relative importance.

	Mimic Myocardial Fiber Alignment	Able to support cells	Reproducible	Manipulate	Easy to Use	Total
Mimic Myocardial Fiber Alignment	X	1	0	1	1	3
Able to support cells	0	X	0	1	1	2
Reproducible	1	1	X	1	1	4
Manipulate	0	0	0	X	1	1
Easy to use	0	0	0	0	X	0

Table 4: Design Team Pairwise Comparison of Objectives

	Mimic Myocardial Fiber Alignment	Able to support cells	Reproducible	Manipulate	Easy to Use	Total
Mimic Myocardial Fiber Alignment	X	0.5	0.5	1	1	3
Able to support cells	0.5	X	1	1	1	3.5
Reproducible	0.5	0	X	1	1	2.5
Manipulate	0	0	0	X	1	1
Easy to use	0	0	0	0	X	0

Table 5: Client Pairwise Comparison of Objectives

The design team focused on the device being able to produce consistent results and properties, while the client was more concerned with the devices ability to create a scaffold with properties that would be advantageous for eventual myocardial regeneration. After further discussion with the client, it was determined that the client’s PCC was the most appropriate for the project because it is the main purpose to have a scaffold that will achieve regeneration of tissue. Secondly, in order to validate these characteristics, the scaffold should additionally be reproducible. With this in mind, the following primary objectives were ranked (most important to least important) as shown below in Table 6. Additionally, corresponding secondary objectives were established for each.

<i>Initial Primary Objectives</i>	<i>Initial Secondary Objectives</i>
Able to support viable cell culture for 7 days	<ul style="list-style-type: none"> - Promote cell alignment - Promote cell proliferation - Promote cell infiltration
Mimic myocardial fiber alignment	<ul style="list-style-type: none"> - Stackable layers - Alignment - Efficient degradation

	<ul style="list-style-type: none"> - Mechanical strength - Planar orientation
Reproducible	<ul style="list-style-type: none"> - Accuracy - Precision
Able to be manipulated	<ul style="list-style-type: none"> - Transferable - Support mechanical and structural testing - Attachment of layers
Easy to use	<ul style="list-style-type: none"> - Fabrication time - Number of steps - Automated - Intuitive

Table 6: Ranked Objectives Primary Objectives

The primary objectives encompass the most important characteristics that the scaffold must meet in order to be successful and satisfy the needs of the client, while the secondary objectives are specific attributes that will allow the primary objectives to be met.

3.4 Final Needs, Wants & Constraints

After reevaluating the objectives, the design team wanted to further clarify the needs, wants and constraints of the client and user before finalizing their objectives and moving forward to establish alternative designs. Therefore, the team conducted a second interview with the client and user to develop a comprehensive understanding of their ideal system, creating a more in-depth list of their specific needs, wants, and constraints. From this, the team developed the final set of needs, wants, and constraints for each contributor (Table 7):

Design Team	Client	User
--------------------	---------------	-------------

<p><i>Final Needs:</i></p> <ul style="list-style-type: none"> - To be finished by end of D term - A working prototype by the end of C term - A final design needs to be validated through experimentation 	<p><i>Final Needs:</i></p> <ul style="list-style-type: none"> - A system to create linearly aligned fibrin thread layers - A method to adjoin two linearly aligned layers into a biaxially aligned orientation - For each scaffold to consist of 50-70 threads 	<p><i>Final Needs:</i></p> <ul style="list-style-type: none"> - To be easily maintained and repaired - To be transferable - To be sterilizable - To be reproducible - To be easy to use
<p><i>Final Wants:</i></p> <ul style="list-style-type: none"> - To satisfy client and user's needs - To produce working prototype - To create an innovative product for user 	<p><i>Final Wants:</i></p> <ul style="list-style-type: none"> - To decrease fabrication time significantly - A reproducible method for scaffold creation 	<p><i>Final Wants:</i></p> <ul style="list-style-type: none"> - To minimize handling of threads - To minimize number of steps of the fabrication process - To minimize fabrication time - To minimize supplies wasted during process
<p><i>Final Constraints:</i></p> <ul style="list-style-type: none"> - Time - Budget 	<p><i>Final Constraints:</i></p> <ul style="list-style-type: none"> - Budget - Limited team members to assemble product 	<p><i>Final Constraints:</i></p> <ul style="list-style-type: none"> - Supplies - Budget

Table 7: Needs, Wants, and Constraints for Primary Stakeholders

After examining the final version of the needs, wants, and constraints, the team created final objectives and systematic constraints that needed to be overcome in order to proceed and begin establishing alternative designs for the automated system. While many of the initial needs, wants and constraints, and thus initial objectives, revolved around the scaffold design and its ability to support cell culture, this new list encompassed the needs, wants and constraints for an automated system that would account for reproducibility. Therefore, the team narrowed their focus to primarily cover the desired characteristics of the actual fabrication system in order to generate reproducible aligned scaffolds. Throughout the rest of this report, the constraints and other characteristics primarily pertain to the fabrication system.

3.5 Final Objectives

After confirming with the client and user that the needs, wants and constraints, shown in Table 7 in the previous section, were an appropriate representation of their goals for the project, the design team was able to establish the final set of objectives that was carried throughout the whole design, manufacturing and testing process. These objectives are represented below in Table 8:

Primary Objectives	Secondary Objectives
<i>Reproducible</i>	<ul style="list-style-type: none"> - Accuracy - Precision - Consistent layer properties - Reusable - High scaffold production rate - Able to be scaled
<i>Ease of Use</i>	<ul style="list-style-type: none"> - Fabrication time - Automated/ limited steps - Intuitive - Reliable - Easily Maintained <ul style="list-style-type: none"> - Easy to clean - Easy to repair
<i>Transferable</i>	
<i>Mimic Myocardial Fiber Alignment</i>	<ul style="list-style-type: none"> - Maintain thread mechanical integrity - Minimize thread handling - Stackable layers - Alignment - Efficient degradation - Mechanical Strength - Planar Orientation - Customizable number of threads - Customizable types of threads
<i>Able to be manipulated</i>	<ul style="list-style-type: none"> - Support mechanical and structural testing - Combined into layered scaffold - Support addition of hydrogel

Table 8: Final Objectives and Corresponding Second Objectives

While the final primary objectives were relatively similar from the initial ones, the secondary objectives were modified to characterize the desired automated system for the fabrication of the scaffolds in addition to the scaffold itself. The final objectives needed to be met in order to successfully design a biaxially aligned scaffold. In order to decide the ranking of the final objectives, the team developed a final pairwise comparison chart as shown below in Table 9.

	Able to Support Culture	Mimic Myocardial Fiber Alignment	Reproducibl e	Manipulate	Ease of Use	Transferable	TOTAL
Mimic Myocardial Fiber Alignment	0.5	X	0.5	0	0	0.5	1.5
Reproducible	0.5	0.5	X	1	0.5	0	2.5
Manipulate	0	1	0	X	0.5	0	1.5
Ease of Use	0.5	0.5	0	0.5	X	0.5	2
Transferable	0	0	1	0.5	0.5	X	2

Table 9: Final Pairwise Comparison Chair for Ranked Final Objectives

Below are the objectives explained in further detail:

Reproducible

Reproducibility is necessary in order to ensure the fabrication of accurate and precise scaffolds that allow for testing. The automated device must be able to produce scaffolds with a consistent range of fiber alignment and allow for the stacking of fiber sheets that mimic the complex angular fiber alignment and layers of the myocardium. This also applies to the ability of the system itself to produce scaffolds of reproducible properties with multiple users. High precision and accuracy will result in less variation when testing the scaffold and therefore consistent properties throughout samples.

Easy To Use

The user would like the automated system to allow for the scaffold fabrication process to be done with relative ease when compared to the current system. This includes the fabrication time that is required from start to finish to create these scaffolds, the number of steps that are needed in this process and having a process that is intuitive so that it does not require complex and detailed instructions. This is only the second highest objective, because while it is important to provide the client with a process and end product that is simpler and less tedious than the current method, it is more important to ensure the fabrication process can reproducibly create scaffolds to mimic myocardial fiber alignment.

Transferable

At the beginning of the scaffold production process, the alignment and creation of the threads take place on a non-sterile bench top in a laboratory. In order to seed the cells onto the scaffold, the scaffold must be able to be transferred from the bench top to the sterile hood for sterilization and cell seeding. The scaffold may also need to be taken from the bench top for mechanical testing and imaging. For any *in vivo* experiments these scaffolds must also be able to be easily moved before and during implantation. Therefore, the automated system should be able to accommodate for movement of the scaffold around the lab without compromising the scaffold integrity.

Mimic Myocardial Fiber Alignment

It is necessary for this scaffold to mimic the myocardial fiber alignment so that the developed tissue is homogeneous with the healthy surrounding myocardial tissue. *Figure 2* shown previously depicts the multiple fiber orientations of the myocardium in porcine specimens that the team aimed to reproduce with the alignment of fibrin microthreads in the aligned scaffold.

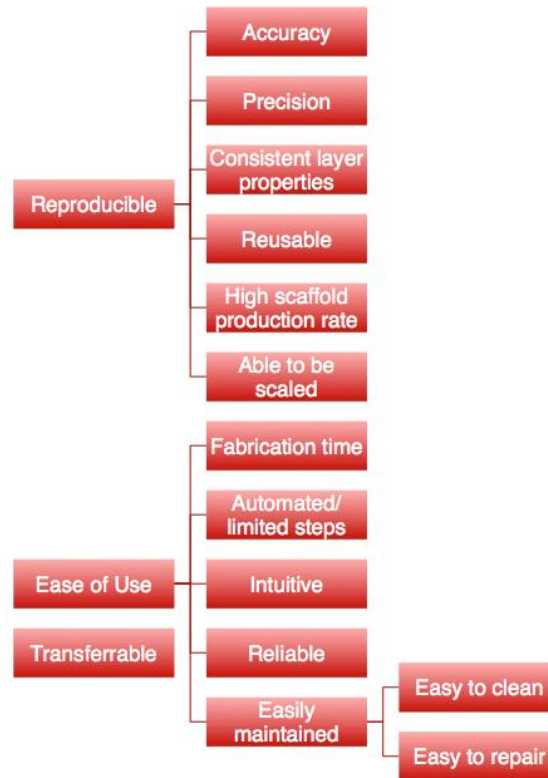
Each fibrin planar sheet should be composed of aligned microthreads with optimal spacing of 50 μ m between each thread. These sheets will make up each layer of the scaffold. The myocardium is composed of multiple layers oriented at multiple angles, and so these sheets will be positioned at angles that vary from 0° to 90° to simulate this variance in orientation. This desired alignment would also produce scaffolds with mechanical properties that are consistent between scaffolds and therefore would have similar mechanical properties of the myocardium. Keeping all of this in mind, the steps involved within the automated process should minimize the physical handling of the threads in order to maintain their structural and mechanical integrity, while simultaneously ensuring proper alignment and orientation.

Ability To Be Manipulated

The ability of the scaffold to be manipulated relies on its transferability, or the ability of the scaffold to be easily moved between workspaces following fabrication. This objective includes the ability of the scaffold design to support mechanical and structural testing in order to validate the design's reproducibility and ability to mimic the complex myocardial fiber alignment. Additionally, each layer must be manipulated so that two or more layers can be stacked together in order to form the multilayered composite. This stacking can simulate the multiple angles of alignment within the myocardium tissue. Due to these criteria, the automated system must facilitate the mechanical testing and stacking of scaffold layers, as well as support the addition of a hydrogel.

While the first three objectives are ranked highest, all five are needed for our design process to ensure the most successful outcome. Ultimately, the team aims to develop an automated system that can consistently reproduce scaffolds that mimic the fiber alignment shown in tissue of the myocardium.

Finally, the design team created a hierarchy graph to summarize their final objectives into a ranked list, which can be seen below in Figure 6:



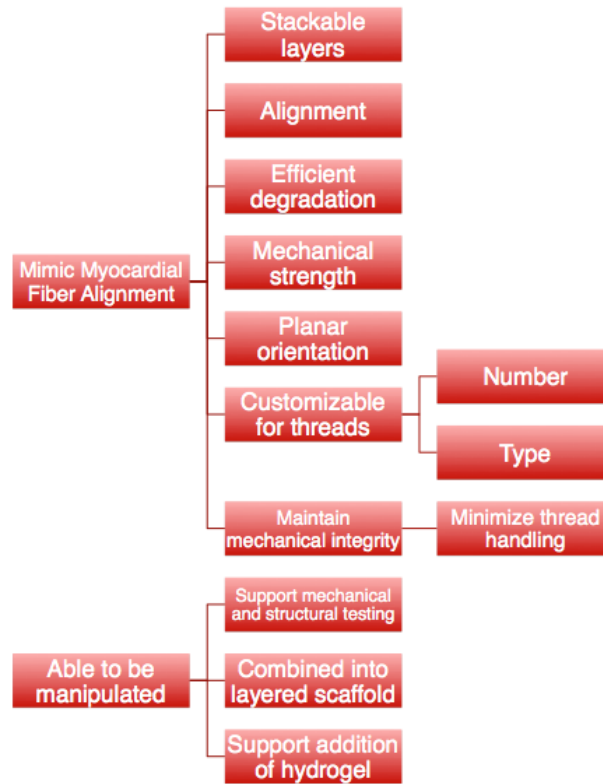


Figure 6: Hierarchy of Primary and Secondary Objectives in Ranking Order

3.6 Revised Client Statement

After solidifying the needs, wants and constraints of the client and user, and establishing concrete objectives, the team was able to determine that the focus of the project is to develop an automated system to facilitate the reproducible construction of a scaffold, which mimics the mechanical and structural properties, excluding functional properties, of myocardial tissue. The team decided to use two terms interchangeably when describing their fabrication system as either “automated” or “semi-automated”. As the scaffold materials are fragile in nature, and it is challenging to eliminate all manual steps while protecting the integrity of the fibrin microthreads, the team refers to this semi-automated process as automated throughout the project.

The client provided the design team with desired specifications for the scaffold, including an overall area of 1 cm² and a range between 20-75 threads per sheet that the system

must accommodate for. The client also expressed the desire for the system to allow for the transfer of the individual sheets between multiple surfaces in the lab, as well as provide a platform construct to facilitate the assembly and testing of the scaffold sheets. Additionally, the system should allow for the orientation of the individual sheets to be customized. From these additional details, the design team was able to modify the initial client statement to produce a final client statement:

“Design and develop a fabrication system to reproducibly construct bi-layered 1cm² fibrin scaffolds whose layer orientation can be customized between 0° and 90° and consists of planar sheets of 20-75 aligned fibrin microthreads to mimic the complex fiber alignment of the myocardium. The system should accommodate for the addition of a hydrogel, and enable the manipulation of the threads to facilitate the mechanical and structural testing of the composite scaffold in order to determine the precision and consistency of thread alignment.”

It is from this final client statement that the team was able to establish a project approach in order to meet the wants and needs of the client.

4 Device Design

After establishing a revised client statement, the team explored methods to meet the wants and needs of the client and user. In order to accomplish this, the team determined the functions of the design and the specifications and parameters needed to achieve them. Through first compiling a list of individual design elements to perform each of the desired functions, the team combined the elements together to develop several design alternatives.

4.1 Functions and Specifications

To generate several alternative designs, the design team first needed to establish a list of functions that the device needed to perform. The list was based off of the needs and wants of the client and user. Below, in no particular order, are the initial functions that the design team established before pruning them down to only the most important functions that the device would need to perform:

- Allow for threads to become a laminated composite through gel adherence
- Gather multiple threads at once
- Provide frame to support threads
- Anchor threads
- Facilitate thread alignment
- Allow threads to be transferable
- Allow for mechanical and structural testing

In order to create a successful scaffold, the device would need to complete a series of chronological steps. Firstly, the device would need to gather the threads. Next, it would need to align and anchor the threads uniformly, and lastly the device would need to provide a frame structure to support the aligned threads and allow for gel adherence. With this in mind, the team

simplified the above list of functions into four main functions, which reflected these chronological steps. Additionally, the team outlined several sub-functions that corresponded to each of the four main functions seen below in Table 10.

Functions	Sub-Functions
Gathering Threads	<ul style="list-style-type: none"> - Collect multiple threads at once - Avoid tangling of threads - Avoid unnecessary breakage of threads - Allow for multiple thread types
Aligning Threads	<ul style="list-style-type: none"> - Allow for equal spacing between threads - Allow for customizable spacing between threads - Allow for customizable number of threads - Allow for use of multiple types of threads
Anchoring Threads	<ul style="list-style-type: none"> - Hold threads in place - Maintain structural and mechanical integrity of threads
Frame to Support Aligned Threads	<ul style="list-style-type: none"> - Protect threads from breakage - Allow for movement around the lab - Allow for mechanical and chemical testing - Allow for addition of a gel

Table 10: Functions and Sub-Functions

From this list of functions, the team developed a set of parameters and specifications that the device needed to accommodate based on the wants of the client. With this in mind, the threads of the scaffold should be composed of an extrusion of fibrinogen and thrombin with a final dry diameter of 100-150 μm . The fabrication of these threads will consist of an automated process with an intermediate drying stage and a final stretch of 150% of the initial extruded length. The total fabrication time should ideally be less than one hour. The scaffold produced should contain 20-75 threads with a 50 μm gap between each thread. In addition, the final scaffold will consist of two or more layers of the aligned threads, each with dimensions of 1 cm

x 1 cm. The thickness of the overall scaffold containing the fibrin microthreads and gel must not exceed 300 μm . The hydrogel that will be added to the two layers of aligned threads will be composed of fibrinogen. A summary of the parameters and specifications for the desired scaffold can be seen below in Table 11.

Parameters	Specifications
<ol style="list-style-type: none"> 1. Thread composition 2. Thread diameter 3. Thread processing techniques 4. Thread fabrication time 5. Number of threads 6. Spacing between threads 7. Number of stacked layers 8. Scaffold fabrication time 9. Scaffold dimensions 10. Scaffold thickness 11. Hydrogel composition 	<ol style="list-style-type: none"> 1. Fibrinogen and thrombin 2. 150 μm 3. Automated process with intermediate drying step and stretch to 150% 4. 2 hours 5. 50-75 threads per layer 6. 50 μm 7. Two layers 8. Less than 1 hour 9. 1 cm x 1 cm 10. Maximum of 300 μm (including gel) 11. Fibrinogen hydrogel

Table 11: Parameters and Specifications

From these specifications, the team brainstormed preliminary conceptual designs for their device.

4.2 Conceptual Design Phase

After establishing functions and specifications, the design team determined a variety of different design elements that could accomplish each of the individual functions as described in Table 10. Once established, the design team outlined the pros and cons of each of these individual elements. Next, the team quantified, ranked and determined the highest ranked elements for each function. By combining these top ranked elements, the team was able to establish an overall design for their alignment device.

4.2.1 Brainstormed Design Elements

Using the four main functions outlined in Section 4.1, the design team brainstormed different design elements that could accomplish each of the main functions. The individual team members first brainstormed different ideas separately with preliminary sketches of different elements, which can be seen later in this chapter. The team then had a collaborative brainstorming session where they combined these ideas and additionally developed several new ideas together. At this stage, the team was not concerned with feasibility of each element to accomplish each of the functions. Instead, the goal was to generate as many diverse design ideas as possible. A complete summary of all the design elements the design team created can be seen in the morphological chart shown below:

Feature/ Function	Means						
Gathering Threads	Spool Storage	Box Remover (Thread Scooper)	Rolling grabber	Lint roller			
Aligning Threads	Threaded rod	Hinge mechanism	Clips on a rail	Grooved device	Pot holder maker	Roller	Shaker
Anchoring Threads	Suction Mechanism (Anchoring)	Saran wrap	PDMS sandwich	Clips	Glue/Tape	Funnel	
Frame to Support Aligned Threads	Washer & Peg	PDMS Frame	Square platform	Loom platform			

Table 12: Initial Brainstorm of Design Elements

Several of these design elements were established from different technologies currently used in the textile industry, food sorting, among others. For example, spool storage for gathering threads and a loom platform for aligning and supporting threads are both elements used for textile fabrication. Working from these initial ideas, the team investigated how other items are currently gathered, aligned, anchored and supported in everyday life in order to generate further design elements. For example, a lint roller is commonly used to gather lint, so the team determined this concept might apply to gathering threads. Additionally, clips, glue and tape are all items used to secure different items, so the team determined they could also be used for anchoring threads. Lastly, the team was able to come up with several different design elements of their own creation, which will be discussed in more detail in the following section.

4.2.2 Evaluation of Design Elements

After design concepts were organized into a morphological chart, the design team began to further develop each of the different elements. For each of these elements, the team established a list of pros and cons for each design concept. These pros and cons explained the potential capabilities and limitations of each of the design elements. These descriptions then aided with the quantitative assessment of the design elements that is discussed in Section 4.2.3. A description and detailed set of pros and cons for each design element can be found below.

Gathering Threads

The first function of the team's device is gathering threads. After the threads are drawn, stretched and hung to dry, they need to be gathered into a bundle before being aligned. The team was able to design several different design elements to accomplish this function. The different elements are described in detail below and the pros and cons of each are laid out as well.

Spool storage

This means of storing microthreads mimics the textile industry where the threads are stored in a continuous spool. This would require a modification in the fabrication of the microthreads in order to be possible. Like a spool of fabric threads, the goal of this mechanism is to allow an easier manipulation of the threads and generation a continuous spool. This could then allow for the threads to be manipulated with similar technologies already found in the textile industry. A model of the spool storage can be seen below in Figure 7 and an overview of the pros and cons for this particular element can be seen below in Table 13.

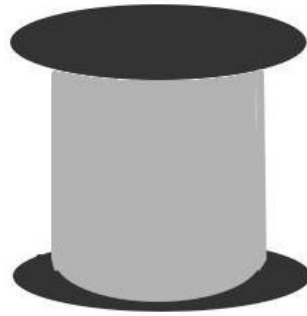


Figure 7: Spool Storage

Pros	Cons
<ul style="list-style-type: none">- Ease of use- Simple procedure- Time saving method- Minimizes thread handling	<ul style="list-style-type: none">- Difficult to wrap around spool- Can cause thread breakage due to stiffness- Require modification of microthread fabrication

Table 13: Pros & Cons of Spool Storage

Box remover

At the end of the fabrication process, fibrin microthreads are hung to dry on an open frame. The thread scooper would then be able to remove the threads from this frame and scoop them into a disorganized bundle. On the outsides there would be two sharp blades that would cut

the thread at the junction with the frame where they are connected on either side. A platform would be under the threads to catch them as they are removed from the frame. The sides would be open and would allow for the bundles to be removed easily to be further processed. A model of the box remover can be seen below in Figure 8 and an overview of the pros and cons for this particular element can be seen below in Table 14.

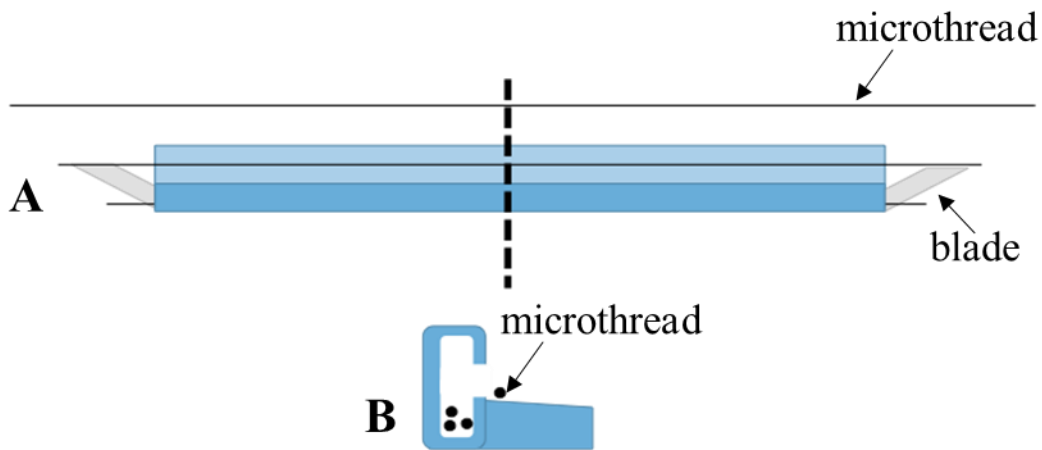


Figure 8: Box remover from a (A) top view and (B) cross sectional view.

Pros	Cons
<ul style="list-style-type: none"> - One-motion process to cut and gather threads off frame - Minimal damage to threads - Supports entire length of threads - Aligns the ends of the threads together 	<ul style="list-style-type: none"> - Threads may become tangled

Table 14: Pros & Cons of Box Remover (Thread Scooper)

Rolling grabber

This will work similarly to the box grabber where the threads will be collected from the frame which they are hanging to dry. This would also use the two sharp blades to remove the threads from the box. As the thread is collected it will be placed into a single slot of a rotating rod. This will allow them to be kept individually without any chance of tangling with other

threads. They can then be individually emptied for the next step in the alignment process. The rotating grabber will be operated manually by twisting the outer handles. A model of the rolling grabber can be seen below in

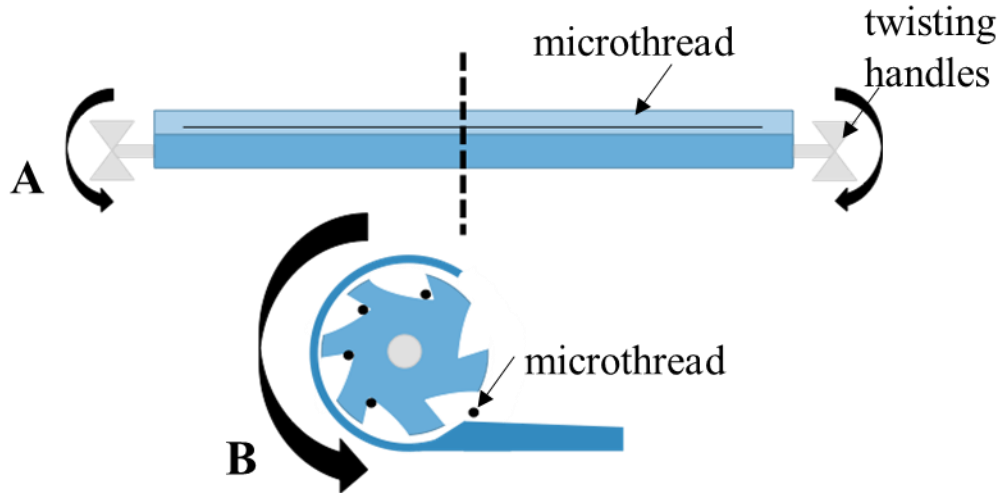


Figure 9 and an overview of the pros and cons for this particular element can be seen below in Table 15.

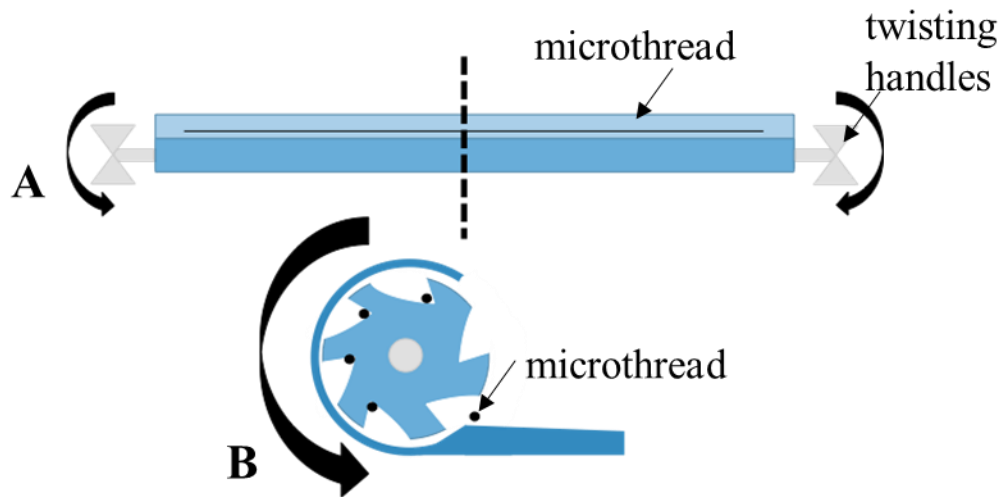


Figure 9: Rolling Grabber from a (A) top view and (B) cross sectional view

Pros	Cons
------	------

- Keeps threads separated to avoid tangling	- Limited number of threads able to be collected at once - Complex parts - Potential damage to threads when spinning
---	--

Table 15: Pros & Cons of Rolling Grabber

Lint roller

The lint roller is a simple design element that mimics an existing technology. By rolling the tube of adhesive paper along the collection of threads, the lint roller design can easily gather the threads with minimal physical handling. The drawback of this design, however, is that the adhesive paper can compromise the sterility of the threads and additionally poses the risk of the threads becoming tangled or even breaking. A model of the lint roller can be seen below in Figure 10 and an overview of the pros and cons for this particular element can be seen below in Table 16.

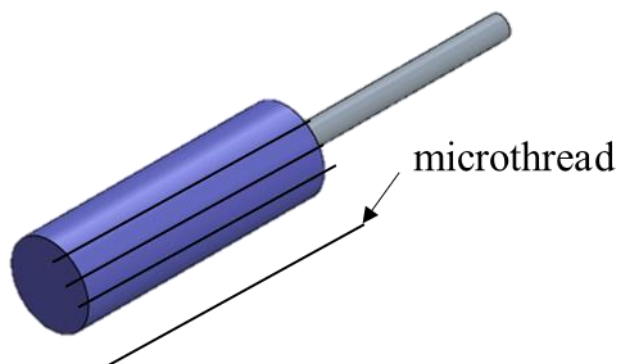


Figure 10: Lint Roller

Pros	Cons
- Easy to use - Simple concept - Less handling of threads	- Risk of tangling and breakage - Human error - Sterility

Table 16: Pros & Cons of Lint Roller

Shaker

The shaker is a simple design adapted from technologies used in the food and manufacturing industry. After the threads are fabricated and removed from the box, they are in a disorganized bundle. Currently, to proceed to the next step of scaffold creation, the threads are manually separated with forceps. This handling of the threads can potentially damage the mechanical integrity of the threads, and is an inefficient process. With the shaker device, the threads are put into the top, where there are slits cut into the bottom, as wide as one single thread. By shaking the device from side-to-side, the threads separate and exit through the slits on the bottom where they will be aligned. This minimizes handling of the threads and is a more automated system than that which currently exists. A model of the shaker can be seen below in Figure 11 and an overview of the pros and cons for this particular element can be seen below in Table 17.

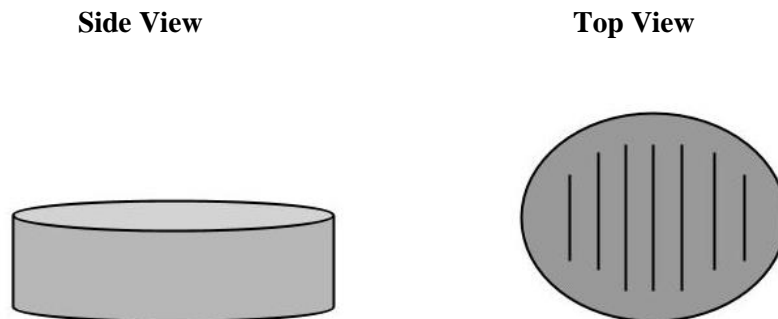


Figure 11: Shaker

Pros	Cons
<ul style="list-style-type: none">- Easy to use- Less handling of threads- Separates threads easily	<ul style="list-style-type: none">- Tangling dependent on static electricity- Spacing and width of slits precision- Threads sticking together

Table 17: Pros & Cons of Shaker

Aligning Threads

After the threads are gathered, the device must then align them. This particular function posed the greatest challenge to minimize the physical handling of the threads in the alignment process. Details of the elements the design team brainstormed can be seen below as well as pros and cons for each.

Threaded rod

The threaded rod design uses a singular part to precisely align a bundle of threads. This design idea was adapted from a strategy used in the creation of beaded bracelets using a bead loom. The threaded rod helps to ensure the threads for the bracelet stay separated, but aligned, during the bracelet making process. The team thought that this concept would translate well into the aligning of threads for a fibrin scaffold. The drawback of this particular concept, however, is that it may require the threads to be manually placed in the threads of the rod. A model of the threaded rod can be seen below in Figure 12 and an overview of the pros and cons for this particular element can be seen below in

Pros	Cons
<ul style="list-style-type: none">- Simple design- Good precision- Singular part	<ul style="list-style-type: none">- Manual placement of threads may be required

Table 18.

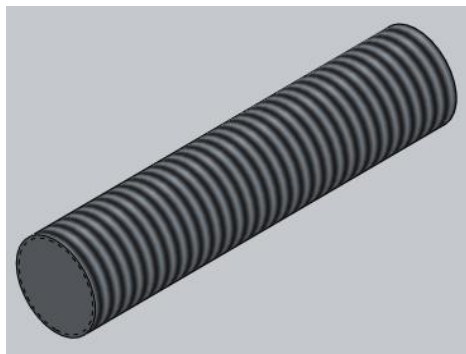


Figure 12: Threaded Rod

Pros	Cons
<ul style="list-style-type: none"> - Simple design - Good precision - Singular part 	<ul style="list-style-type: none"> - Manual placement of threads may be required

Table 18: Pros & Cons of Threaded Rod

Hinge Mechanism

This concept to align threads operates by folding the threads into desired lengths. The device would fold on alternating sides, and the user would then attach the folded thread to the center alignment on each fold. The user would manually move the side pieces alternating with each folding of the thread. Additional threads can be added to reach 20-75 total aligned threads in the centerpiece or the spool storage could allow for continuous folding of the microthreads with this device. A model of the hinge mechanism can be seen below in Figure 13 and an overview of the pros and cons for this particular element can be seen below in Table 19.

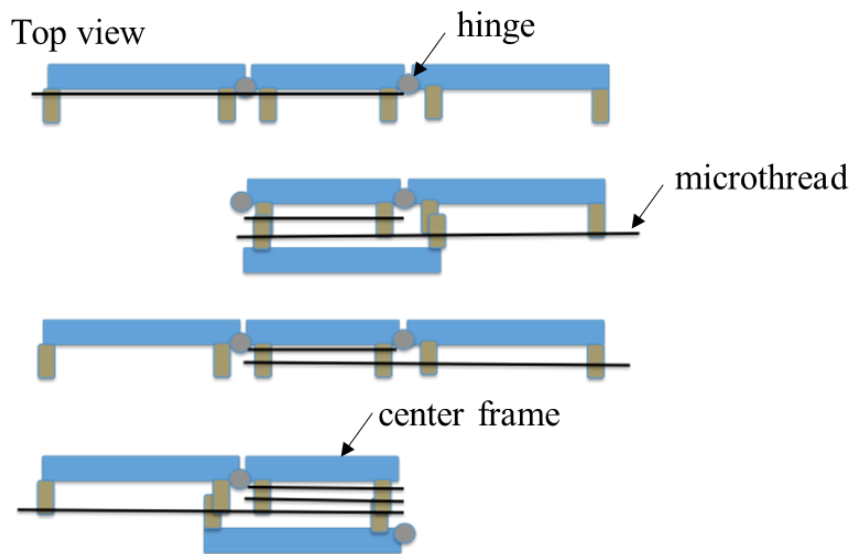


Figure 13: Hinge Mechanism

Pros	Cons
<ul style="list-style-type: none"> - Equal length for each thread 	<ul style="list-style-type: none"> - Manual manipulation needed

- | | |
|-----------------------------------|--|
| - Internal frame can be removable | |
|-----------------------------------|--|

Table 19: Pros & Cons of Hinge Mechanism

Clips on a Rail

This mechanism is manual and requires a constant manipulation of the thread. It relies on having a mobile platform that first secures both ends of the thread and then slides together to fold the thread. The device would join the ends of the thread, making the thread bend, break in half where it is secured to an additional clip. The process is repeated multiple times until a substantial number of threads have been joined together. A model of the clips on a rail can be seen below in Figure 14 and an overview of the pros and cons for this particular element can be seen below in Table 20.

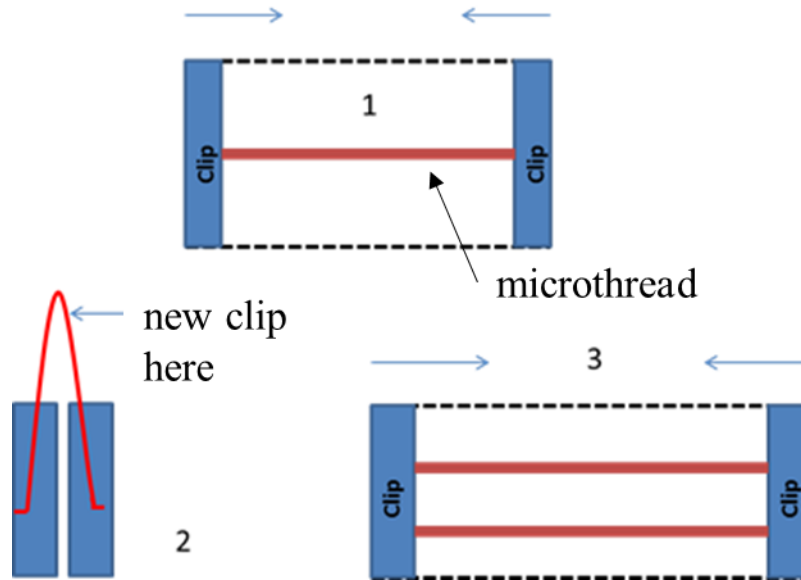


Figure 14: Clips on a Rail (top view)

Pros	Cons
- Intuitive process	- Manual process
- Easy set-up	- Requires constant assistance
- Non-electrical	- Constant thread manipulation

Table 20: Pros & Cons of Clips on a Rail

Grooved Device

The grooved device is a novel idea to align the threads by placing the threads into pre-cut holes which align them in order to create the scaffold. This device is easy to use because the threads can be slowly and lightly pushed across the surface of the device causing them to fall into place without having to manually place each one individually into the grooves. Each groove is only large enough for a singular microthread to fill. The threads can then be held together on the ends and moved to create the ideal scaffold. A model of the grooved device can be seen below in Figure 15 and an overview of the pros and cons for this particular element can be seen below in Table 21.

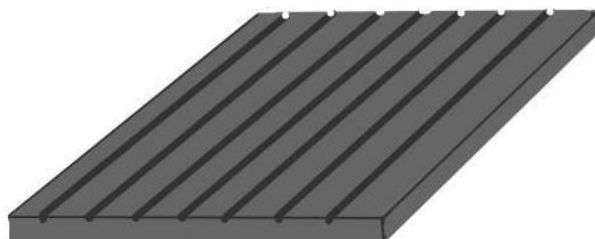


Figure 15: Grooved Device

Pros	Cons
<ul style="list-style-type: none">- Simple design- Equal/consistent spacing- Reusable	<ul style="list-style-type: none">- Could damage mechanical and structural integrity of threads- Could cause breakage on ends of threads

Table 21: Pros & Cons of Grooved Device

Funnel

This device component already exists on the market and can be used to separate each thread from the bundle of threads. This device is reusable and simple. As the threads fall into the funnel, they are separated into individual threads, which can then be used later to align into scaffolds or can be directly aligned at the bottom of the funnel. A model of the funnel can be

seen below in Figure 16 and an overview of the pros and cons for this particular element can be seen below in Table 22.

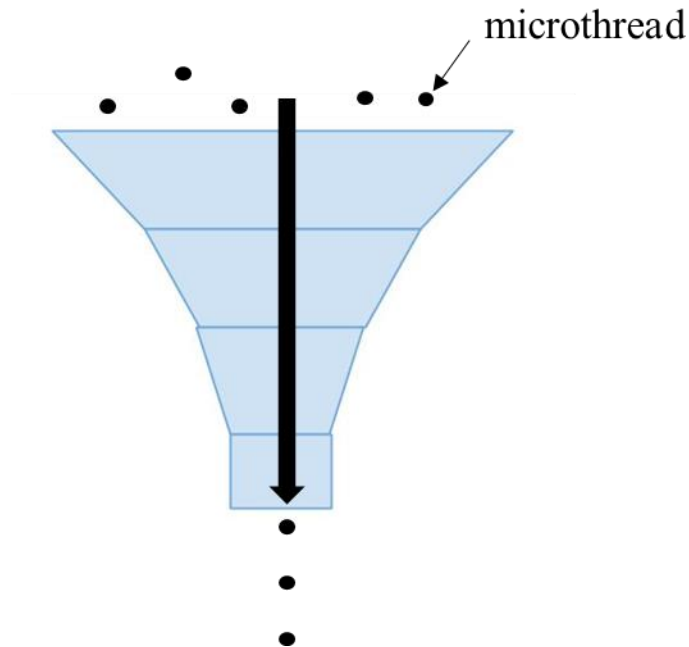


Figure 16: Funnel

Pros	Cons
<ul style="list-style-type: none"> - Simple - Reusable 	<ul style="list-style-type: none"> - Threads tangling/get stuck - Static electricity can affect

Table 22: Pros & Cons of Funnel

Pot holder maker

This design works to align threads in both axes by placing them in between the posts that are on the outsides of the platform. This gives the user the capability to align threads in both axes on a singular platform. It does require the manual placement of the threads into each of the grooves, however. A model of the pot holder maker can be seen below in Figure 17 and an overview of the pros and cons for this particular element can be seen below in Table 23.

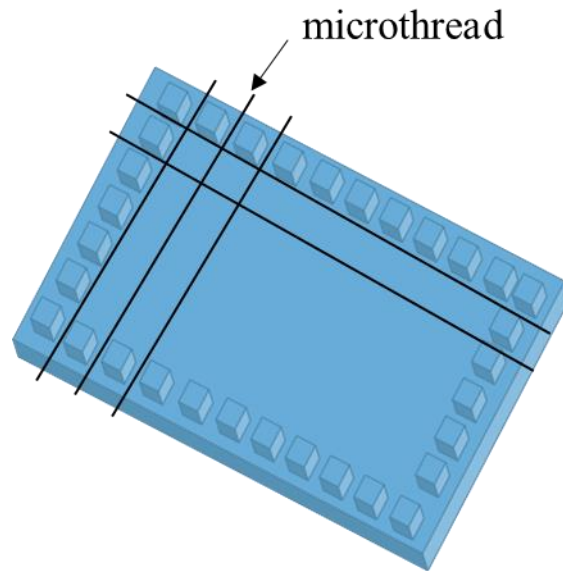


Figure 17: Pot Holder Maker

Pros	Cons
<ul style="list-style-type: none"> - Simple design - Allows for biaxial crossing of threads 	<ul style="list-style-type: none"> - Thread placement could be a tedious process - Limited angle of orientation of the threads

Table 23: Pros & Cons of Pot Holder Maker

Anchoring Threads

Once the threads have been aligned, the device needs to anchor them in such a way that will maintain their alignment. The challenge with this particular function is ensuring the physical and mechanical integrity of the threads is maintained by reducing tensions placed on the threads. Descriptions of the different elements the design team created can be found below as well as pros and cons of each.

Suction Mechanism

Once threads are in a bundle, they can enter in the direction seen below and will be separated and aligned immediately. Suction will be applied in both directions, parallel to the threads in order to bring them into the device, and perpendicular to the threads to anchor them to

the surface. Suction allows for the threads to be pulled down to the surface of the platform in order to prevent unwanted movement. Similar to an air hockey table, this design will work in reverse, securing the threads to the surface instead of pushing air out. A model of the suction mechanism can be seen below in Figure 18 and an overview of the pros and cons for this particular element can be seen below in Table 24.

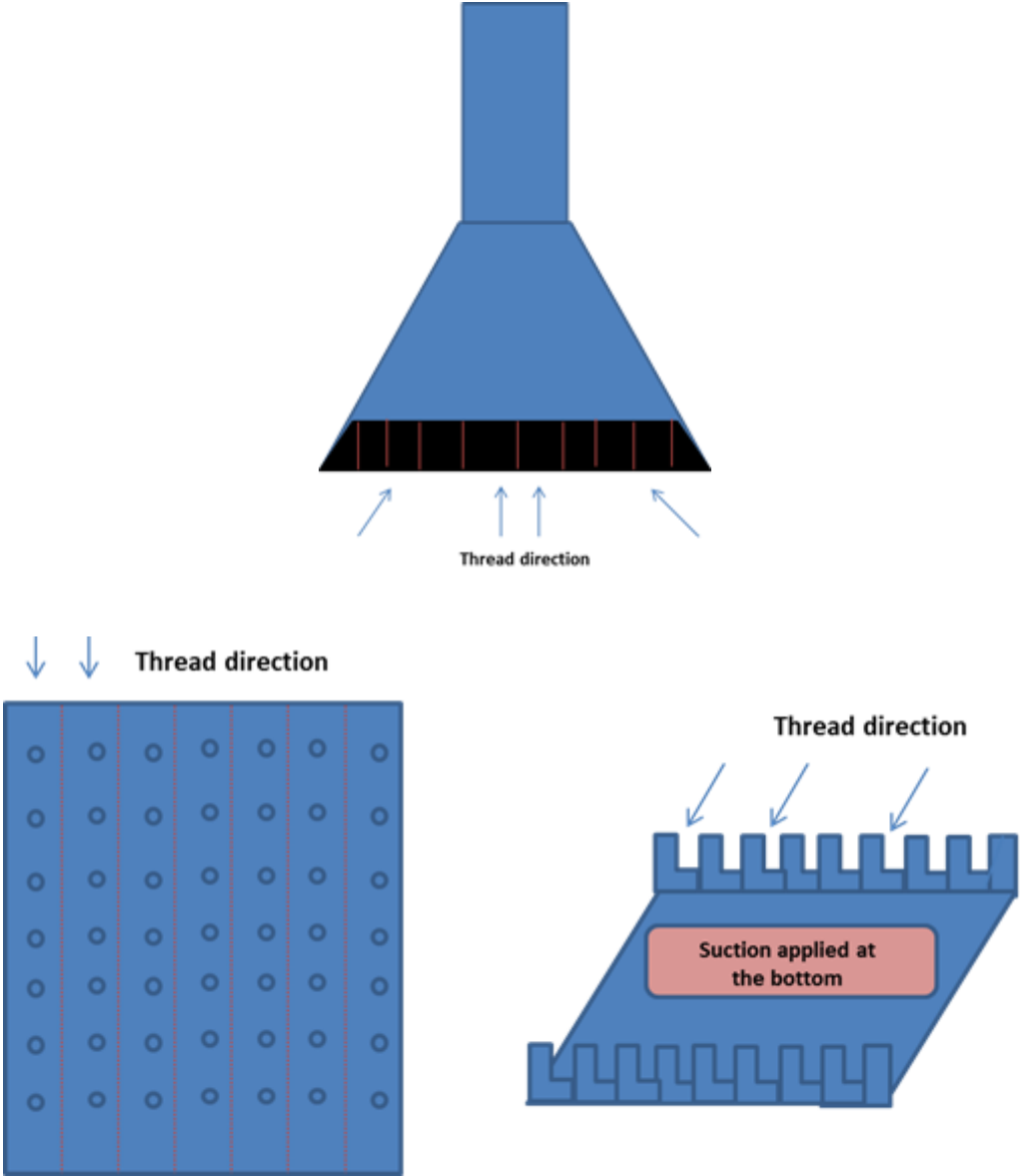


Figure 18: Suction Mechanism

Pros	Cons
<ul style="list-style-type: none"> - Aligns threads into a grooved system - Anchors threads to the surface - Automated process - Offers detachable platforms - Minimal thread handling 	<ul style="list-style-type: none"> - Not an organized mechanism - Threads can get tangled - Complicated design since it requires small grooves - Potential thread deterioration

Table 24: Pros & Cons of Suction Mechanism

Saran wrap

This means of securing the threads utilizes saran wrap to hold the threads in place. It is an item that is easily available and inexpensive. It would allow the team to utilize an existing product that is on the market, saving time which would be used to design another element of the device. However, saran wrap is not reusable and can be very hard to handle as it sticks together on itself. A model of the saran wrap can be seen below in Figure 19 and an overview of the pros and cons for this particular element can be seen below in Table 25.

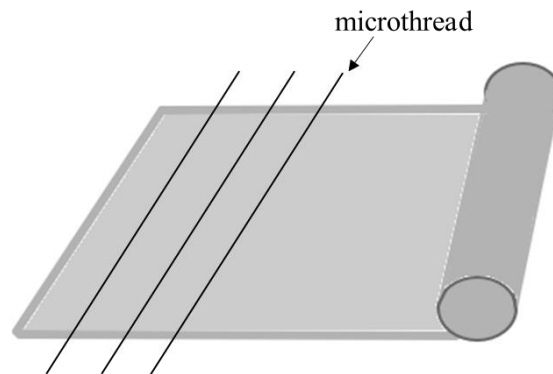


Figure 19: Saran Wrap

Pros	Cons
<ul style="list-style-type: none"> - Potential to hold threads in place - Inexpensive material 	<ul style="list-style-type: none"> - Sticks together on itself - Difficult to handle with gloves - Not durable

Table 25: Pros & Cons of Saran Wrap

PDMS sandwich

This mean of securing threads would work by positioning the threads between two PDMS pieces that would be shaped to allow for them to be held together by friction between pieces. This could be incorporated into many other designs for other frames because of the capabilities of PDMS to be easily molded into any desired shape. Due to its low stiffness, it would have a limited effect on the mechanical and structural integrity of the threads. A model of the PDMS sandwich can be seen below in Figure 20 and an overview of the pros and cons for this particular element can be seen below in Table 26.

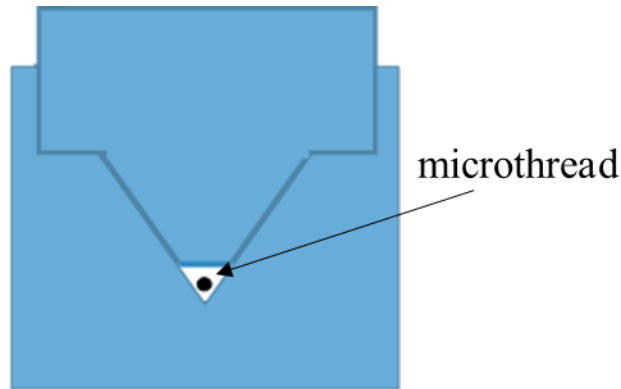


Figure 20: PDMS Sandwich from side view

Pros	Cons
<ul style="list-style-type: none">- Limits mechanical damage to threads- Easy to secure thread in place- Secure connection between PDMS	<ul style="list-style-type: none">- Difficult to fabricate- May not have secure grasp of thread- Multiple molds needed to create

Table 26: Pros & Cons of PDMS Sandwich

Clips

Using clips to hold and anchor the threads in place would be simple and the clips are reusable, thus a cost effective method. The clips would be able to hold the aligned threads together so that they can maintain their specific alignment as well as be able to be transferred

from place to place without disturbing the alignment. Unfortunately, the clips could damage the ends of the threads which are in contact with the clips themselves, potentially breaking them and disrupting the mechanical integrity. A model of the clips can be seen below in Figure 21 and an overview of the pros and cons for this particular element can be seen below in Table 27.

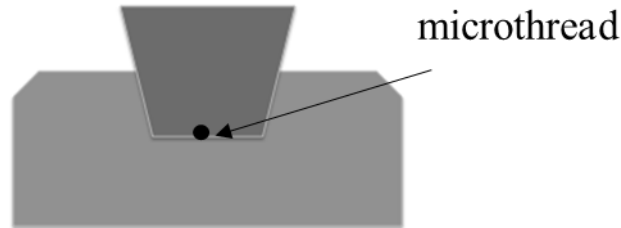


Figure 21: Clips from side view

Pros	Cons
<ul style="list-style-type: none"> - Holds threads in place - Transferable 	<ul style="list-style-type: none"> - Potential thread damage & breakage - Could be hard to release threads at the same time; stick together and to clips

Table 27: Pros & Cons of Clips

Glue/Tape

Utilizing glue or tape as a means of anchoring the threads would be both simple and inexpensive. It would allow the team to utilize an existing product and thus save time and resources that would be required for design a unique element. However, glue and tape could damage the threads and threaten the sterility of them. Table 28, below, outlines these pros and cons.

Pros	Cons
<ul style="list-style-type: none"> - Simple - Inexpensive 	<ul style="list-style-type: none"> - Sterility - Damage to threads

Table 28: Pros & Cons of Glue/Tape

Frame to Support Aligned Threads

Lastly, the team's device must incorporate a frame to support the aligned threads. Not only must this frame be able to allow for mechanical and structural testing, but it should be able to be transferable between surfaces without compromising the integrity of the scaffold. Details of the different elements the design team established are below as well as the pros and cons of each.

Washer & Peg

This frame design would allow for the customizable addition of aligned layers at the desired relative angles. The threads would be already in the aligned layer, with anchors on either end. These anchors would then secure into the washer shaped frame, one layer at a time. This could then be used the addition of a gel and other testing purposes as the frame would allow for easy transferability of the scaffold between working surfaces. A model of the washer & peg can be seen below in Figure 22 and an overview of the pros and cons for this particular element can be seen below in Table 29.

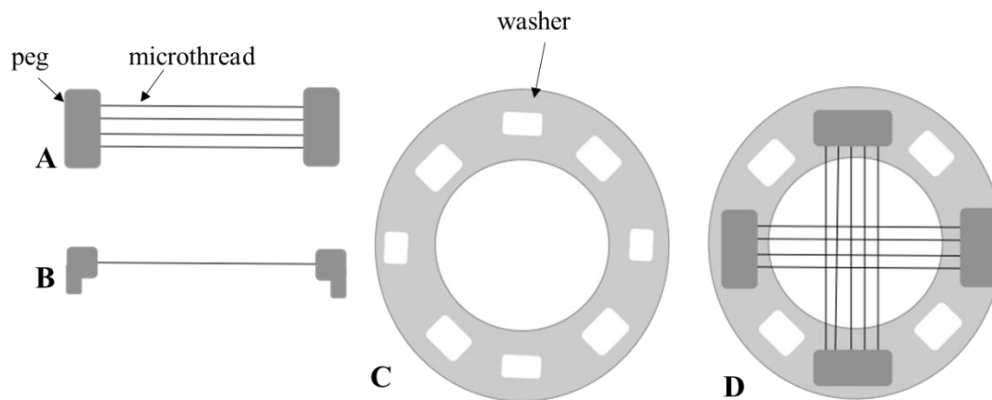


Figure 22: Washer and Peg with (A) top view of aligned threads in peg, (B) side view of aligned threads, (C) top view of washer and (D) top view of washer with two layers of threads

Pros	Cons
<ul style="list-style-type: none"> - Customizable angle orientation of aligned threads - Ability to add gel - Easily sterilizable - Easily fabricated 	<ul style="list-style-type: none"> - Threads may need extra support to be held securely - Need for multiple small parts

Table 29: Pros & Cons of Washer and Peg

PDMS Frame

This frame would be made out of PDMS and allow for the adherence of the scaffold to the well of the frame. This could be customizable in different volumes and shapes depending on the testing that it would be used for. It could be easily transferable to different work spaces due to the outer frame that would also protect the threads within the well. A model of the PDMS frame can be seen below in Figure 23 and an overview of the pros and cons for this particular element can be seen below in Table 30.

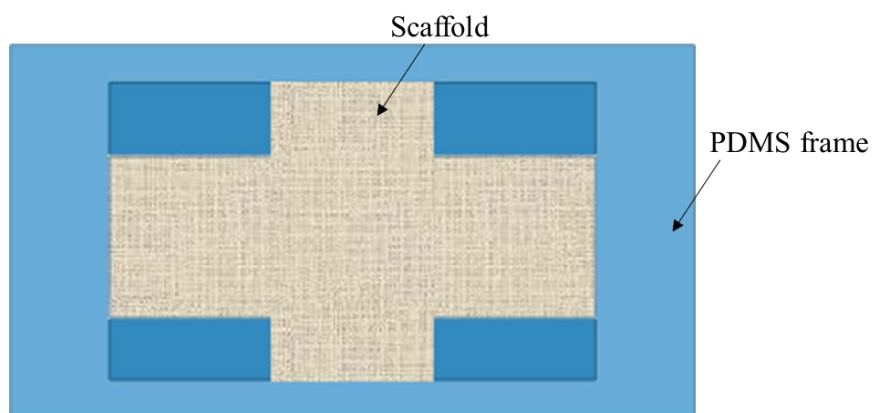


Figure 23: PDMS Frame, top view

Pros	Cons
<ul style="list-style-type: none"> - Allows for customizable shape of final scaffold - Allows for addition of gel in customizable volume 	<ul style="list-style-type: none"> - Securing threads to frame might be difficult - Low resistance to tearing - May interfere with mechanical testing

Table 30: Pros & Cons of PDMS Frame

Square Platform

As its name denotes, this design consists of a platform with a hollow interior in which threads can be positioned. The borders of the platform allow for the addition of a hydrogel in order to hold the threads together. In addition these borders are detachable to facilitate the process of placing the threads in and taking them out at the end once the gel has been added. A model of the square platform can be seen below in Figure 24 and an overview of the pros and cons for this particular element can be seen below in Table 31.

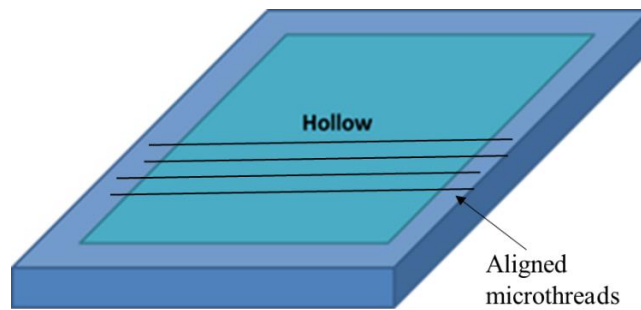


Figure 24: Square Platform

Pros	Cons
<ul style="list-style-type: none">- Simple and intuitive- Allows for containment of gel- Cheap- Sterilizable	<ul style="list-style-type: none">- Complicated separation of platform after placement of gel

Table 31: Pros & Cons of Square Platform

Loom platform

The loom platform mimics an existing loom structure designed for the creation of bracelets and other handmade jewelry. The loom consists of a wire frame and incorporates the threaded rod design element that was discussed above. It also includes two anchoring cylinders which are able to be adjusted by loosening or tightening wing nuts on the sides. The aligned threads would be anchored to a spool at one end, extended across the two threaded rods (which

would help to ensure alignment), and anchored to the spool at the opposite end. The adjustability of the anchoring spools would allow for the tension of the threads to be modified. Additionally, the open structure of the loom platform would allow for easy access to the fibrin scaffold, but one drawback of this particular design is that it may require too much physical handling of the threads/scaffold. A schematic of the loom platform can be seen below in Figure 25 and the pros and cons of this element can be seen in Table 32.

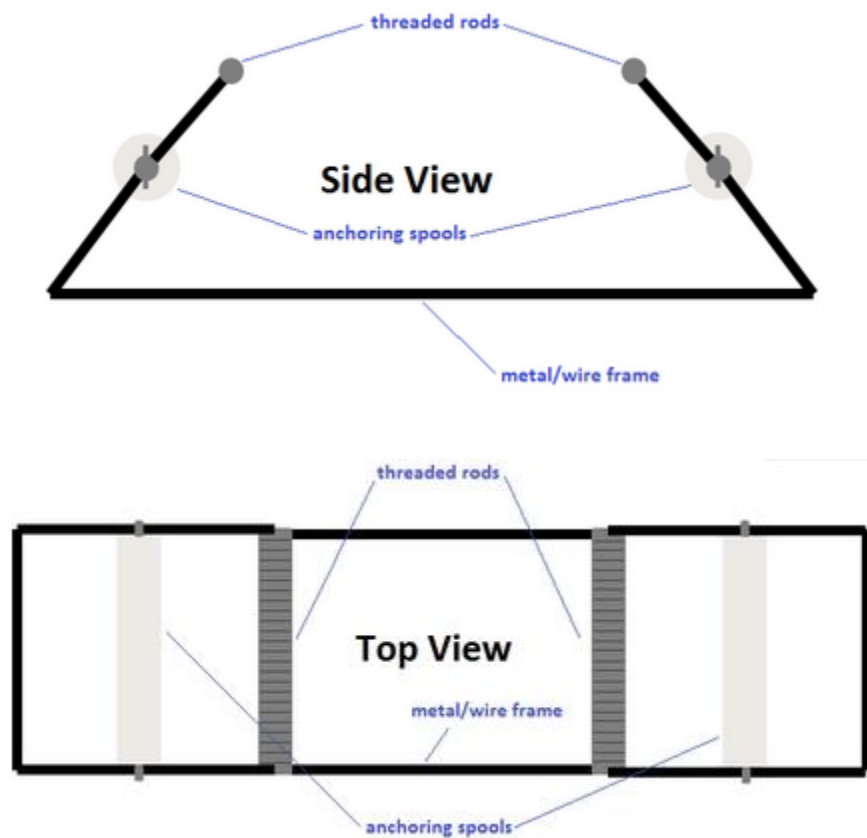


Figure 25: Loom Platform

Pros	Cons
<ul style="list-style-type: none"> - Simple - Open design structure allows for easy access - Easy to maintain 	<ul style="list-style-type: none"> - Manual placement of threads may be required - Doesn't allow for the incorporation of a gel

Table 32: Pros & Cons of Loom Platform

4.2.3 Quantitative Assessment of Design Elements

A numeric scale was established to determine whether the elements achieved the objectives established in Chapter 3. The scale consisted of a rating from 0 (lowest score) to 2 (highest score). The detailed scale information can be found in *Appendix A - Metrics Rubric*. Based on this scale, two assessments were created; a preliminary study and the final decision matrix which allowed for the selection of the final elements of the desired design.

The preliminary quantitative assessment consisted in rating the elements in a scale from 0 (lowest score) to 2 (highest score), according to the objectives shown in Chapter 3. The rating presented an alternative to understand the feasibility of the elements. However, since it was not a weighted mechanism, it did not account for the relevance that each objective represented to the client.

The second quantitative assessment was more complex and was used in the final evaluation. Four decision matrices were established in order to separate the elements in each of the main functions established earlier in this chapter (gathering, alignment, anchoring or framing of threads) according to their utility and function. Once the matrices were created, the elements were assessed on whether or not these complied with the constraints. If the elements didn't pass the constraints, they were rejected; if they did pass the constraints the rating continued. An example of this rating is shown below in Table 33. On the left side of the table, constraints and objectives are specified with either a C or an O respectively. Constraints were assessed qualitatively with either a Y (Yes) or N (No).

Objectives were assessed quantitatively. The elements were ranked in a scale of 0 (lowest score) to 2 (highest score) according to the attributes established for each objective. These scores were then normalized by dividing the score given by the highest rating, which in this case was a 2

score. These normalized scores were then summed and weighted according to the importance of each objective. The weight that each objective received had been previously established based on the client’s needs. Each weighted sum, pertained to the 5 objectives that the device needed to fulfill, were added and the final score was obtained. The elements with the highest scores were then selected for further proof of concept. Table 33 shows the decision matrix template used for the rating system used.

C/O	Weight (%)	Attribute	Element 1			Element 2			Element 3			Element 4		
			Score	Normalized Score	Weighted Sum	Score	Normalized Score	Weighted Sum	Score	Normalized Score	Weighted Sum	Score	Normalized Score	Weighted Sum
C		Time												
C		Budget												
C		Safe for user												
C		Supplies												
C		Limited Team members												
Obj 1	40	Reproducible												
O		Accuracy - thread separation												
O		Precision - Consistent layer properties												
O		Reusable												
O		High Scaffold production rate												
O		Sterilizable device												
O		Able to be scaled up												
Obj 2	10	Easy to use												
O		Automated												
O		Intuitive												
O		Reliable												
O		Easily maintained												
Obj 3	20	Transferable												
Obj 4	20	Mimic Myocardium Structure												
O		Maintain thread mechanical integrity												
O		Minimize thread handling												
O		Stackable layers												
O		Alignment												
O		Efficient degradation												
O		Mechanical Strength												
O		Planar orientation												
O		Customizable number of threads												
O		Customizable types of threads												
Obj 5	10	Able to be manipulated												
		TOTALS												

Table 33: Decision Matrix Template

By using this system, the team assured that the ratings given to each element were normalized by the weight that each objective represented. Thus, the team could make a more informed decision of the best elements to be incorporated in the final design. In the following section the results obtained through these decision matrices are presented.

Decision Matrix Results

The results below are separated in four categories, each representing the four functions the elements needed to comply with. The top of each table presents the highest ranked elements.

Gathering threads

Element	Score
Box Remover	355
Rolling grabber	340
Spool	170
Lint roller	85

Aligning threads

Element	Score
Grooved device	275
Roller	255
Shaker	250
Funnel	235
Clips on a rail	210
Threaded rod	195
Hinge Device	185
Pot holder	110

Anchoring threads

Element	Score
Suction	225
Sandwich	225
Clips	205
Glue/Tape	75
Saran wrap	70

Framing Threads

Alternative	Score
Washer and Peg	255
Square platform	225
Loom platform	205

Table 34: Results from Decision Matrix

Function	Alternative	Score
Gather	Box Remover	355
Align	Grooved device	275
	Roller	255
	Shaker	250
Anchor	Suction	225
	Sandwich	225
Frame	Washer and Peg	255
	Square Platform	225

Table 35: Final Top Scores

The Table 35 shown above depicts the elements rated with the top scores that in the next section will be explored further in Section 4.3 in order to select the components of the final design.

4.3 Development & Verification of Final Design

From the quantitative assessment seen in the previous section, the design team was able to consolidate their design elements into one design alternative for each function. For gathering, the team decided to move forward with the concept of the box remover. To align the threads, the team selected the grooved device, while additionally choosing to incorporate the suction element in order to anchor them. Lastly, the team decided to move forward with the washer and peg design to provide a supportive frame for the aligned threads. After receiving approval of these elements from the client and user, the team was able to further develop these elements in order to establish their final design.

4.3.1 Gathering Threads – Box Remover

The box remover received the highest ranking from the team's quantitative assessment for accomplishing the function of gathering the threads. A CAD model of this element can be seen below:

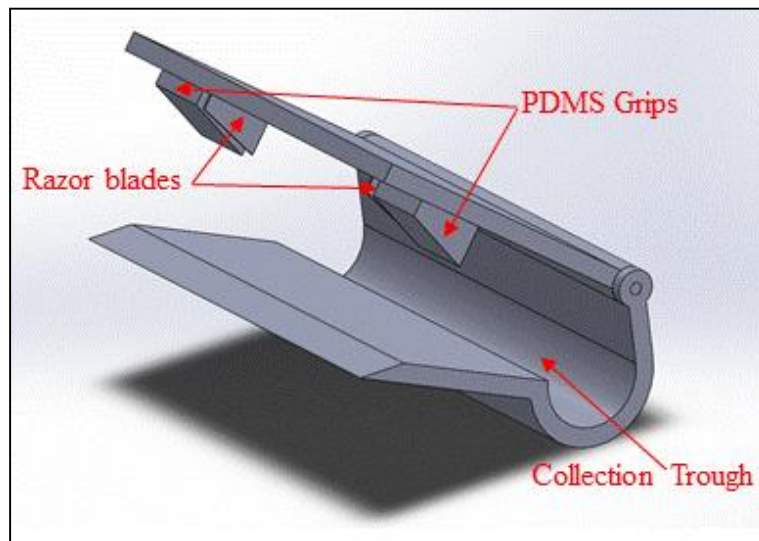


Figure 26: CAD Model of Box Remover

The device would consist of mainly a plastic material such as acrylic, with two regions of PDMS to first grip the threads and additionally two adjacent razor blades to then simultaneously cut the threads off the frame. A small trough at the back would serve as a collection location for the cut threads. As mentioned above, once the threads are drawn, they are placed across an open box frame. From here, the PDMS grips would hold the thread securely while the razor blades cut to ensure that if one end of the thread is cut slightly before the other the thread will remain secure and not displaced by tension. Next, releasing of the grips and tilting the box remover slightly backwards will allow the cut thread to fall into a collection trough at the back of the device. After this process is repeated several times, a small bundle of threads will be gathered in the trough.

After reassessing whether this process was the most straightforward option, the design team decided to design a system that would skip the step of gathering all together by altering the step of drying the extruded threads on the simple box frame. Instead the extruded threads could be placed onto a frame that to align them following fabrication. A CAD drawing of this modified frame design can be seen below in Figure 27.

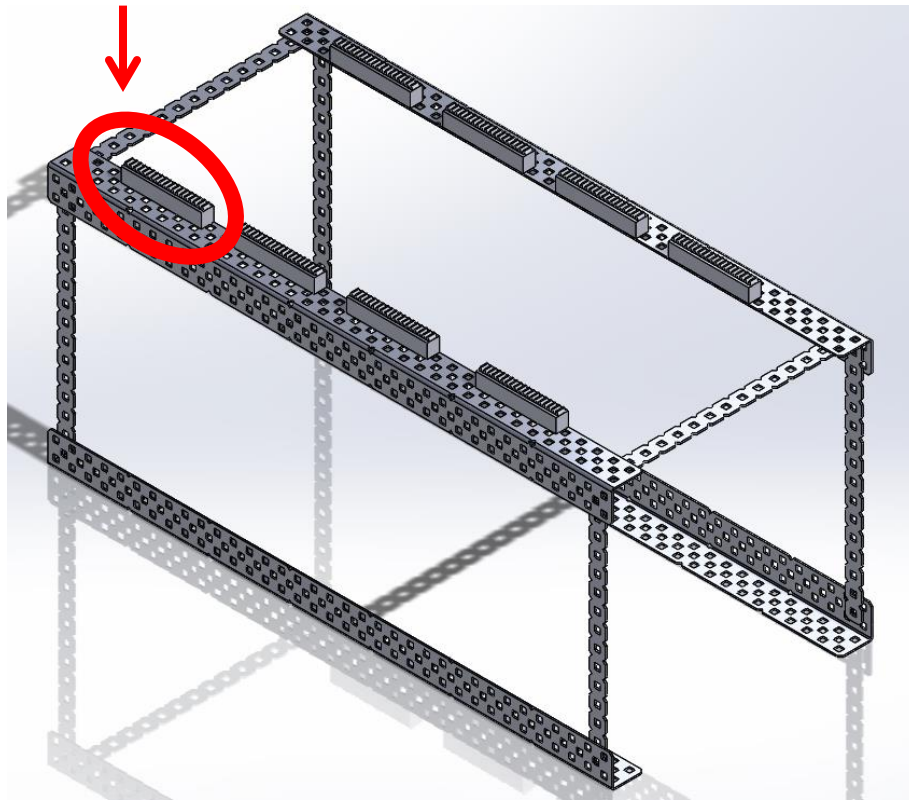


Figure 27: CAD of Extrusion Alignment Frame

This device would consist of an inexpensive metal frame made out of mostly VEX Robotics parts. On top of this frame would be several small plastic pieces with grooves in them (circle in the picture above), into which each of the threads could be laid in. These grooved pieces are gear treads used with VEX motors. Using these VEX parts would eliminate the need for them to be 3D printed or manufactured in-shop, saving time and resources. Lastly, each groove in the gear treads would be color coded with its corresponding groove on the opposite

side of the frame to aid in visualization of thread placement. This will help to ensure proper alignment and spacing of the threads.

4.3.2 Aligning Threads – Grooved Device

While the grooved device scored the highest for accomplishing the task of aligning threads, the concept itself was further modified by the design team. The initial grooved device concept involved a collection of grooved platforms on either side of a cylindrical rod that allowed the bundled threads obtained from the box remover separate from each other and fall into the grooves due to gravity. A CAD model of this idea can be seen below in Figure 28:

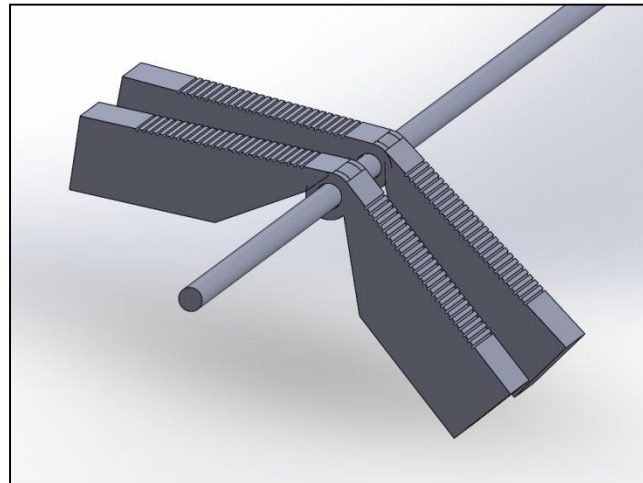


Figure 28: CAD of Sliding Pyramid Grooved Device

Each platform shown in the device would be free to move along the rod as well as rotate in a plane perpendicular to the rod in order to match up with its corresponding grooved platform on the other side of the rod. To operate the device, the rod would first be positioned on a stand that would support it horizontally, with each side of the individual platforms open and resting on the bench top at a 45 degree angle. The angle would be such that the threads wouldn't fall out of the grooves once initially positioned. A sketch of this concept can be seen in Figure 29.

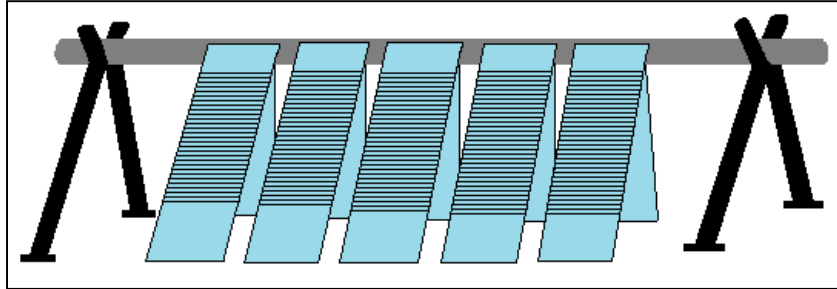


Figure 29: Folding Pyramid Grooved Device Sketch (Step 1)

The gathered threads (spanning the entire length of all the individual platforms) would be gently rolled down each side of the row of platforms until a singular thread was positioned in each groove. Upon filling each groove, the stray ends of the threads extending out from either of the two outer platforms would be taped to the edge of these platforms to secure them. At this stage the support frame would be removed and the platforms would be laid out flat on the bench top. From here, the two groups of platforms on either side would be folded together, which can be seen in Figure 30.

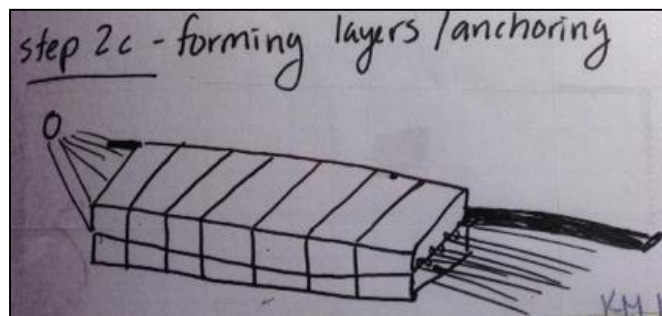


Figure 30: Sliding Pyramid Grooved Device Sketch (Step 2)

The grooves on opposite sides would be staggered in such a way that when folded together, the resulting aligned threads would be positioned slightly closer to each other. This concept is illustrated in Figure 31 below with the staggered grooves highlighted in red.

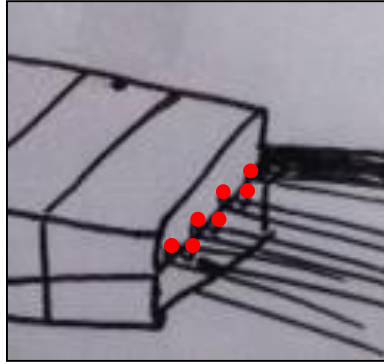


Figure 31: Close-up of Aligned Threads Using Sliding Pyramid

At this point, the tape on the outer platforms can be removed as the joined platforms would provide enough security to keep the threads aligned. Next, each paired platform would be slid apart gently in pairs of two and at equal increments as can be seen below in Figure 32.

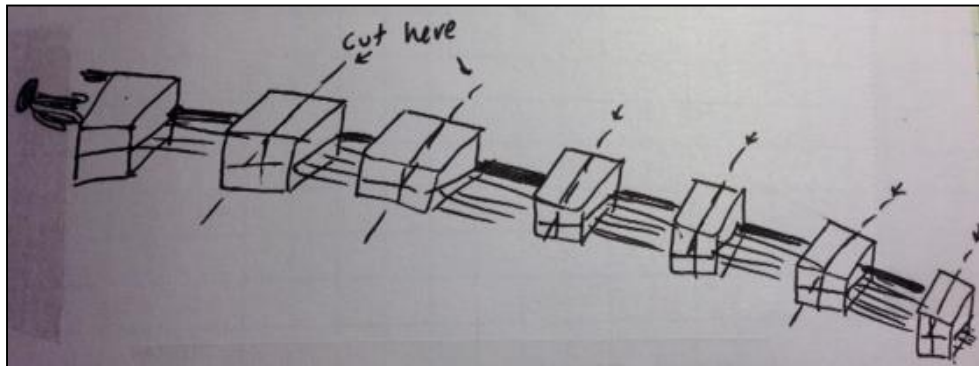


Figure 32: Sliding Pyramid Grooved Device Sketch (Step 3)

From here, each pair would be separated slightly to allow the threads to be cut in between each pair, which can be seen above. The result would be a smaller sample of threads with one set of folded platforms on either side, providing an anchor at each end (Figure 33). These separate samples of aligned threads could then be placed in a frame and stacked on top of each other according to the needs and desires of the user.

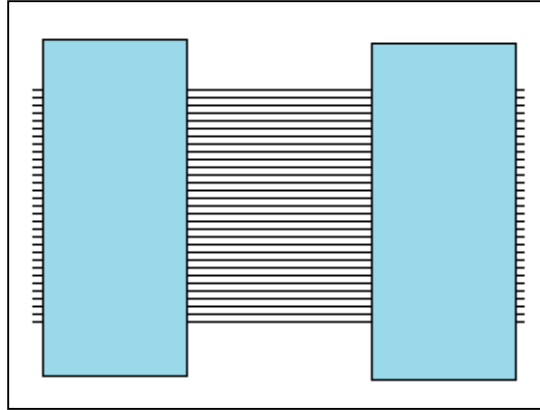


Figure 33: Segmented Portion of Sliding Pyramid Grooved Device

Ultimately, the team decided to abandon this particular design due to the complex steps involved in this alignment process. The concept itself was over-engineered, with many moving parts and as a result the team returned to a flat grooved platform to facilitate the alignment process. This would still incorporate the grooved platform as seen in the previous design but would allow for fewer steps and less complexity in the manufacturing and use of the device. The final CAD model of this design can be seen below:

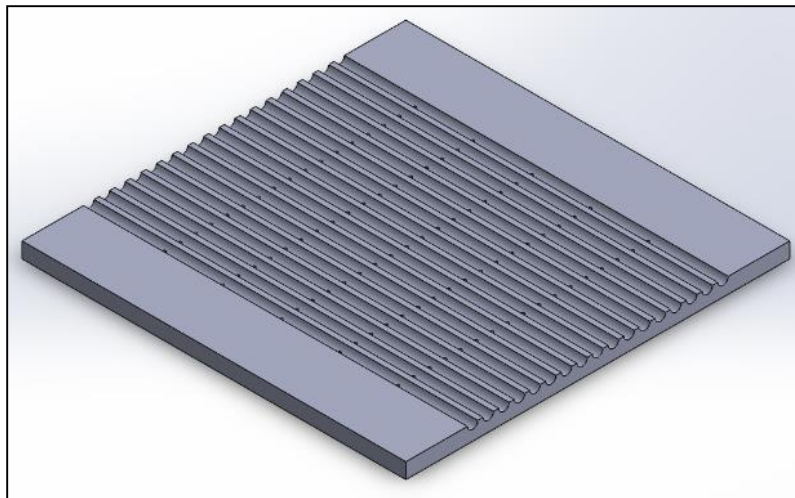


Figure 34: Grooved Device (Flat Platform)

This platform, made out of a polycarbonate cast acrylic, has shallow grooves that secure a singular thread per groove. Additionally, a series of holes are placed along the trough of each

groove. This flat platform combined with a suction element would allow for an applied suction to pull the threads securely into each groove, allowing them to be anchored into the grooves. This alternative facilitates the alignment process, and anchoring of threads.

To improve the manufacturability of this design, the team developed a design that incorporating a separate mesh layer under a completely open groove instead of using drilled holes in the platform to provide the suction to align and anchor the threads. A sketch of this design can be seen below:

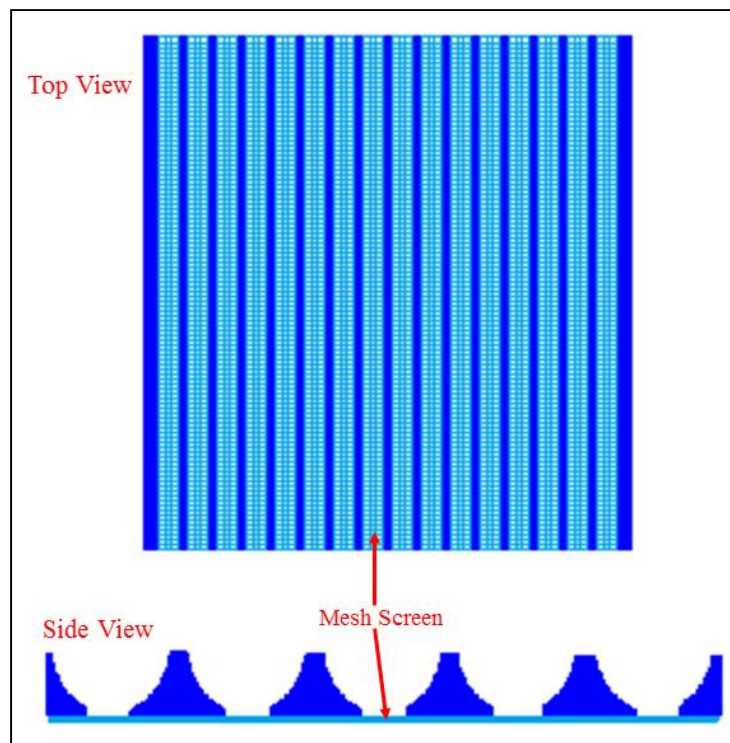


Figure 35: Grooved Device (Mesh Screen Element)

This device would consist of polycarbonate ridges (dark blue) adhered to a mesh platform (light blue). The mesh would function in much the same way as the drilled holes in a solid platform in that it would allow for suction to facilitate alignment and provide a method for anchoring the threads. This would decrease the difficulty of manufacturing the small holes in the bottom of the grooves.

Since the initial concept of alignment changed, the team needed to determine how to move from the gathering step to the aligning platform shown above in Figure 35. Therefore, the microthreads in the gear treads would be placed on top of the grooved platform and removed from the gears using a blade. Then using a shaker plate (Figure 36) the threads would automatically fall into the grooves.

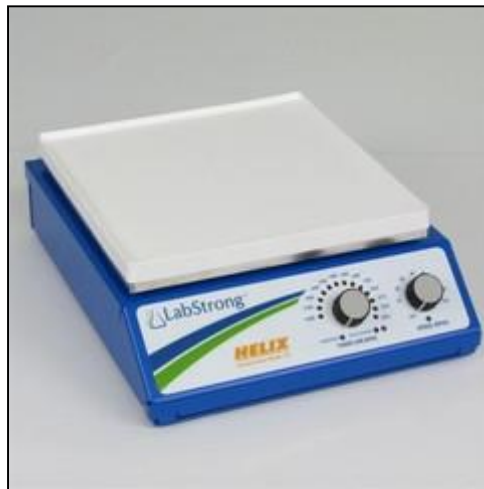


Figure 36: Laboratory Shaker Plate (<http://orbitalshakers.net/products/helix-150-150bl>)

Above, Figure 36 shows an example of a shaker plate that is commonly used in laboratories to stir liquids. The oscillating motion of the plate in combination with the flat platform design could help to promote better migration of the threads into the grooves while minimizing the amount of physical handling needed to achieve complete alignment.

4.3.3 Anchoring Threads – Suction Element

The concept of the suction element was one of the top three highest scoring elements in the design team's quantitative evaluation. Therefore, the team decided to pursue this idea, due to its ability to be incorporated with the grooved device design. The element would consist of a small box that would be able to be integrated with the flat grooved platform. A CAD model of the team's design can be seen below:

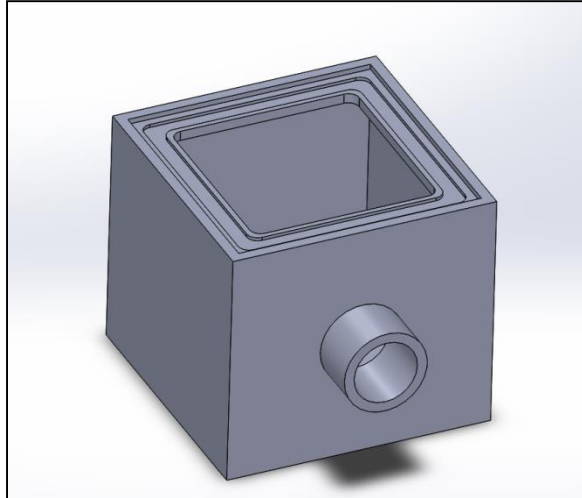


Figure 37: Suction element

On the side of the box would be a nozzle for a hose to be hooked up to for supplying the box with suction. The top of the box would be cut out just enough to securely fit the flat grooved platform. Additionally, it would incorporate a space for a rubber gasket to be laid in order to ensure an air tight fit of the platform. The CAD model in Figure 38 shows the integration of these two elements.

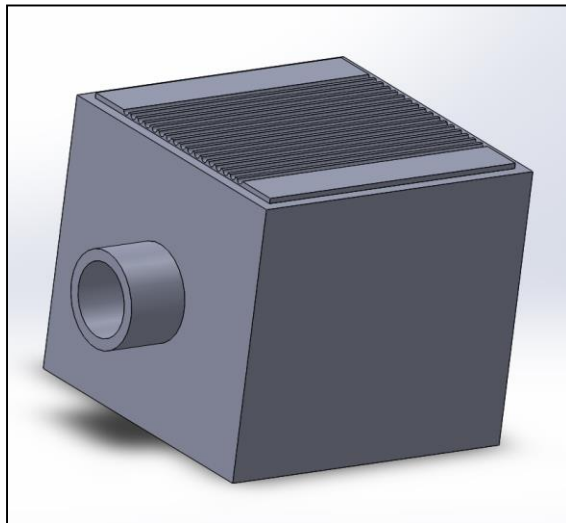


Figure 38: Suction element with grooved platform

4.3.4 Providing a Supportive Frame – Washer & Peg

The last function the device needs to accomplish is providing a supportive frame for the threads post-alignment. From the grooved platform, the team needed to carefully gather the aligned threads and place them into a platform that would allow for the addition of a hydrogel and also for a customizable orientation of the layer. With this in mind, the team developed clamps that would be used once the threads are aligned and would facilitate the transferability of the thread sheet. *Figure 39* shows this concept.

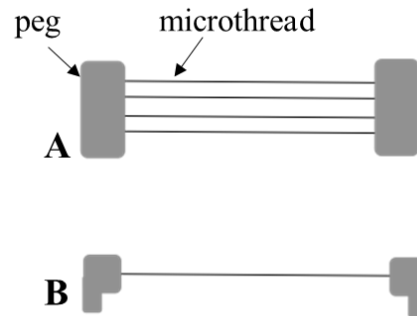


Figure 39: Pegs/clamps and aligned threads in (A) top view and (B) side view

These clamps would not only hold the threads but also have a shape that would allow them to be inserted inside of the holes of the washer and peg component (Figure 40). The design is composed of a circular platform with multiple anchors that allow for the customization of the sheet angle. The team decided to encompass the end goal of the client, which was to create a scaffold composed of multiple fibrin microthread layers. Therefore, this design allows for multiple layers to be positioned in multiple angles as the user desired. The design also allows for the addition of the gel on top of the thread layer post alignment.

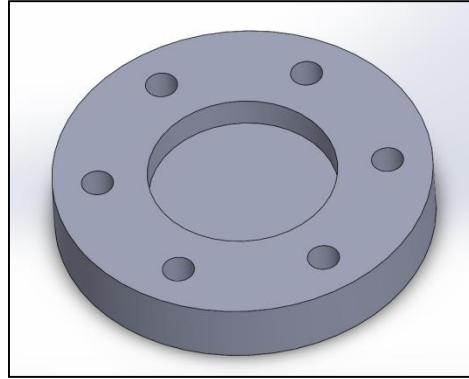


Figure 40: Washer and Peg Design

4.3.5 Final Modifications, Adjustments & Design Verification

After establishing the four main elements of the final design, the design team made additional modifications and adjustments before establishing the final scaffold fabrication system. These included solidification of the thread extrusion process and extruding hardware, modifications to the suction element design, replacement of the washer and peg system with a more intuitive, simplified adhesive framing system and the introduction of an additional framing unit to allow for the casting of gels.

Thread Extrusion Process and Hardware

The fabrication process of fibrin microthreads can be performed either manually or automated depending on the equipment available. For improved precision in the properties of the threads, an automated extrusion and stretching system is preferable. For this project, both manually produced and automated threads were utilized for the scaffolds. 73Figure 41 below shows the frame and motors of the automated biopolymer printer that fabricates automated fibrin microthreads.

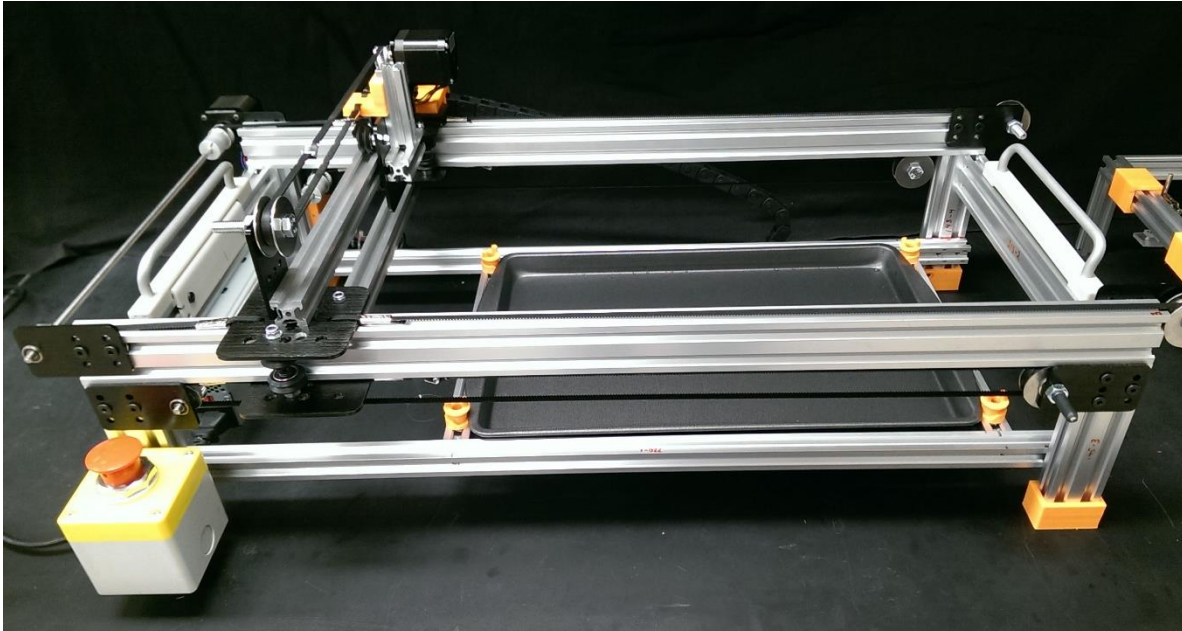


Figure 41: Automated Machine

The automated system works by first using a syringe pump for the coextrusion of fibrinogen and thrombin at a rate of 0.225 ml/min through polyethylene tubing that is then drawn into a HEPES Buffered Saline (HBS) bath at an automated rate on a customized frame as seen in Figure 42.

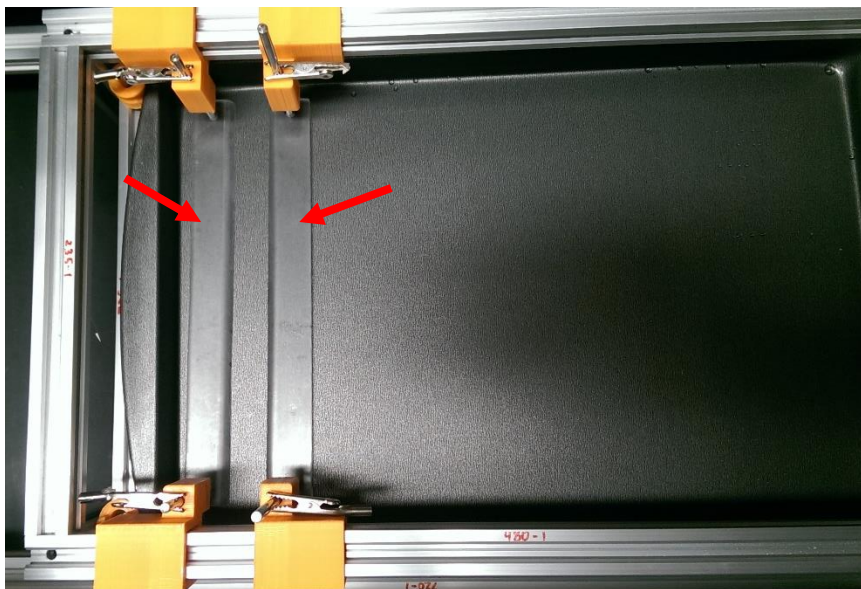


Figure 42: Frame for the coextrusion fibrin microthreads with red arrows pointing to anchors for ends of fibrin microthreads.

After ten minutes, the threads can be removed from the buffer for an intermediate dry step for 24 hours before returning to bath to be rehydrated and stretched to increase the tensile strength of the threads if desired. Once the threads are secured onto the bath frame manually, they stretched to 100%, 150% or 200% of their original length using an automated strain rate. These stretch percentages will tune the mechanical, structural and degradation properties of the microthreads as desired. Following stretching, the threads then be removed from the bath supported on the anchors shown in Figure 42. The threads are then allowed to dry for 24 hours, after which they can be removed from the frame and moved onto the next steps in the scaffold production.

Suction Box

In addition to solidifying the thread extrusion hardware for use in the scaffold fabrication system, the team also made modifications to their alignment component design due to manufacturing constraints. The desired groove diameter was initially 150 μm because the average thread diameter is 150 μm . However due to the team's resources, the smallest groove diameter possible was 250 μm . The smallest holes that were able to be fabricated within the grooves to secure the threads were 150 μm in diameter by utilizing the tapered edge of a drill bit. Any smaller drill bits would have a high probability of breaking and were not able to be used with the team's resources. These grooves were made within a cast acrylic sheet because of its ability to have clean cuts for the grooves without breaking during manufacture.

An initial prototype for proof of concept testing was fabricated with three 250 μm grooves, each with five holes for suction. The grooved top plate was then placed on a box that was fabricated from polyacrylamide. The diameter of the grooves in this prototype was 0.25mm (250 μm). Each groove contained five small holes, each with a diameter of 0.15mm (150 μm). The separation between each of these grooves was 0.50mm (500 μm). On one side of the box

was the addition of a fixture that allows for the attachment of tubing of an aspirator for application of a suctioning force. Two small plates are placed on top of the grooved top plate with four screws to secure in place, while also allowing the grooved top plate to be removed when necessary. This preliminary prototype can be seen below in *Figure 43*:

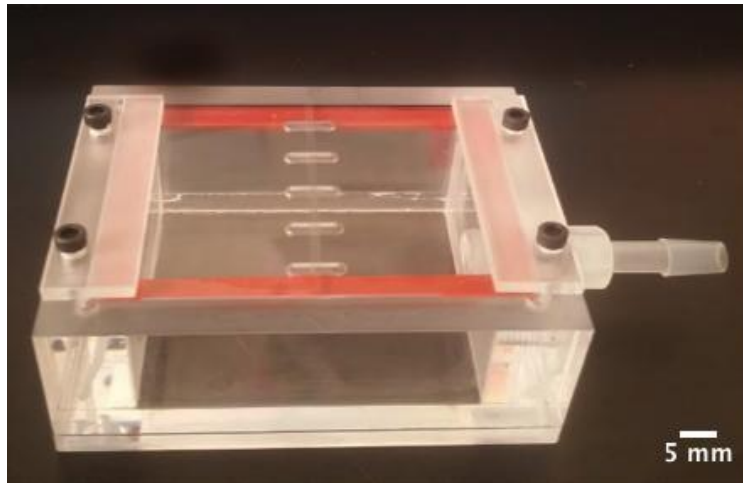


Figure 43: Preliminary Suction Box Prototype (3 grooves)

After successfully determining the ability of the suction box to hold threads in place in the desired spacings, a final prototype was created with 21 grooves. The number of grooves was chosen as the lower limit of the desired number of threads for scaffold creation (20 to 50 threads). With the dimensions used for this grooved plate, 21 grooves will create a scaffold of approximately 1.5cm. The client desired a scaffold that would be around 1 cm x 1 cm and so the lower limit of 21 threads was able to achieve these dimensions. Although, this did not meet the ideal thread separation due to size constraints and materials, this model allowed the team to create scaffolds as a close to the ideal as possible. This new plate can be seen below in Figure 44, with an image at 2X magnification shown in Figure 45.

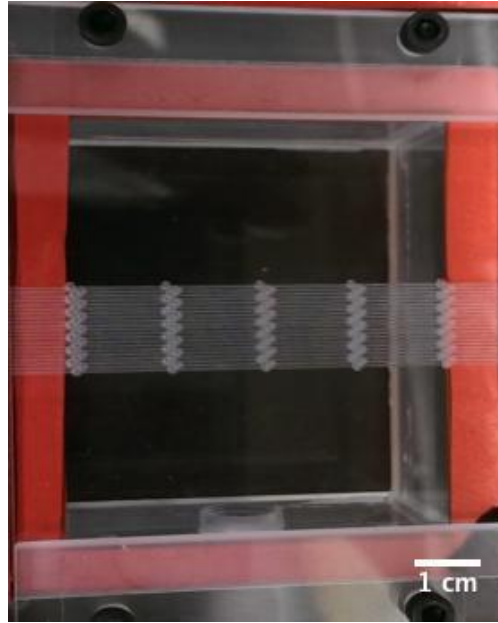


Figure 44: Final Suction Box Prototype (21 grooves)



Figure 45: Suction Box Plate at 2x Magnification

Overall, the suction box fulfilled the design team's device criteria, as it was a small box with an integrated flat grooved platform in order to align and secure the threads. The aim was for the team's designs for the automated scaffold production system to increase efficiency, precision and reproducibility of thread fabrication and allow for the advancement of this technology towards the regeneration of cardiac tissue following myocardial infarction. It will limit the steps needed, increase the amount of microthreads aligned per minute and protect the mechanical and structural integrity of the microthreads compared to the current manual method.

Adhesive Framing Mechanism

As mentioned in Section 4.3.4, one of the elements of the scaffold production system is a framing mechanism to support the threads once they are aligned. The team made further modifications to the peg and washer mechanism in an effort to decrease the number of steps and handling necessary. The simpler mechanism to frame the aligned threads is also simple and low cost. It consists of adhesive paper that sticks to the surface of the platform and the threads in order to maintain alignment and allow for transferability of the scaffold. This mechanism creates a smooth interface between the frame and the suction box that is easy for the user to handle. In addition, because of the simple nature of the adhesive frame, the structural integrity of the suction box platform wouldn't be compromised after each use. Additionally, the adhesive of the frame is gentle enough that it won't alter the mechanical properties of the threads from adhesion and removal from the threads. It can also be disposed after use, making it cost effective, quick and efficient to use. A diagram of this adhesive framing mechanism can be seen below in Figure 46.

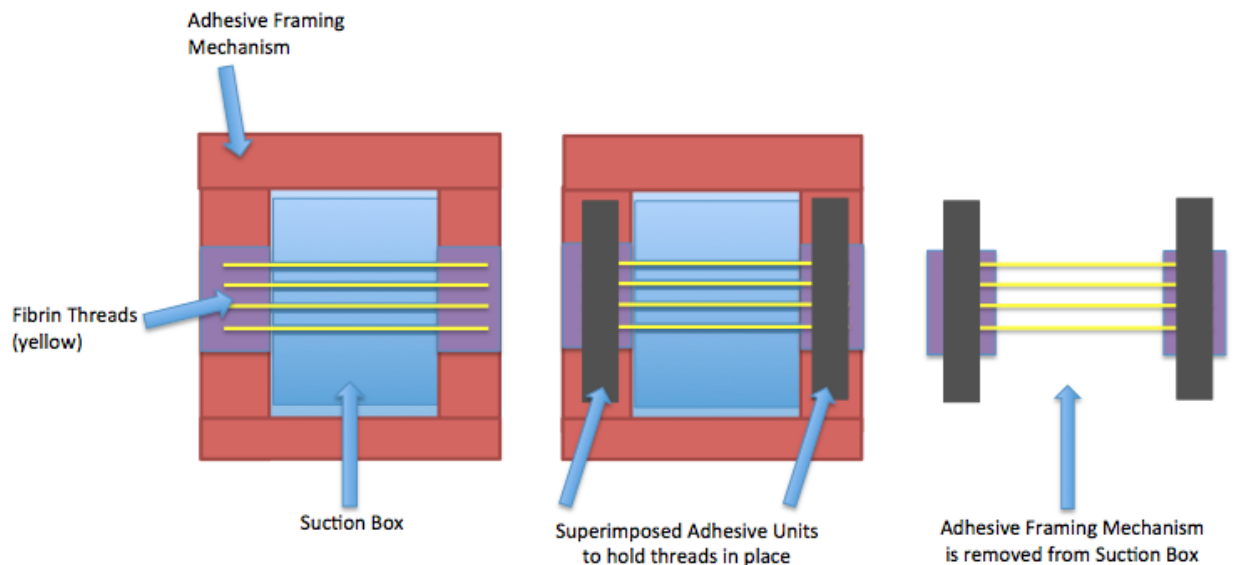


Figure 46: Steps for Use of the Adhesive Framing Mechanism

The frame has two main parts, the initial adhesive frame (represented in red and blue) and the superimposed adhesive units (represented in orange). The initial adhesive frame needs to be placed on the suction box (represented in red and blue) prior to the alignment of threads, for this is where the threads will be placed as they are being aligned. This initial frame is made preliminarily from four pieces of tape, folded over and attached with a small amount of adhesive exposed on either side of the grooves for the threads. Once this size-customizable adhesive paper is placed on the platform, the threads can be aligned. To secure the threads, an adhesive strip (represented in orange) of tape come into place on top of the threads to secure the alignment and allow for the threads to be transferred from the suction box.

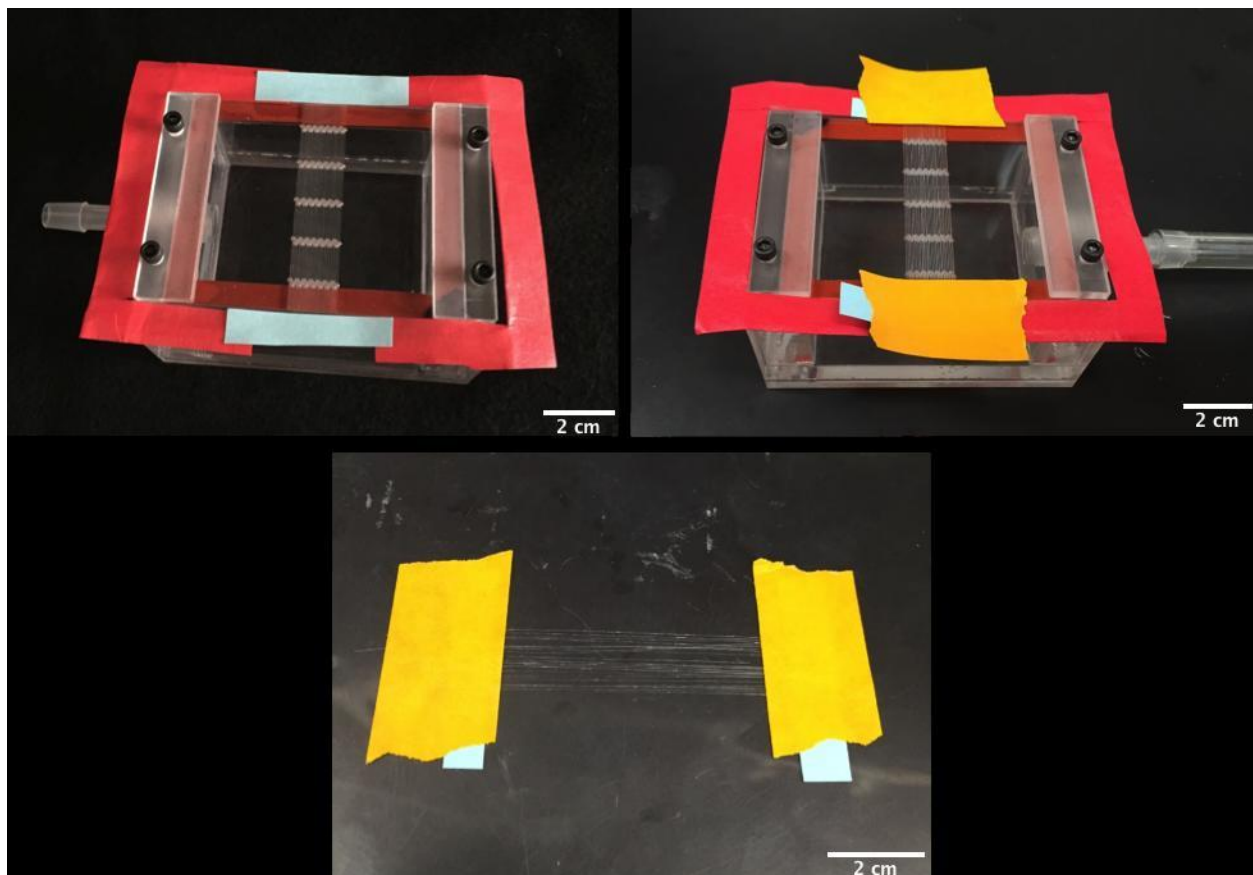


Figure 47: Adhesive Framing Mechanism Process with Alignment and Fibrin Thread Removal

Framing System (Gel Casting)

After the alignment of the threads and securing the alignment, a fibrinogen gel is added to encompass the threads before the threads are ready for testing. The team incorporated an additional framing process, which was established prior to their project and allows for the casting of the gel. Several of the components for this framing process were originally created for the client during a prior project and were ideal for the team's current process as well. The team was comfortable incorporating them into their system as it had been tested previously and the client felt comfortable and confident using it.

For each set of aligned threads on the suction box, there are two scaffolds created. A simplified schematic of this is shown in Figure 48 below. To begin the process of gel casting, the threads are aligned and removed from the suction box and are attached to a vellum paper frame (represented in grey) using silicone glue (represented as dark grey ovals). This vellum paper frame allows for the fibrinogen gel to be incorporated into the scaffold and provide a flexible frame. This is an easily made, customizable, and cheap frame that facilitates the transferring of the scaffold between different experiments. After the glue is dried, the scaffold can be removed from the adhesive frame for the addition of the fibrin gel.

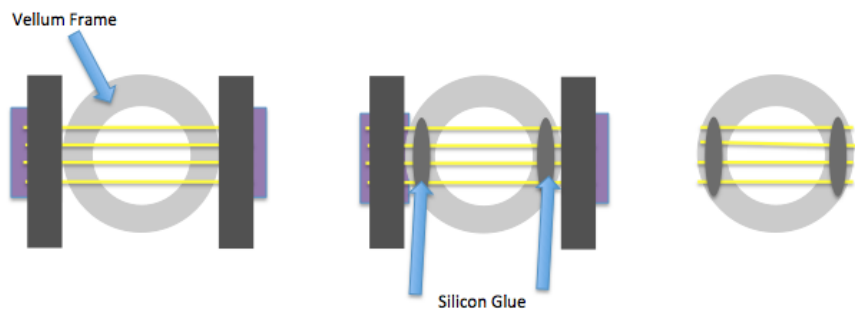


Figure 48: Steps to adhering threads to vellum paper frames for gel casting

The scaffolds are then moved to the frame for the addition of the gel. A plastic slide (the size of a glass microscope slide and made of black acetal plastic) is used to aid in better contrast between the threads and the background (Figure 49). The plastic has a thickness of 1mm, and was cut into 74 mm x 24 mm rectangular pieces using laser cutting. These plastic pieces also act as a form of stability for the casting of gels onto the threads, to be used in testing. The acetal plastic also allows for easy removal of the scaffold after the gel is added because the gel does not adhere to the plastic.

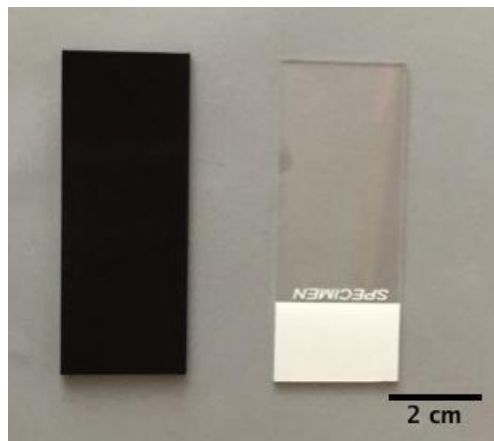


Figure 49: Part 1 of the framing system, compared to the slide

The second part consists of polydimethylsiloxane (PDMS) framing wells (Figure 50). To create the model for the PDMS layer, a CultureWell product is used (Figure 51). This acts as well divider that can be snapped onto a glass slide for cell culture and imaging use. The PDMS wells allow for defined sections to be created on the acetal plastic, as the gel casting of the scaffolds requires a seal to separate the wells.

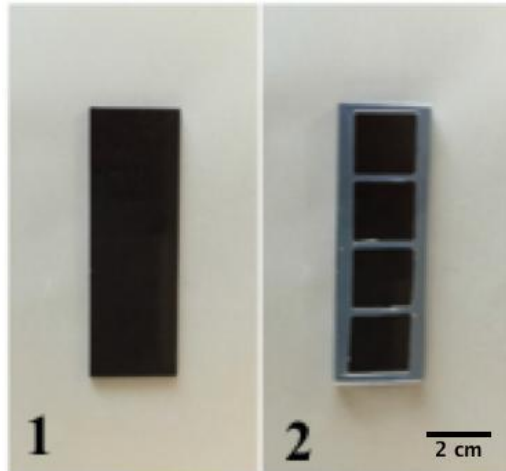


Figure 50: Series of images showing (1) black acetal plastic, (2) the PDMS wells

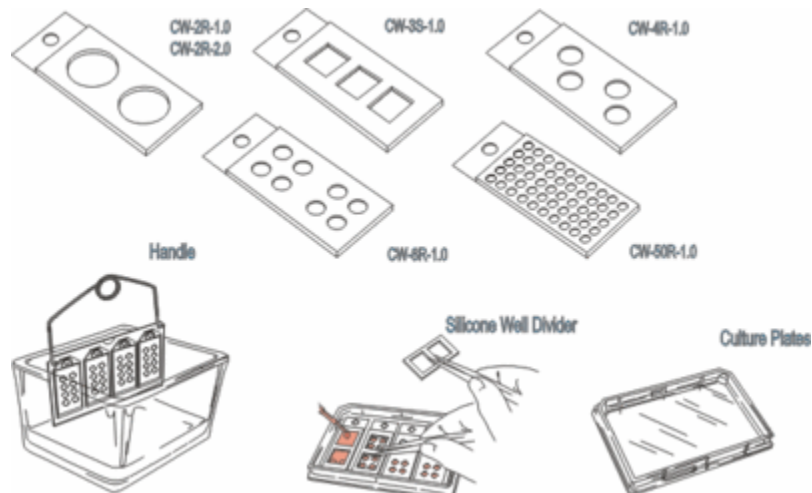


Figure 51: Examples of well dividers used by the past project groups to create the PDMS wells for the client (Lifetechnologies)

Once the threads are aligned these are secured on the vellum frames, they are transferred to the acetyl plastic surface seen above. The PDMS is sealed to this surface using vacuum grease to prevent any gel spill and finally the gels are casted. This entire framing procedure is user friendly and is able to be successfully integrated into the team’s scaffold creation process without major changes or problems.

The detail designs shown above for the automated scaffold production system will fabricate scaffolds that will reproducibly mimic the anisotropic fiber alignment of myocardium

structure. This process will increase efficiency and precision and allow for the advancement of this technology towards the regeneration of cardiac tissue following myocardial infarction. It will allow for a more superior fabrication method that facilitates the alignment of fibrin microthreads for the consistent creation of composite scaffolds, while maintaining the mechanical and structural integrity of the microthreads. It will additionally accommodate for manipulation of the threads and composites to allow for the validation of the reproducibility of the automated system to advance this platform technology.

4.3.6 Complete Design of Production System

The complete production system was aimed to limit steps, be easy to use and produce reproducible scaffolds that will mimic the aligned myocardial fiber structure. It includes three distinct steps for the creation of the composite scaffold. This process incorporates aligning, anchoring and providing a frame to support the threads for testing. The goal is to fabricate reproducible, customizable and aligned fibrin microthreads scaffolds. The following figures below outlines the process for the final conceptual design for the creation of these scaffolds.

Secure Alignment

This process begins by placing the threads into the grooves of the suction box that is shown in as a side view in Figure 52 that is attached to the tubing of an aspirator. The threads are held in place in the grooves from the negative pressure of the suction applied by the vacuum through the small holes in each groove. The suction within the grooves allows for the threads to be anchored into each groove, as the light weight and delicate nature of the microthreads makes it challenging to keep the threads in place, despite being in grooves.

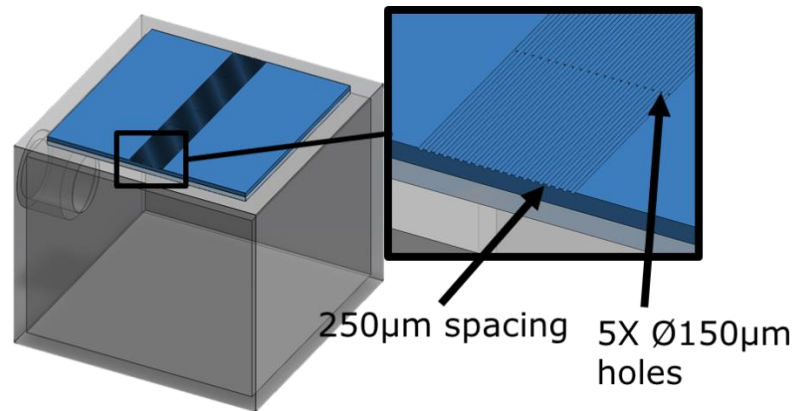


Figure 52: Suction box with zoomed in grooved platform

Once the desired number of threads are placed into the grooves, these are then secured onto the adhesive frame in alignment using tape on either end as shown in orange rectangles in Figure 53.

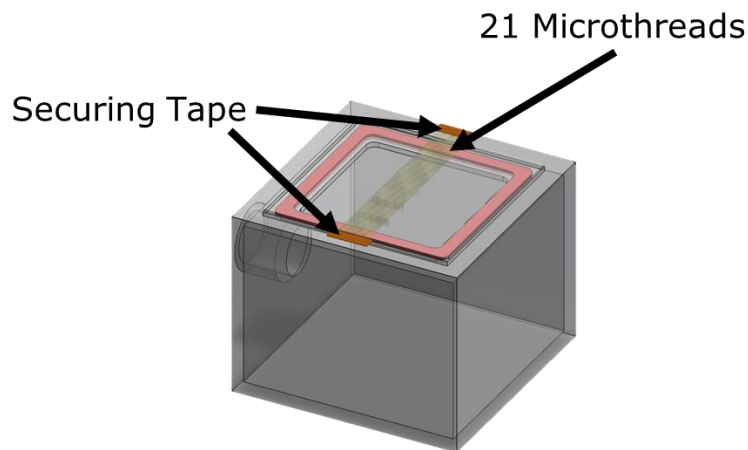


Figure 53: Suction box with secured threads in grooved platform

Adhere to Frame

Once the threads are aligned by using the suction box, they must be transferred onto a transferable frame. The threads are removed from the suction box and placed over a vellum paper frame as seen in Figure 54. The threads remain aligned as they are secured onto either side of the vellum frame using silicon glue to maintain alignment. After the glue dries for 24 hours the scaffold is then ready for the addition of the fibrin gel.

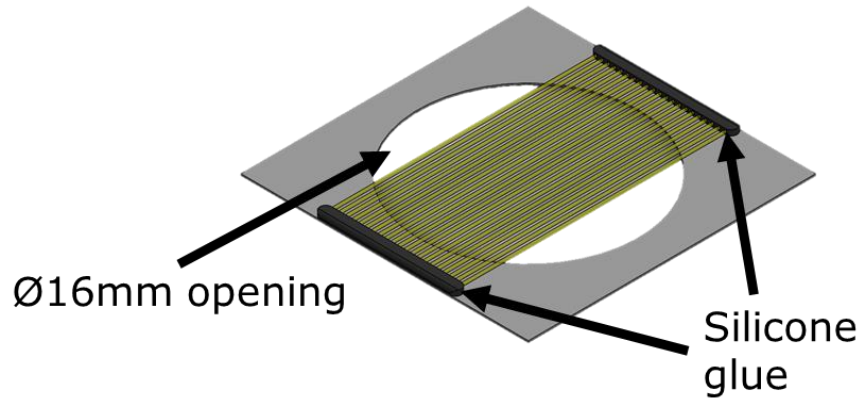


Figure 54: Microthreads adhered to vellum frame

Addition of Fibrin Gel

For the addition of the fibrinogen gel, the threads are placed onto a sheet of black acetal plastic and then are secured into place with a PDMS mold around the scaffold as shown in Figure 55.

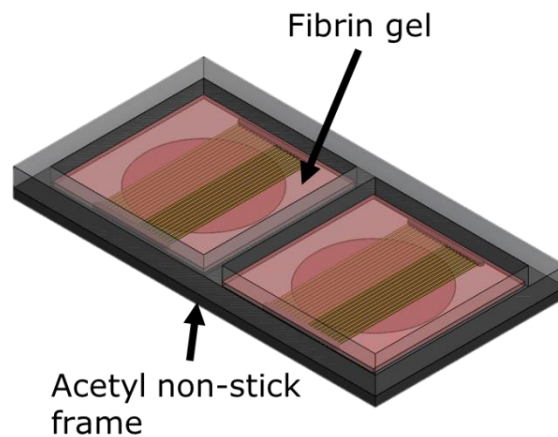


Figure 55: Frame for addition of fibrin gel

The fibrinogen gel is then added to the frames, shown as red in the figure. Once the gel is set after about 30 to 40 minutes, the scaffolds can be removed from the frame and manipulated for use in testing. The final composite scaffold combining the aligned fibrin microthreads within a fibrin gel is shown in Figure 56.

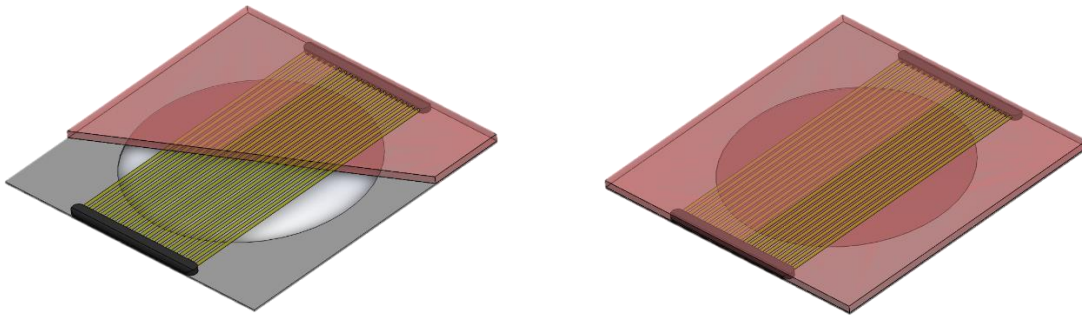


Figure 56: Final composite scaffold, with fibrin gel (red) and fibrin microthreads (yellow)

Through the described design process, the team was able to establish objectives, functions, specification and parameters that guided the development and modification of design elements into a final production system. This final system incorporates aligning, securing and providing a frame to support fibrin microthreads. This system was then tested to determine its ability to produce reproducibly aligned fibrin microthread composite scaffolds when compared to the current manual process.

5 Device Validation & Results

The team used several quantitative tests to validate the device and assess the completion of our objectives. By comparing the manual and automated scaffolds through multiple testing mechanisms the team was able to evaluate the desired objectives of the final production, most important of which was the validation of the reproducibility of the automated system. Two major testing methods were conducted:

- Alignment and Spacing Analysis
- Ball Burst Compression Testing

The goal of these validation methods was to determine if the new automated system produced scaffolds that achieved the outcomes outlined in the final client statement and met the primary objectives. The methods utilized to test for the system's ability to meet the primary objectives and their significance is detailed below in Table 36:

Primary Objective	Testing Methods	Data collected
Reproducibility	Measuring alignment	Width of spacing between threads, standard deviation of spacing, difference in thread alignment between users
	Customizable spacing	Width of spacing between threads with altered spacing (125 μ m and ~ 0 μ m)
	Ball burst testing	Maximum mechanical loading
Ease of Use and Transferability	Duration of fabrication	Timing of automated and manual scaffold fabrication
	Visualization of process	Any points of difficulty, amount of handling of threads, common areas of error

Mimic Myocardium Fiber Alignment	Measuring alignment	Width of spacing between threads, standard deviation of spacing, difference in thread alignment between users , comparison to native myocardium tissue
	Ball burst testing	Maximum mechanical loading, comparison to native myocardium tissue
Able to be manipulated	Failed tests due to frame	Number of failed tests due to frame failure

Table 36: Primary Objectives, Testing Methods and Significance of Data

As mentioned above, the most important objective of the project was for the final device design to be able to reproducibly construct composite scaffolds. Therefore, this became the main focus of device testing in order to provide the client with a reliable process that can be used for further research into this platform technology.

5.1 Comparison of Fabrication Processes

In order to assess qualitatively the process of scaffold fabrication, the team decided that they would compare observations acquired from visualizing the process that the client currently performs in order to align the threads and cast the gel. These observations were then compared to the automated process and helped the team to identify any points of difficulty that would need to be modified such as the amount of thread handling, common errors or failures and the duration of both the manual and automated fabrication processes. The observations gathered through this process are shown below:

Points of Difficulty

For both systems, the team combined personal observations of the process with information from the client to identify certain points of difficulty for both systems. A point of difficulty is anything determined by the team or the client to cause frustration, is not intuitive or

affects the resulting scaffold. This allowed the team to determine if any difficulties were solved with the automated system or additional ones arose. These are seen below in Table 37.

Scaffold	Manual	Automated
Observed Difficulties	<ul style="list-style-type: none"> Excessive handling of threads Long alignment process (>1hour) Breakage of threads 	<ul style="list-style-type: none"> Groove visualization Movement of threads during securing process

Table 37: Difficulties observed from manual and automated processes

This demonstrates that both processes have difficulties. However, the automated process is more optimal than the manual process, as the difficulties in the automated process have the potential to be improved upon, unlike those of the manual process. One of the most important difficulties that was overcome with the automated process, was the decrease of thread handling by the user.

Thread Handling

The structure of fibrin microthreads can be compromised with the application of mechanical force from handling with forceps. This can cause defects within the thread structure, resulting in breakage and/or reduced mechanical strength. Therefore, thread handling should be limited as much as possible except in regions of the thread that are not within the scaffold. Figure 57 below shows where the threads for the manual and automated system are handled during fabrication with forceps, scissor or tape.

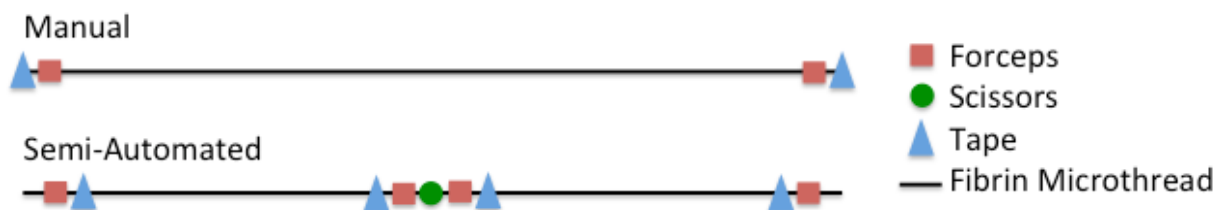


Figure 57: Thread handling for manual and automated processes by forceps, scissors and tape

There are four points of handling with the manual process and 9 with the automated process. The manual process has four handling points total with two handling points with forceps and two with tape. Therefore the thread's structural and mechanical integrity may be compromised in these regions. Of the nine handling points with the automated process, five handling points are not involved in the region used for the final scaffold because they are outside of the four tape points used to secure the threads. Therefore the region of the thread that is involved in the final scaffold is not compromised with the automated process by thread handling.

Overall it was found that the automated method provides scaffolds with fewer failures. This suggests that the team's new process is qualitative better than the manual method. It also proposes an improvement in the efficiency with which these scaffolds are currently built. To prove these improvements, in the next sections detail the quantitative testing performed.

5.2 Quantitative Testing

The team looked to quantitative testing to determine the mechanical and structural properties of the scaffolds from both fabrication systems. This allowed the team to analyze the automated scaffold in order to ensure that it met the primary objectives of the project. Of the objectives listed in Table 36, the main objectives tested quantitatively were the reproducibility of the scaffolds' properties and how successfully these could mimic myocardial fiber alignment.

The design team tested these two objectives by measuring the alignment of threads, customizing the spacing, and performing ball burst testing. These testing methods assessed the consistency in alignment of the threads (noting any variation between users), the accuracy when customizing the spacing and the maximum compressive load sustained. The testing variables examined were single layer scaffolds at a spacing distance of 250 μ m. The control variable was a single-layer manually aligned microthread scaffold. Statistical comparisons between manual and

automated scaffolds were drawn using tools that analyzed the variances and means of the data. Tests such as T-test, F-test and ANOVA were performed to examine the differences between manual and automated scaffolds.

5.2.1 Alignment and Spacing Validation

Understanding the separation between fibrin threads in scaffolds is important for assessing the alignment between the fibers and to validate the reproducibility of the method used to build the scaffold. The more aligned the scaffold is, the more fibers will be oriented in parallel to each other and the more constant separation the threads will have. We hypothesize that the manual fabrication of the scaffold will most likely show a non-parallel structure due to the low accuracy and precision of this method. Through the automated alignment platform, the team anticipates finding a higher percent of fibrin threads aligned in parallel to each other.

Validation of Testing Method

Previous work has been done to determine alignment of electrospun fibers using 2D Fast Fourier Transform (Ayres, 2008). Because of the increased spacing of the scaffolds compared to the electrospun fibers, this imaging process could not be utilized for our scaffolds. Instead, to measure the alignment and spacing between threads, the gaps between threads were measured on scaffolds made with the automated method and manual method. The protocol used to measure the separation distances between threads is shown in detail in *Appendix D – Alignment Testing Method Validation Procedure*. Using this method helped to determine whether the automated method improved the consistent spacing and alignment of the threads in the scaffolds. It can be assumed that if there is a high level of alignment and consistency, the standard deviation for the spacing will be lower than that of a non-aligned scaffold since there is less variability in the distances between threads. To validate this testing method, the team referred to the analysis of

alignment of electrospun scaffolds using 2D Fast Fourier Transform (FFT) (Ayres, 2008). The pictures below in Figure 58 are of spaghetti that was aligned in different angles to demonstrate how the 2D FFT can determine the alignment of the fibers in the study performed by Ayres. Three samples with multiple alignment arrangements (n=3) were chosen to validate the method of measuring the spacing in order to determine alignment. These three are shown below in Figure 58. Once the distances were measured between each thread in three parallel regions of the sample, the means and standard deviations of these measurements were calculated. Results from these calculations are shown in Table 37.

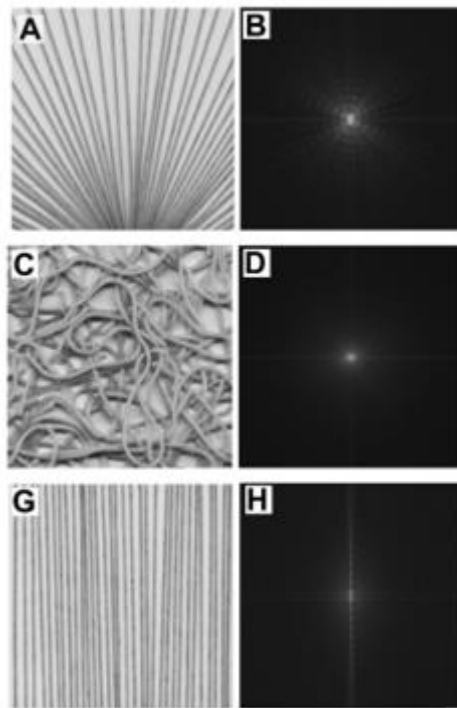


Figure 58: Pictures of aligned fibers for validation of space measuring method (Ayres, 2008).

Sample	Average Thread Separation (nm)	Standard Deviation
A	3.01	1.40
C	2.58	2.18
G	1.70	0.83

Table 38: Spacing method calculations used to validate alignment

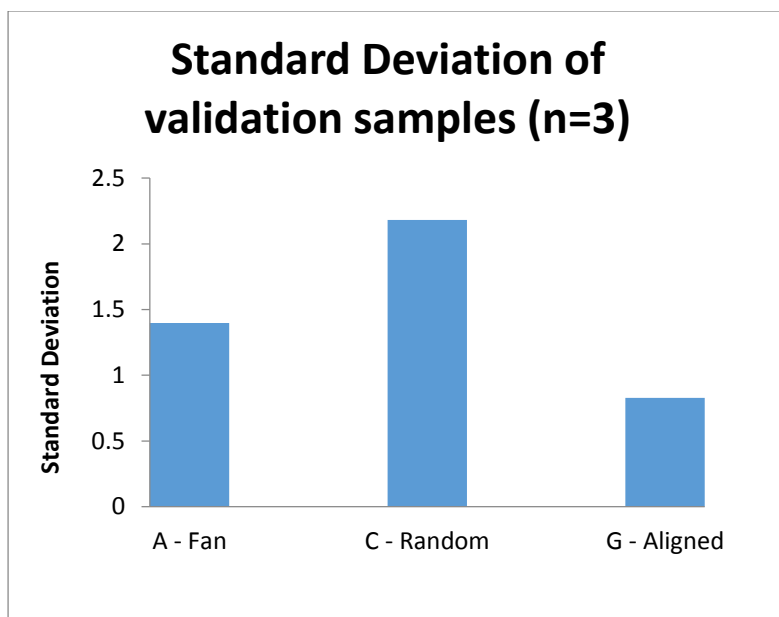


Figure 59: Results of validation testing of spacing method compared to FFT method.

Using the results summarized in Table 39, the standard deviation was compared visually and displayed in Figure 58. Each sample (n=3) displays a different standard deviation due to its variability in the alignment as seen in Figure 57. In order to assess whether or not these differences were significant an analysis of variance (ANOVA) single factor was performed at a confidence level of 95%. A significant difference between each sample was found for $p < 0.05$. Through ANOVA, the team was able to analyze the differences between groups and therefore, finding statistical differences between them.

The statistical difference found between these samples shows that the visual difference between the different pictures is reflected during the comparison of their standard deviation, which the most visually aligned picture having significantly lower standard deviation than the other two non-aligned pictures. This allows us to hypothesize that this similar pattern would be seen when measuring the fibrin microthread spacing in scaffolds. Preliminary analysis from the data collected suggested that when the automated scaffolds were compared to the manual scaffolds, there was a noticeably lower standard deviation, which could lead us to believe that

the threads within the automated scaffold have consistent spacing and therefore higher alignment. The complete set of results is explained in detail in the following sections.

Methods

After each user created scaffolds using both the manual and automated method, JPEG images were taken of each scaffold (n=38) using an upright brightfield microscope. From this pool the scaffolds were classified as either ‘automated’ (n=16) since these were constructed using the automated system, or ‘manual’ (n=22) because these were constructed manually. A total of nine images were taken of each scaffold, three images per row and per column of the whole scaffold as seen below in Figure 60. The rectangles shown in red represent the nine images taken of each scaffold that were then used for analysis of the alignment and spacing of the threads.

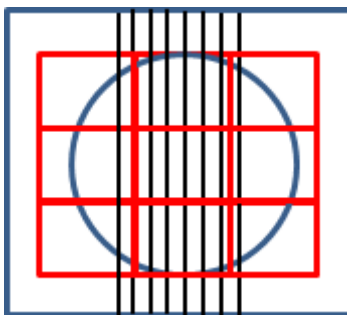


Figure 60: Frames used for scaffold alignment analysis

To analyze these images, the NIH software Image J was used to measure the distances between threads in each frame. This was accomplished by measuring the thread separation in three parallel regions of each frame. A visual explanation of how to measure the distances between threads is seen in Figure 61. The complete protocol used to measure the distances between threads is shown in *Appendix E – Alignment Testing Protocol*. These measurements were then analyzed using multiple statistical tools described in detail in the next section.

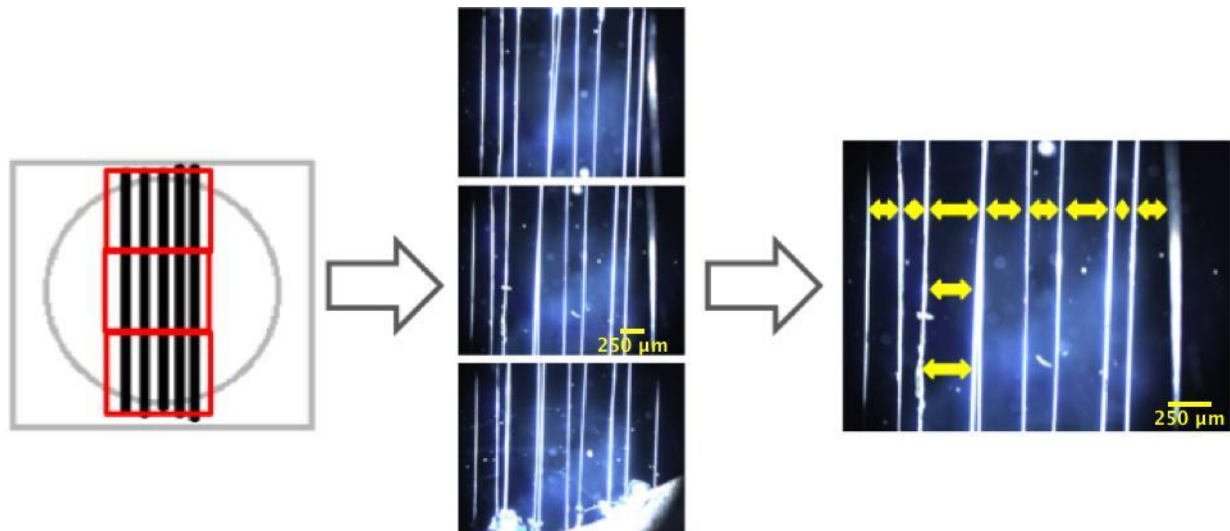


Figure 61: Method for measuring spacing between threads

Statistical Analysis

Multiple statistical analysis tools were used to analyze the alignment between threads in both manual and automated scaffolds. All these analysis were completed at a 95% confidence interval. In the next paragraphs the tools used for this measuring alignment are explained more in detail.

An F-test was used to determine the differences between the variances of the threads separation in both manual and automated methods. A higher variance and higher standard deviation means that the measurements collected are more spread out. Therefore, if the data collected from the manual scaffolds are more spread out compared to the automated system these would present a higher standard deviation. With this in mind, a significant difference in the variance and standard deviation would suggest that the method with highest variability would have lower precision.

Additionally, a two-sample t-test for unequal variances was used to compare the thread gap measurements between automated and manual scaffolds. A t-test allows comparing two sets of data and analyzing if these sets are significantly different from each other. A Welch t-test was used in this study since the variances of each set are not assumed to be equal and the sample sizes differ.

Finally, an analysis of variance (ANOVA) was performed to assess the variability between users. ANOVA allows for the analysis of the differences between group means. In this study a 2-factor ANOVA was used to compare the manual and automated method with the average thread separation in scaffolds according to each user. The test assumes independency of the data, which the data measured in this study presents.

Results

Visually, automated scaffolds looked very different from the manually constructed ones. Figure 62 shows the discrepancy of the frequency distribution between the thread spacing measurements in two scaffolds, one from each sample type randomly chosen from the sampling pool (n=38).

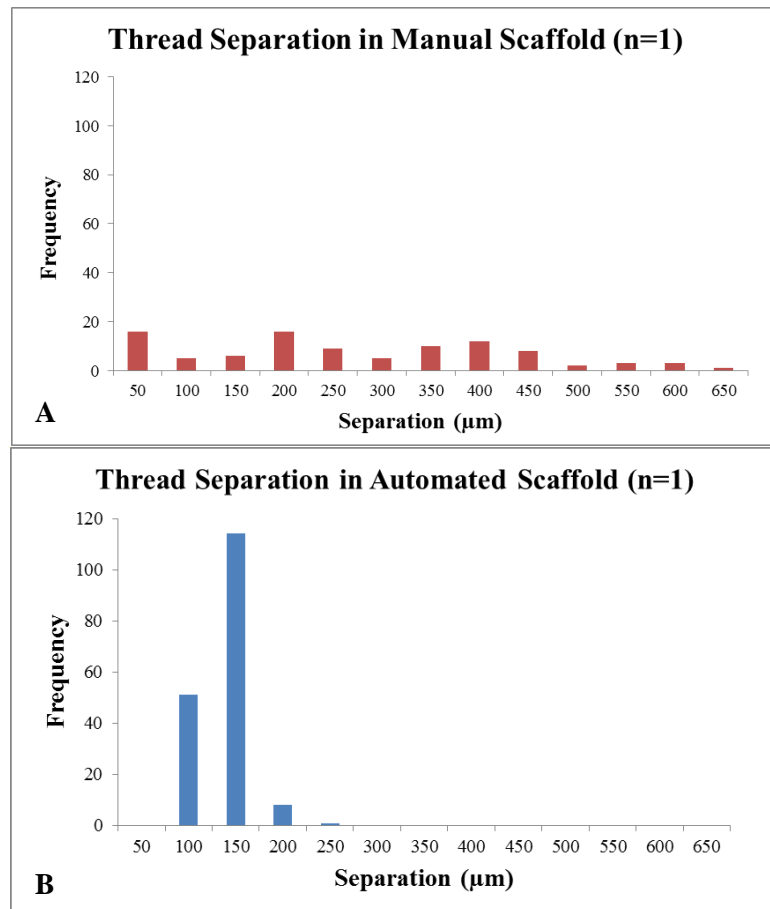


Figure 62: (A) Thread separation in manual scaffold (n=1). (B) Thread separation in automated scaffold (n=1).

In the figures shown above a visual difference can be seen between these two scaffolds. For instance, a more consistent distribution can be seen through the alignment of the automated scaffold. The automated method shows an average thread separation of 111.78 μm and a standard deviation of 21.23 μm . In contrast, the manual scaffold has an average separation of 247.39 μm and a standard deviation of 157.37 μm . However, in order to validate a significant difference between the thread separation in each method all samples had to be considered. Results are explained in the following paragraphs.

Using the spacing measurements from all samples, the following histograms were generated, shown below in Figure 63. This figure shows the thread separation frequency in scaffolds created using both the automated and manual methods.

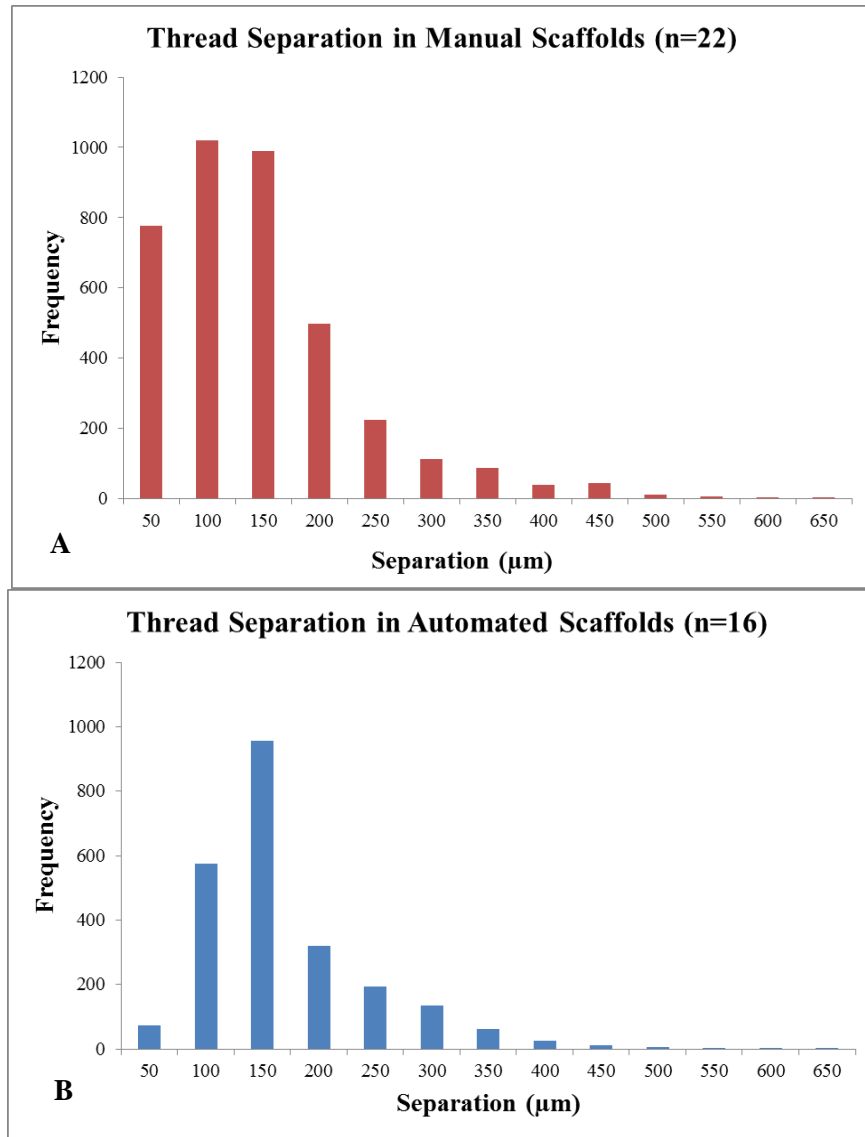


Figure 63: (A) Thread separation in manual scaffolds (n=22) (B) Thread separation in automated scaffolds (n=16)

Through the histograms shown in Figure 63, the highest frequency of thread separation in the manual system (Figure 63A) ranges between 50 μm to 150 μm . However, the automated method (Figure 63B) presents more accurate and concise results regarding the separation of threads since the highest frequency of thread separation lies between 100 μm and 150 μm , which represents a shorter range of variability compared to the manual method.

Additionally, the standard deviation between the average separation of threads using the manual and automated methods were calculated. The average thread separation of the automated

scaffolds was 145.63 μm , compared to the manual scaffolds separation, which was 127.03 μm .

Figure 64 shows the average thread separation using the manual and automated method.

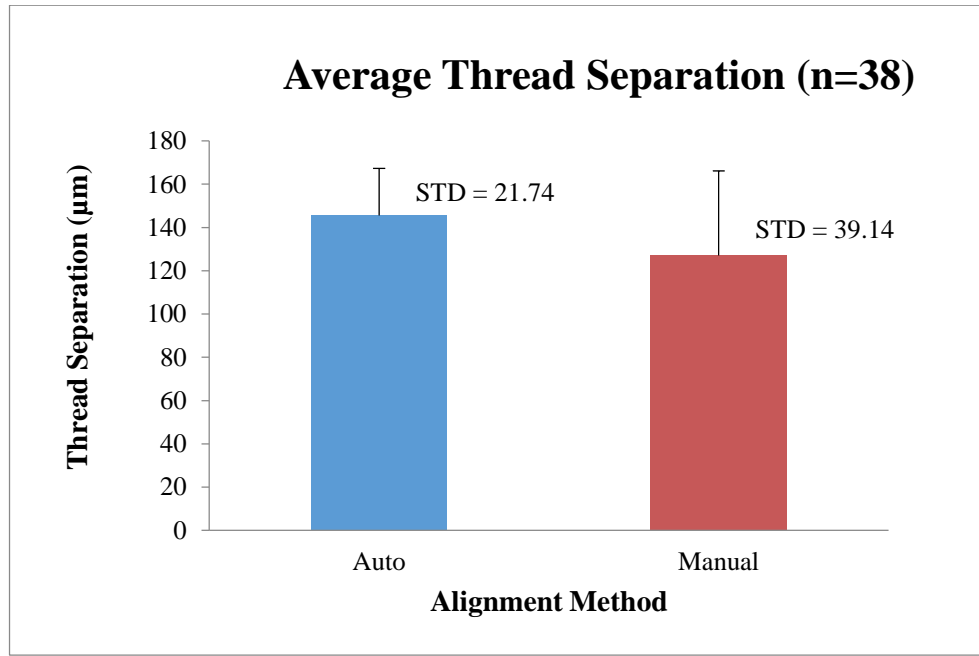


Figure 64: Average thread separation for (n=38)

As seen above in Figure 64, although the thread separation is smaller using the manual method, the standard deviation is larger. For instance, the standard deviation of the automated method was calculated to be 21.74 μm compared to 39.14 μm separation found in the manual method sample group. Using an F-test for variances with a p-value of 0.05, the variances of the average thread separation were found to be statistically different ($p=0.012$). Additionally, using a two-sample t-test for unequal variances with p-value of 0.05, a significant statistical difference was found between the automated and manual scaffolds ($p=0.035$).

Furthermore, an analysis to compare the variability in thread alignment between different users was also performed. Figure 65 below shows the average thread separation between different users using both the automated and manual method to construct the scaffolds.

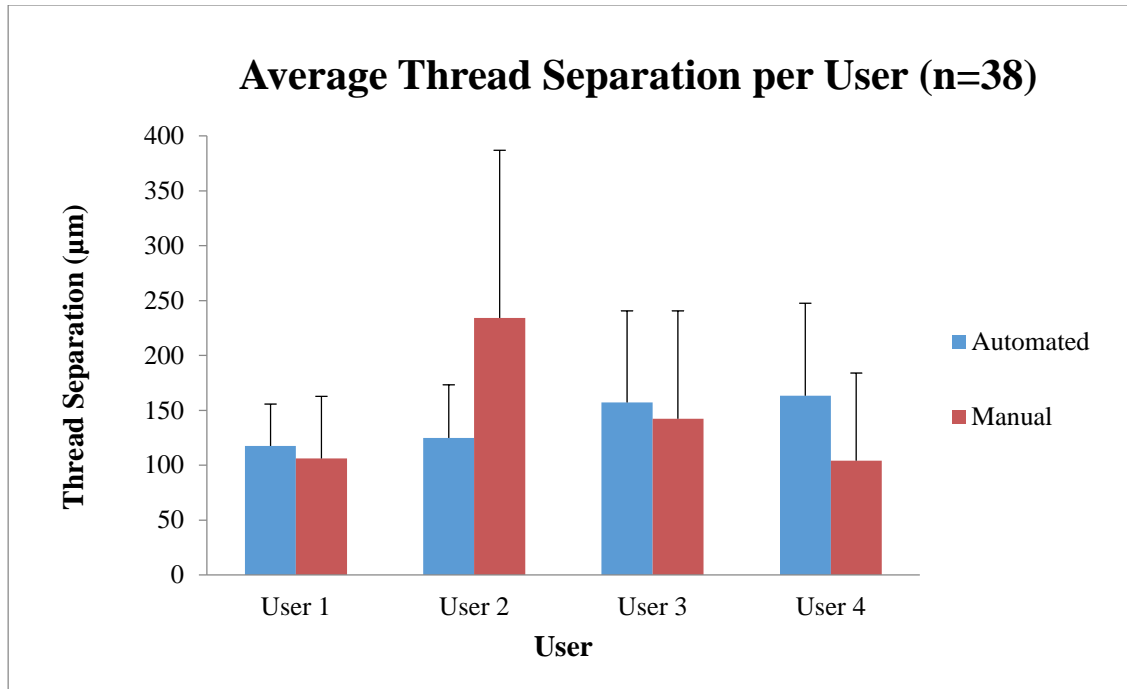


Figure 65: Average thread separation between users for (n=38)

An analysis of variance (ANOVA) was performed to assess the variability between users. Using a p-value of 0.05 no significant difference in thread separation measurements was found between users ($p=0.65$). Therefore, the method is not user-dependent and the thread separation is only dependent of the method used to align them. The complete analysis of this data and the full set of measurements in the alignment testing can be found in *Appendix E – Alignment Testing Protocol*. Furthermore, in the following chapter a more thorough analysis of the data presented above will be explained.

5.2.2 Ball Burst Testing

The next form of testing the design team performed was ball burst compression testing, which involves driving a spherical probe through a clamped sample to test for the maximum load the sample can sustain prior to failure. An example of a burst testing fixture for the testing of different types of biomaterials can be seen below in Figure 66:



Figure 66: Ball Burst Testing Fixture (Washington University School of Medicine in St. Louis)

The testing methods and parameters the team used were based off of ISO 7198: Cardiovascular Implants—Tubular Vascular Prostheses (AAMI, 2001), which is a modified version of the standard ASTM D3787: Bursting Strength of Textiles—Constant-Rate-of-Traverse (CRT) Ball Burst Test (ASTM, 2011). The team decided to follow the testing methods outlined in this particular standard(s), as they were cited for use in testing a variety of other biological tissues such as urinary bladder matrix (UBM), small intestinal submucosa (SIS) and cardiac extracellular matrix (ECM) (Cloonan et al., 2011; Wainwright et al., 2010). The team investigated literature that performed this type of testing on similar biological scaffolds in order to determine appropriate testing parameters. A group at the University of Limerick in Ireland utilized ball burst as a testing method for acellular porcine UBM and SIS ECM. They used a spherical probe with a diameter of 25.4mm and a rate of traverse of 25.4mm/min (Cloonan et al., 2011). This rate was also cited as being used for ball burst testing of multilaminated ECM scaffolds (Freytes et al., 2004). These scaffolds were similarly derived from porcine UBM and SIS, as well as from urinary bladder submucosa (UBS). A third study, mechanically tested cardiac ECM, also using a 25.4mm/min rate of traverse to test their samples (Wainwright et al., 2010).

Having an understanding of the standard test parameters needed to perform ball burst testing on their samples, the design team investigated what types of metrics would be acquired from this form of testing. The raw data from this test would include time (s), load (N) and extension (mm). From this, the maximum load sustained by each sample could additionally be calculated. The goal of this testing was to ensure that each scaffold created with the automated system had consistent mechanical properties, to achieve reproducibility. The team hypothesized that the manual scaffolds will have more variability in the maximum loads when compared to the loads sustained by the automated scaffolds. This will validate the reproducibility of the automated scaffold fabrication system.

Proof of Concept Testing

The team next created a custom testing set-up that met the criteria outlined above in order to begin testing their scaffolds. Not having access to a ball burst testing compression frame, they purchased several different materials at Home Depot in order to create their own. Using a bolt, cap nut, metal washers, nylon washers and small PVC pipe fittings, the team made a custom set-up on an Instron Universal Testing System. This set-up can be seen below in Figure 67:



Figure 67: Ball Burst Testing Set-Up

To test a sample, the bolt with the cap nut, which mimicked the spherical probe of a standard ball burst compression fixture, would be brought down to the surface of the sample. Next, a standard compression test would be run using a rate of extension of 25.4mm/min as cited above. The sample would be loaded to failure and the resulting load vs. extension data could be observed to determine the maximum load sustained by the sample. A detailed explanation of the testing set-up and procedures as well as details of all the necessary components can be found in *Appendix G - Ball Burst Compression Testing Procedure*. For proof of concept testing, a moist piece of notebook paper was used to simulate a scaffold sample, the result of which can be seen below in Figure 68:

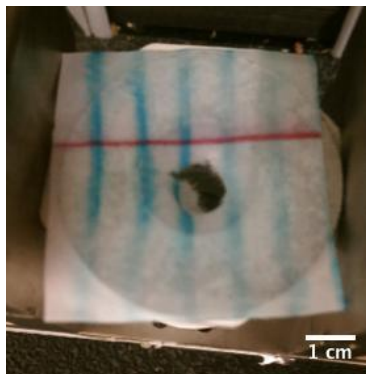


Figure 68: Burst to Failure of Moist Paper

Additionally, the load vs. extension data from this test was graphed using MatLab software and the result of this can be seen below in Figure 69:

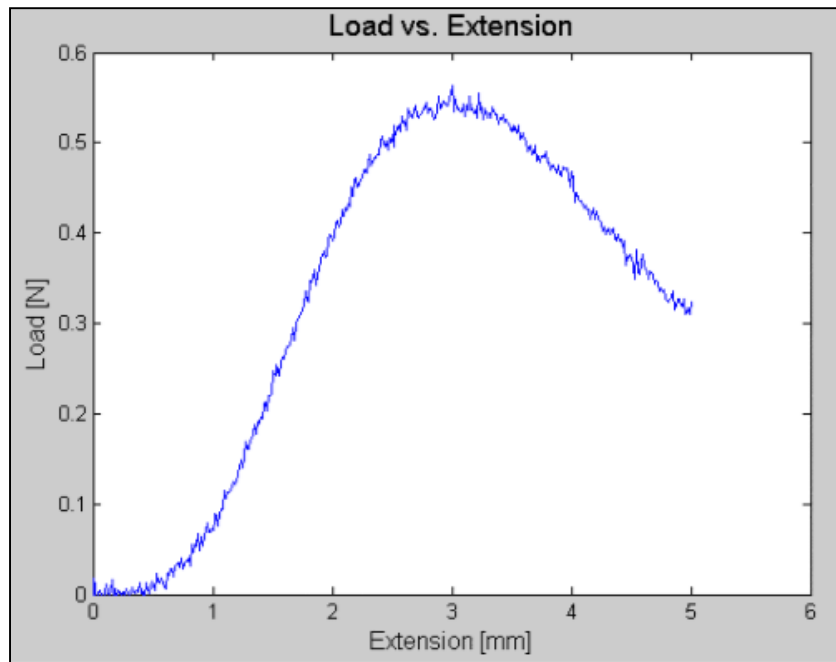


Figure 69: Ball Burst Load vs. Extension of Moist Paper

In achieving a load vs. extension curve similar to that seen in the test procedure section of ISO 7198 (AAMI, 2001), the team was satisfied with the result of their mock test and thus determined that their set-up would be a feasible method for testing the strength of their scaffolds. Before the team could begin testing their own samples, however, they first needed to validate their testing method.

Validation of Testing Methods

In order to validate their testing set-up, the team decided to perform the ball burst test on samples of gelatin, which would be similar to the consistency of their scaffolds (gel-thread composite). This validation would determine if the team could achieve different load values for different consistency gel samples. If the testing method could measure these differences, the method would be valid for testing the loads sustained by the team's different scaffold sample types. By assessing differences in variability of loading for each sample group, the team would be able to validate the reproducibility of their automated fabrication system.

The team utilized Knox Original Unflavored Gelatine to make their samples. For this validation test, they created two batches of four different gelatin sample groups (batch #1 was left to set for longer). A summary of these different test groups can be seen below in Table 39:

Test Group	Environment	Concentration
Test Group #1 (Fridge Concentrated – FC)	Fridge	1.25 grams gelatin powder/10mL water
Test Group #2 (Fridge Regular – FR)	Fridge	0.625 grams gelatin powder/10mL water
Test Group #3 (Room Concentrated – RC)	Room	1.25 grams gelatin powder/10mL water
Test Group #4 (Room Regular – RR)	Room	0.625 grams gelatin powder/10mL water

Table 39: Validation of Testing Method Test Groups

The design team predicted that because the more concentrated samples are likely more elastic (higher gelatin content), they should be able to sustain a higher load than the less concentrated samples. In addition, the samples in the room will likely dry out more than the samples in the fridge, again making them more elastic and able to sustain a higher load. Lastly, the samples from batch #1 had a longer period of time to solidify, therefore the team also predicted that they would be able to sustain a higher load. If the testing set-up could show a statistically significant ($p < 0.05$) maximum load difference between concentrated vs. regular concentration, fridge vs. room and/or batch #1 vs. batch #2 using a paired t-test, then the testing set-up could be considered valid.

Validation of Testing Methods Process

The team made two batches of samples. The batches were made 24 hours apart; therefore at the time of testing the first batch had been left to set longer. The first batch set just over 48 hours before testing and the second batch had set for approximately 24 hours. The first batch was poured into rectangular vessels (9cm x 4.5cm x 0.6cm) made of tinfoil and the second batch was poured into plastic Tupperware containers (which prevented the issue of leaking). Batch #1

had a sample size of $n=2$ for each group. Batch #2 had a sample size of $n=4$ for each group. The preparation of these samples, however, was the same. Details of these preparation methods can be found in *Appendix F – Ball Burst Testing Method Validation Procedure* (for one out of every four samples per group in the second batch, a piece of vellum paper was used instead of tissue for reinforcement and this paper was placed on the surface for all sample types).

After the gels had set for the times specified above, a scalpel was used to cut them to size and remove them from their respective containers (Figure 70).

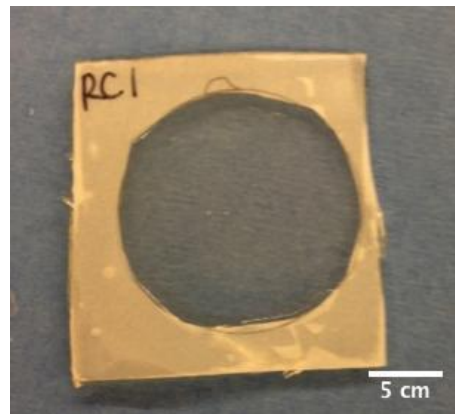


Figure 70: Cut-to-Size Sample

They were then testing utilizing the ball burst testing procedure referenced above. The full testing procedure can be seen in *Appendix G - Ball Burst Compression Testing Procedure*.

Validation of Test Method Results

In investigating the statistical significance in maximum load sustained between concentrated vs. regular concentration, fridge vs. room and batch #1 vs. batch #2, the team was able to identify a statistical significance batch #1 and batch #2. This signified that their testing method was indeed valid.

In comparing the fridge samples versus the room samples, the team wasn't able to identify a statistically significant difference. They compared both the fridge and room samples within the first batch as well as the fridge and room samples in the second batch. The load

versus extension of the concentrated batch #1 comparing the samples left in the room versus the samples left in the fridge can be seen below in Figure 71 (n=2 per each group).

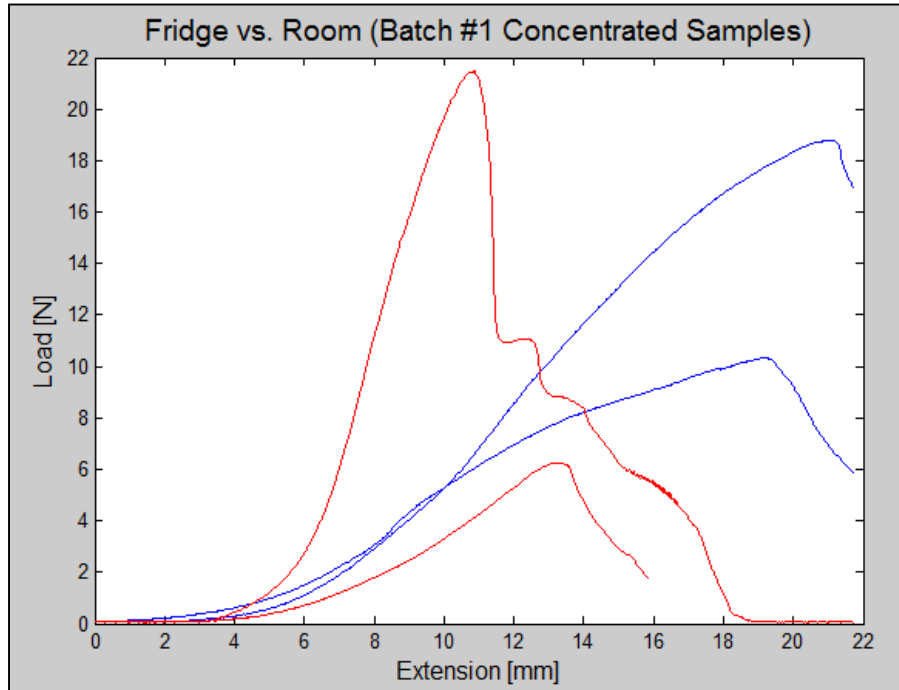


Figure 71: Load vs. Extension of Batch #1 Concentrated Samples (Fridge (blue) vs. Room (red))

The samples left in the fridge are represented by the blue curves and the samples from the room are represented by the red curves. While there is a slight difference in the maximum loads sustained by the two groups, the difference was not found to be statistically significant ($p=0.964$). Additionally, concentrated samples from batch #2 from both the fridge and room were compared. A graph of load vs. extension of these samples can be seen below in Figure 72 (n=4 per each group).

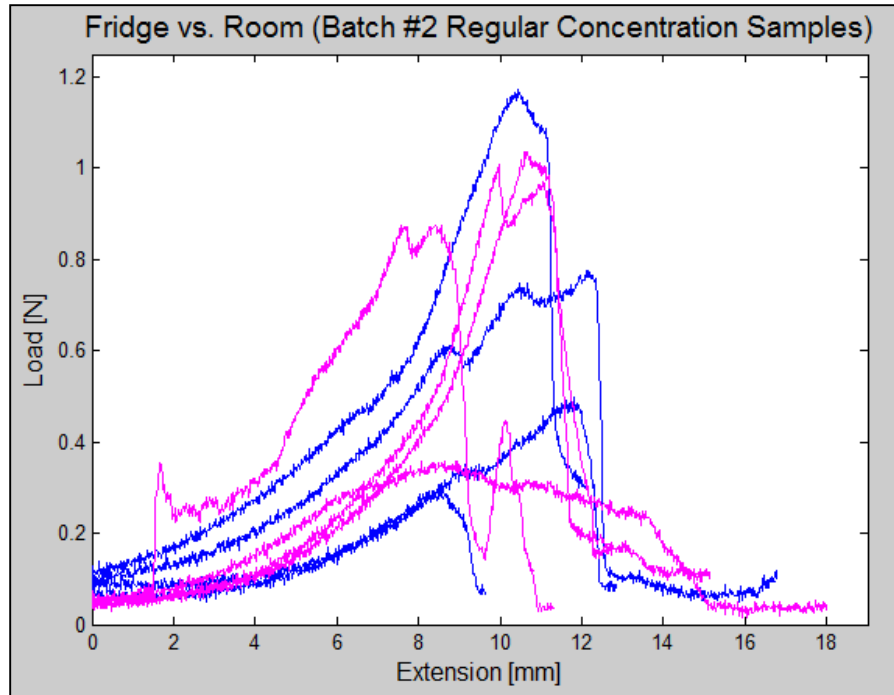


Figure 72: Load vs. Extension of Batch #2 Regular Samples (Fridge (blue) vs. Room (magenta))

The magenta curves represent the samples from the room and the blue curves represent the samples from the fridge. From the graph above, it can be seen that there doesn't appear to be a difference in the maximum loads sustained by the samples from the fridge and samples from the room. Through statistical analysis this was further confirmed by a p-value of 0.718.

Next, the group compared the concentrated vs. regular samples from both batches. Below in Figure 73 is the load vs. extension of these samples (n=8 per each group).

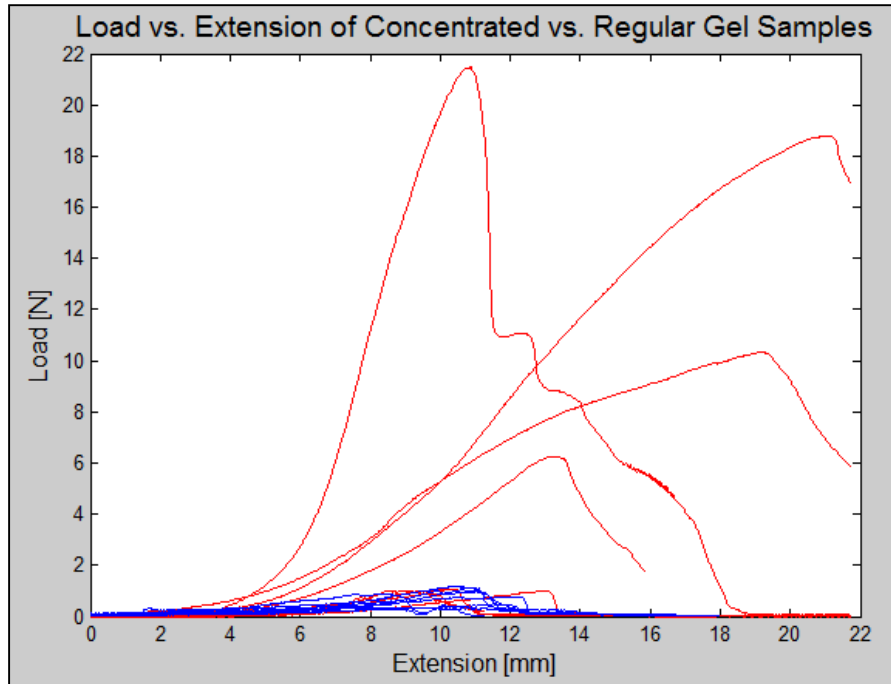


Figure 73: Load vs. Extension of Concentrated (red) & Regular (blue) Samples from both Batches

The red curves above represent the concentrated gel samples and the blue curves represent the regular samples. While a distinct difference in load sustained can be seen between the two groups from this graph, the difference wasn't quite statistically significant ($p=0.059$). This being said, the difference was more significant than the difference between the fridge and room samples.

While a statistically significant difference wasn't found between the fridge and room samples or the concentrated and regular gel samples, a statistically significant difference was found between concentrated samples from batch #1 and batch #2. Figure 74 below shows the difference between the failures of a sample from batch #1 versus batch #2.

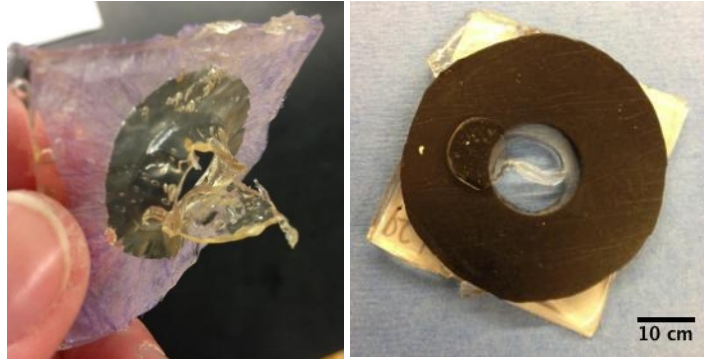


Figure 74: Failure of Batch #1 (Left) vs. Batch #2 (Right)

From this picture, it can be observed that the failure of batch #2 was very uniform, while when the batch #1 sample failed it stretched out before completely failing. Because the samples from batch #1 had longer to set, many of them were stiffer and were therefore able to sustain a higher load for a longer period of time before failure. The load vs. extension plot of these two samples can be seen below in Figure 75 (n=4 per each group), which further supports this observation.

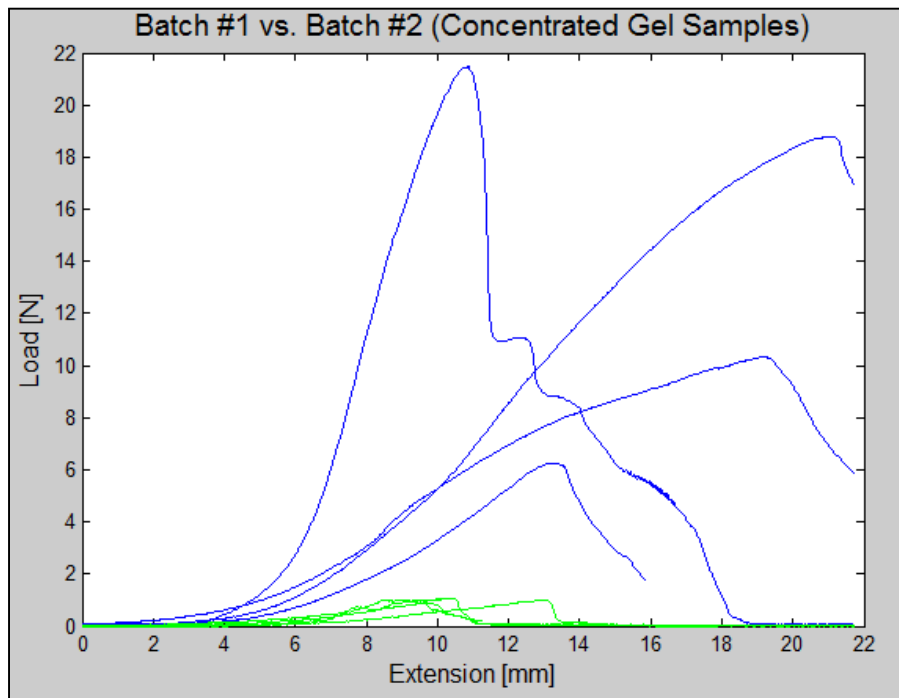


Figure 75: Load vs. Extension of Batch #1 (blue) and Batch #2 (green) (Concentrated Samples)

The blue curves represent the concentrated samples from batch #1 and the green curves represent the samples from batch #2. This graph depicts a clear difference between the concentrated

samples from batch #1 and batch #2. Through statistical analysis, this difference was found to be statistically significant ($p=0.033$).

Due to a slight variance in thickness between samples, the design team did a statistical analysis of sample thickness to determine if the difference in thickness between each of compared groups was statistically significant. These measurements were taken using a set of calipers and this analysis would establish if thickness variation caused the difference in max load readings between tested groups versus the controlled conditions. From this analysis it was found that there was no statistical difference between the thicknesses of the batch #2 regular concentration fridge samples and room samples ($p=0.655$). Similarly, there was no statistical difference between the batch #1 concentrated fridge samples and room samples ($p=0.406$). The team did, however, find a statistical difference between the thicknesses of the concentrated and regular samples ($p=0.034$), but upon averaging the thicknesses between the two (concentrated average=2.54mm; regular concentration average=3.22mm), it was determined that this had no influence on the higher load readings displayed by the concentrated samples, as their average thickness was smaller. Lastly, the difference in thickness between batch #1 and batch #2 was not statistically significant ($p=0.701$). Based on these findings, the team was comfortable in concluding that the variance of thickness did not have a significant effect on the results of their validation testing.

The goal of this validation testing was to determine if the testing method established by the design team could depict a statistical difference for different types of gels. Between the second groups, statistical significance was not obtained, however, a difference can clearly be observed between the two samples. This being said, a statistical significance was observed

between the last two samples. Because of these results, the team felt comfortable declaring this testing method valid for testing their scaffolds.

Methods

After alignment and spacing measurements, the team performed ball burst compression testing on composite scaffold samples to measure maximum load that each scaffold could sustain. This was performed on both manually fabricated (n=20) and automated (n=20) scaffolds per the standards referenced above in Section 0. Following the addition of the fibrin gel, the scaffolds remained hydrated in 1X PBS until transferred for testing. Prior to testing, the width and inner diameter measurements were taken on the frame of each sample, with the width measurement being in the direction of the aligned threads, seen below in Figure 76:

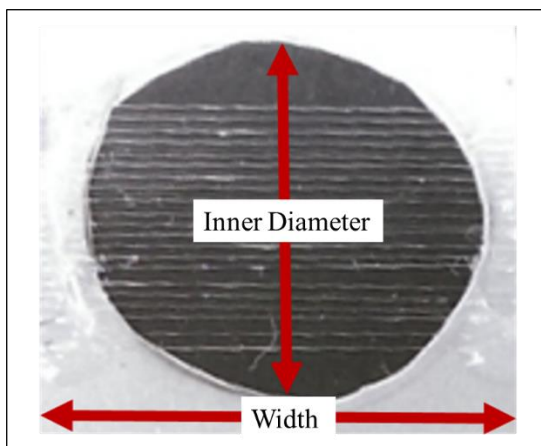


Figure 76: Frame width and inner diameter measurements prior to testing.

To perform the ball burst compression test, the scaffold samples were placed between two nylon washers, making sure the inner circles of both washers and the scaffold frame were relatively concentric by aligning the inner edge of the scaffold frame with the inner edge of the nylon washer (Figure 77). This would ensure that the spherical probe was being driven solely through the threads and gel and not making contact with the frame.

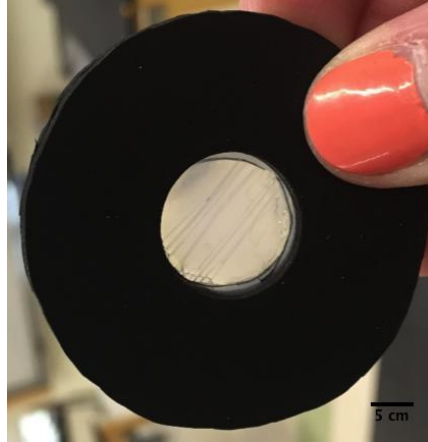


Figure 77: Scaffold between nylon washer prior to testing

Next, a PVC pipe fitting was placed onto the bending platform of an Instron 5544 Mechanical Testing System and a metal washer was placed on top of this. The nylon washers with the sample secured in between were positioned on top of the metal washer. Next, a bolt fitted with a cap nut was secured in the upper tensile grip of the Instron testing frame, making sure to align it with the testing set-up below. This bolt was lowered until it was just touching the surface of the composite in order to set the testing height and safety stops. This was only necessary for the first sample. The upper grip was then raised and a second metal washer and PVC pipe fitting were placed on top of the other components on the bending platform. Once all components were positioned on the bending platform, the movable edges of the bending platform were slid together and tightened to prevent movement of the set-up during testing. This set-up can be seen below in Figure 78:



Figure 78: Ball Burst Compression Testing Set-Up

The upper grip was then lowered back down to the testing height determined in a previous step. Utilizing BlueHill software, a standard compression test was run with a rate of extension of 9.00mm/min. A more detailed explanation of this set-up, procedure and all components can be seen in *Appendix G - Ball Burst Compression Testing Procedure*.

Statistical Analysis

For the statistical analysis, the team investigated if there was a statistical difference between the variances and thus overall distribution of maximum load values for each type of scaffold. This would show if one method was more consistent than the other and validate reproducibility.

For this analysis, the team utilized a Levene's Test for Equality of Variances as the National Institute of Standards and Technology (NIST) cites it as having less sensitivity to skewed data that does not have a normal distribution (NIST/SEMATECH, 2012). There are several variations of this test described in the International Journal of Methodology and Experimental Psychology by Nordstokke and Zumbo, some more robust than others (Nordstokke & Zumbo, 2010).

A traditional Levene's test takes the absolute differences between the values in a particular group and the mean of that group and compares it to those of another group(s). A one-way ANOVA, or analysis of variance for one variable, will then produce a p-value that can be used to determine if there is a statistical difference in the variance or distribution of one group and the other. Like a traditional t-test, a p-value of 0.05 is typically used to determine significance, with a p-value less than 0.05 representing a significant difference. This test can also be done using medians values. However, if there are outliers in a particular set of data, the mean or median often become skewed and the analysis of equality of variances is not as accurate. So while both these tests are more robust when analyzing data that is not normally distributed, an even more robust version of the test is a Non-Parametric Levene's Test for Equal Variances.

A study by Nordstokke and Zumbo provides evidence that the Non-Parametric Levene Test is superior to the mean or median version of the test (Nordstokke & Zumbo, 2010). With this version of the test, data from all groups is pooled and ranked from the smallest value to largest value. This ranking increases the uniformity of the data and strays from assuming normality of a particular population of data when performing a statistical analysis, by accounting for any outliers. The mean of the rankings is taken for each individual group and the absolute difference in mean rank is analyzed using a one-way ANOVA much like the other versions of the test. For this test, the null hypothesis states that populations are identically distributed in shape, which implies that there is homogeneity of variance. Thus, a p-value of less than 0.05 would determine rejection the null, indicating that the distributions are statistically different.

Results

In running ball burst compression tests for both manual (n=20) and automated (n=20) composite samples, the manual samples sustained a mean maximum load of 1.548 N with a

standard deviation of 1.222N, while the automated samples sustained a mean maximum load of 0.7335N with a standard deviation of 0.5353N. The load vs. extension curves for each of the samples can be seen below in the following plots in Figure 79:

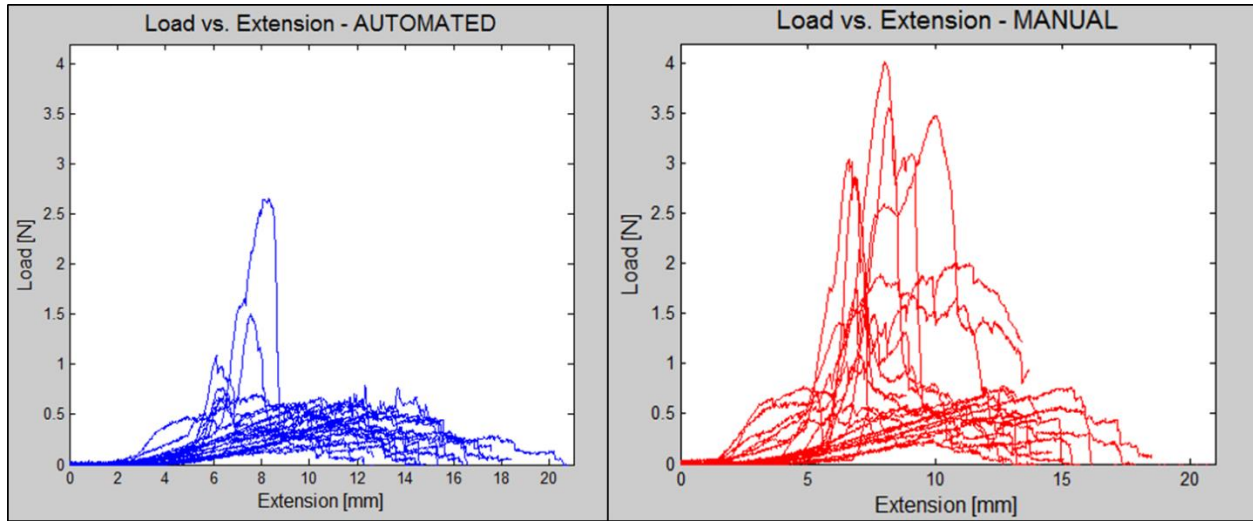


Figure 79: Load vs. Extension of both manual and automated samples (n=20 each)

While the team was assessing for equality of variances between the two data sets to validate the reproducibility of the automated system, and were not testing for differences in maximum load sustained, it is important to note that the manual scaffolds did in fact sustain higher average loads than the automated scaffolds. The team attributed this to overlapping of threads due to the inconsistent thread alignment in the manual scaffolds, therefore increasing the load that scaffolds in that category could sustain. While this appears to a positive scaffold trait, this was not a variable the team was presently testing for, however, the ability for overlapping threads to sustain higher loads is promising for future research of created multi-layered composite scaffolds.

Prior to selecting the appropriate statistical analysis method to compare the variance/distribution of the two different sample types, the distribution type of each of the

samples was analyzed. Below, in Figure 80, is a plot of the maximum loads sustained by both samples as well as a plot more representative of the distribution data fitted with a normal curve.

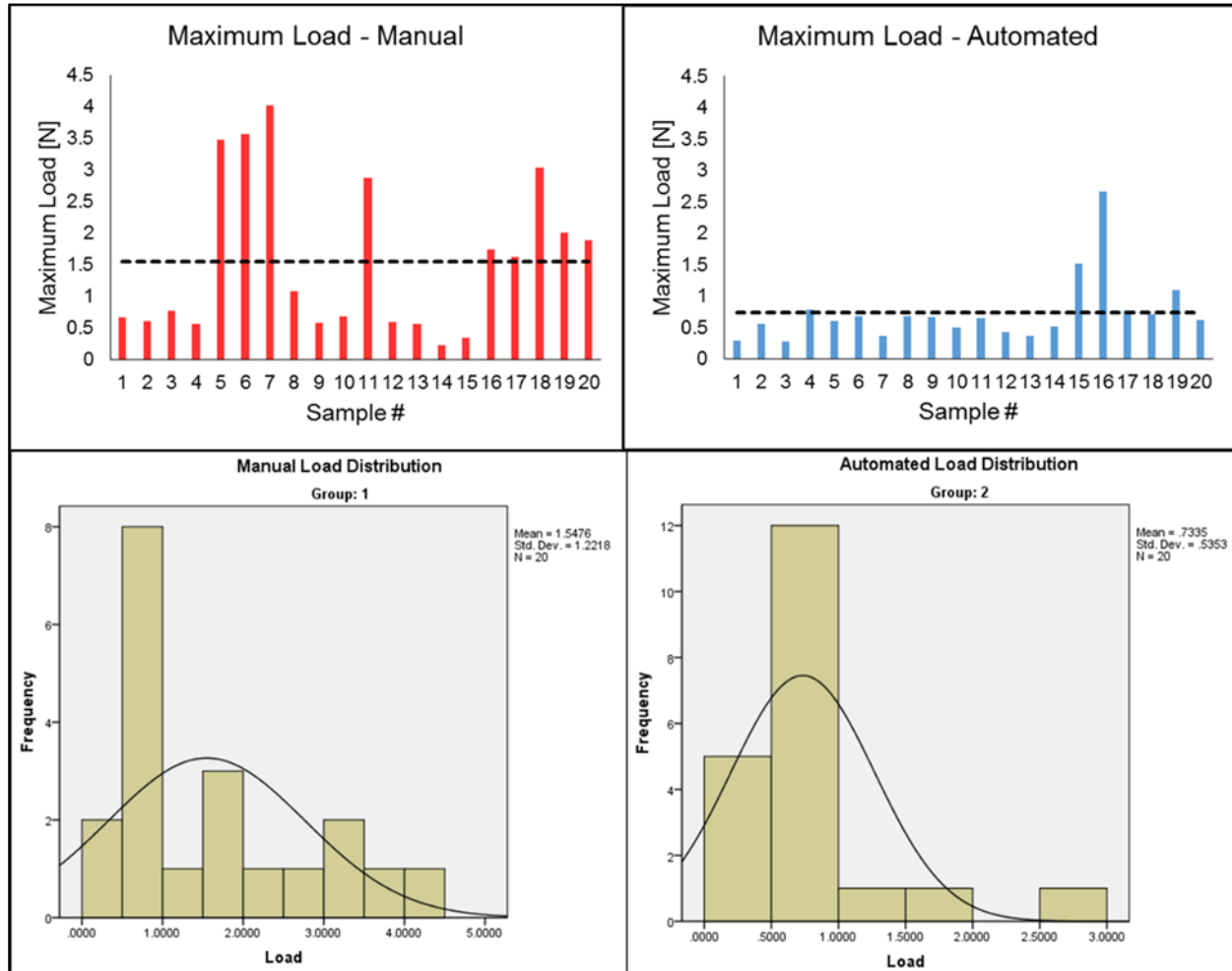


Figure 80: Maximum load values and data distributions for both manual (n=20) and automated samples (n=20).

From these plots it can be seen that both data sets are slightly skewed, thus a Non-Parametric Levene’s Test was used to determine if there was a statistical difference between the variances and distributions of each sample type. This test produced a p-value of 0.244.

The variances of both width and frame inner diameter were compared between the two different sample types as well, to ensure minor inconsistencies in both measurements were not potentially contributing to load variance. The mean width of the manual samples was 19.37mm with a standard deviation of 1.861mm and the mean width of the automated samples was

20.33mm, standard deviation 1.224mm. The mean frame inner diameter for the manual samples was 14.37mm (standard deviation of 0.7680mm), while the mean frame inner diameter for the automated samples was 14.88mm (standard deviation of 1.022mm). Plots of the data distributions of both width and frame inner diameter measurements can be seen below in Figure 81.

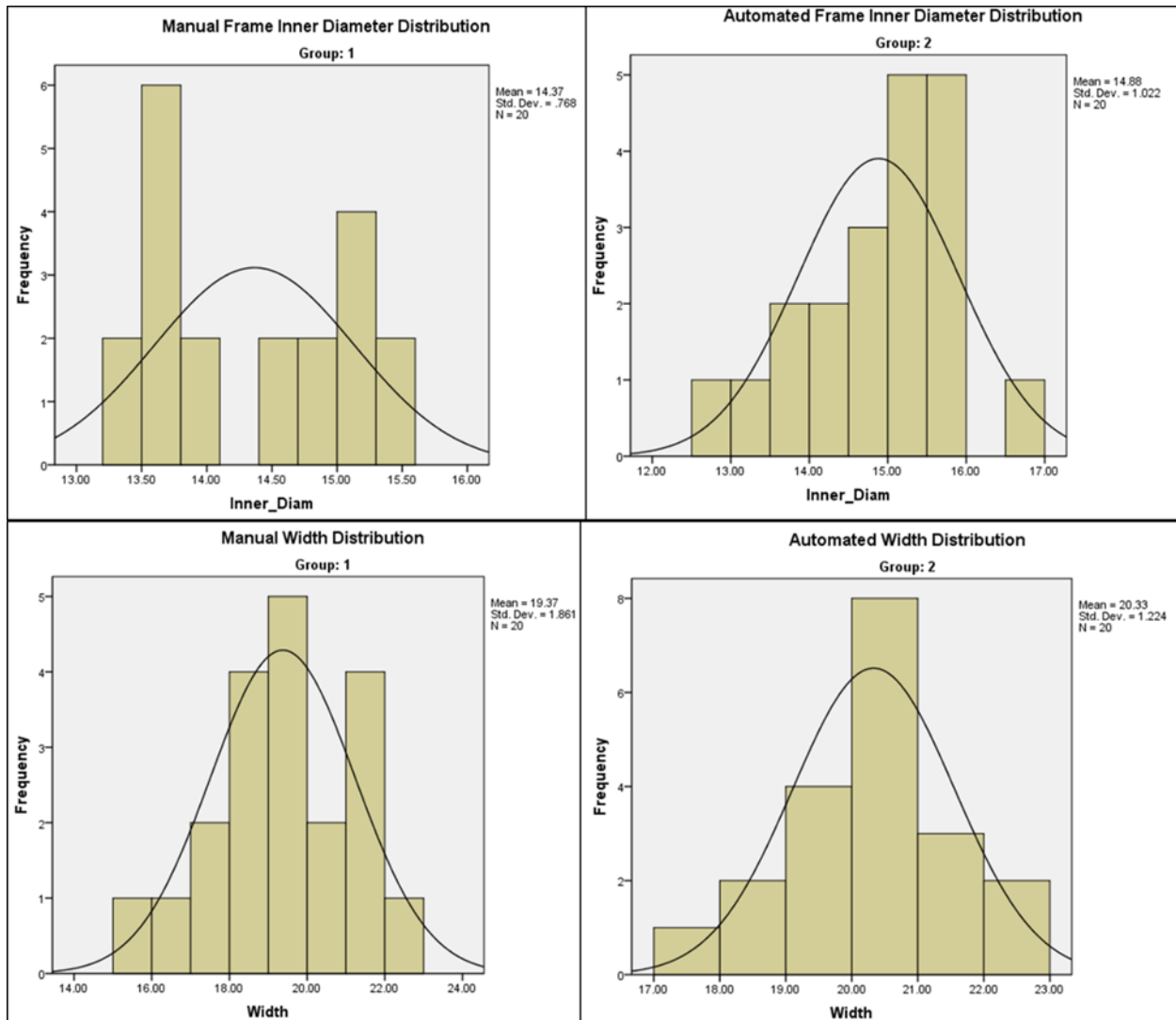


Figure 81: Width and Framer Inner Diameter Distributions for both sample types.

From these plots it can be seen that the width measurements for both sample types have a normal data distribution, while the inner diameter measurements are slightly skewed. For this reason, a traditional Levene's Test was performed to analyze the width measurement data, while a Non-

Parametric Levene’s Test was performed to analyze the frame inner diameter measurements. The p-values as a result of these statistical analyses were 0.089 and 0.359, respectively. A summary of all the calculations and measurements can be seen below in Table 40:

Measurements		Manual	Automated
Width [mm]	Mean	19.37	20.33
	Standard Deviation	1.861	1.224
	Levene p-value	0.0890	
Frame Inner Diameter [mm]	Mean	14.37	14.88
	Standard Deviation	0.7680	1.022
	Non-Parametric Levene	0.3590	
Maximum Load [N]	Mean	1.548	0.7335
	Standard Deviation	1.222	0.5353
	Non-Parametric Levene p-value	0.2440	

Table 40: Summary of Ball Burst Testing Results

6 Discussion of Results

6.1 Alignment & Spacing

Overall, the automated system presents an alternative for an improved and consistent thread alignment and spacing method. The analysis presented in section 0 shows that although the thread separation in any scaffold may be smaller using the manual method, there is less variability using the automated system developed through this project. For instance, the automated method presented a statistical significant lower standard deviation compared to the manual method. This suggests that since there is less variation using the automated system, the user will be able to produce more reproducible scaffolds than using the current manual method.

Moreover, the histograms show that the separation between threads is more accurate and precise using the automated system. Figure 63 displays that both type of scaffolds, manual and automated, show the skewed data. However, the manual method produces scaffolds with threads that are aligned less accurately than those fabricated using the automated method. For instance, the automated scaffolds showed higher precision and accuracy due to the smaller range of thread separation at which threads were aligned compared to the manual scaffolds which presented higher variability.

Additionally, results show that the reproducibility of the scaffolds using the automated system is independent of the user who constructs them. For instance, using ANOVA, the team was able to verify the lack of a significant difference between users. This shows that the automated system can create reproducible scaffolds even when multiple operators use it. Therefore, our novel system is independent of certain external factors such as users, allowing the client to have more freedom when constructing scaffolds while still creating a reproducible product. We can thus conclude that there is less variability of thread spacing using the automated system. The device is

independent of user variability and it allows for the construction of more precise, reproducible scaffolds to be used in cardiac regenerative applications.

6.1.1 Limitations of Alignment & Spacing Results

There were several limitations in the measurement of alignment to validate the reproducibility of the system. For instance there was an unequal number of automated and manual samples due to timing restrictions and the fact that only one user could use the device at the same time for creating the automated scaffolds. If we were to have more automated samples we could have a larger sampling pool to validate our results. Additionally, the measurements of separation between threads collected through Image J, although accurate, depend on the user who measured them. Therefore, this can present a systematic error in the data collection procedure we completed. Due to this factor, in this study we limited the users who collected this type of data to two different users, which reduced the amount of error.

6.2 Ball Burst Testing

The smaller standard deviation between the maximum loads sustained by the automated method versus the manual method suggests that the sustained loads vary less with the automated method, making it more consistent than the manual method. However, in measuring the mean and standard deviation of the data, it is assumed that the data distribution is normal. Figure 80 (above) shows that the maximum load values are not distributed normally for either sample type. Addressing the abnormal distribution, a statistical analysis utilizing a Non-Parametric Levene's Test for Equality of Variances was performed and produced a p-value of 0.244, indicating that there was no statistical difference in distribution of maximum load data between the two sample types and thus homogeneity of variances, but a slight trend suggesting the latter can still be observed.

In addressing the potential possibility that a significant variance in width or frame inner diameter measurements could produce load variance, a traditional Levene's Test and a Non-Parametric Levene's Test were performed for the width measurements and frame inner diameter measurements, respectively. A traditional Levene's Test assumes that the data distributions are normal and in observing the data distribution plots for width measurements above in Figure 81 it can be seen that they are normal, thus making this an appropriate analysis method. The p-value of 0.089 as a result of the traditional Levene's test suggests that there is no statistical difference in the distributions of the width measurements for both manual and automated samples and therefore there is homogeneity of variances.

As mentioned before, a Non-Parametric Levene's Test has proven to be less sensitive to data that is not distributed normally. The data distribution plots in Figure 81 show that the distributions of frame inner diameter measurements are not normally distributed, making the Non-Parametric version of Levene's Test an appropriate analysis method. The p-value of 0.359 as a result of the Non-Parametric Test suggests that there is no statistical difference in the distributions of frame inner diameter measurements for both manual and automated samples and therefore no homogeneity of variances.

Overall, the major limitation of the data acquired through this particular testing method was the use of a 2000N load cell. This load cell is only accurate to about 2N. Most of the load values acquired for the composite scaffolds were less than this value, therefore any readings below this value are not necessarily accurate. For this reason, and being in the early stages of development of a composite scaffold for cardiac tissue regeneration, the team did not compare their load readings to previous literature. Instead they are assessed for consistency among the sample types to validate that the automated method is superior at reproducibly fabricating fibrin

scaffolds. Future testing on these scaffolds could attempt to get more physiologically relevant load values by using a more sensitive load cell.

6.3 Impact Analysis

The semi-automated system developed is intended to be a prototype that can be used to validate the importance of alignment in these fibrin microthreads composite scaffolds in a small-scale, laboratory setting. However, there are potential ways that this system can impact society. This system is the first of its kind to use a suctioning force to secure and align micron-scale fibers, and has the potential to be incorporated into a future mass production system. The following sections analyze the ways in which the semi-automated system may have a societal impact.

6.3.1 Economics

Our scaffold production system has the most impact on economics aspect concerning the manufacture of products, with less on the consumption and distribution of products. Currently the fibrin microthread scaffold technology is focused on research and *in vitro* testing. Our system enables the scaffold production and therefore has potential to validate the composite scaffold on an accelerated schedule. Currently the manufacturing of this system is for research purposes only. However, the system created is able to save money by decreasing the materials wasted and labor time, while increasing the scaffold throughput rates. In the end, it would have an impact on the aspects of consumption or distribution when regenerative myocardial regeneration therapy is approved.

A heart transplant currently costs more than \$900,000.00 (UNOS Transplant Living, 2015). This amount accounts for immune-suppressants and hospital costs. However, it does not assure a successful transplantation, prevent immune rejection and or promote myocardial

regeneration. By using our automated system and furthering developing a regenerative myocardial tissue construct, costs can be reduced dramatically and the issues concerning organ transplantation can be limited.

6.3.2 Environmental Impact

Our system has limited environmental impact from the materials used. The material used for the suction box device is primarily cast acrylic, which has a manufacturing process with negative environmental impacts (EPA, 1994). Acrylic was chosen for this design because of its ease of manufacture, durability, transparency, and biocompatibility. Due to the small amount of acrylic used for this system, this environmental impact would be little to none. If this device is scaled up, further consideration should be reflected in order to reduce the negative environmental effects. For example in the case of the use of reagents for chemical analysis, there is risk of harming the environment through the use of these substances.

6.3.3 Societal Influence

This system has the potential to have a societal impact due to its purpose to validate a platform tissue engineered technology. Validating the platform ensured the team had created a product that met the need for which it was created, which would then benefit not only the client but the user as well, thus impacting society. With reproducible characteristics, the user can collect data that is representative of the alignment in a singular direction. This scaffold will facilitate the regeneration of a patient's heart following myocardial infarction and provide a solution for those unable to receive a life-saving transplant. The prevalence of this condition would then benefit from a consistent source compared to the scarcity of a heart transplant.

6.3.4 Political Ramifications

Directly, the automated system created does not have political ramifications. Globally, tissue engineering constructs have very few clinical applications especially for myocardial infarction scar tissue. This system has the potential to improve the validation of the aligned fibrin microthread scaffold as a replacement for heart transplantation. Because heart disease is prevalent across the world, this technology would have an impact on the global market. Currently, it would have a limited impact on international markets aside from research labs that may find this technology helpful for alignment of fibers. There is much controversy surrounding the government funding of stem cells and their use to treat degenerative diseases, such as those in the cardiovascular system, in particular heart attacks and strokes. These diseases cause lifelong disabilities and reduction of quality of life, creating a need for a more permanent solution for these diseases. After a heart attack, known as myocardial infarction, there is an onset of tissue necrosis and this necrosis is then replaced by the formation of scar tissue. The recent progress in the area of stem cell research has led to the suggestion that stem cells have the potential to be used to regenerate cells in damaged organs, such as the heart. Due to these findings, with the addition of stem cells being incorporated onto microthread composite scaffolds, this would potentially be a solution for cardiovascular diseases.

6.3.5 Ethical Concern

The main ethical concerns with relation to this system would be the materials used with this system as well as in future work. The bovine sourcing of fibrinogen and thrombin for creation of fibrin microthreads would ultimately be then placed into the human body. There are concerns regarding using an animal source for research and medical purposes, even if collected in an ethical manner. In the future, the addition of stem cells within the scaffolds could add

ethical concerns. Concerns around stem cells derived from the use of human embryos and the growth of these cells in a laboratory. The ethical debate begins due to the destruction of human embryos for human embryonic stem cells, with the debate in the United States around the question of when human life begins and abortion. The pros of stem cells is that they have the potential to treat a wide range of medical conditions and problems, such as Parkinson's Disease, heart diseases, organ damage etc. This potentially leads to a cure of these diseases as well. The cons of stem cells is the ethical controversy, including the start of human life, abortion, and cloning. An alternative from the use of embryonic cells is the use of cord blood stem cells. These are harvested from the blood from the umbilical cord during the time of birth. This blood is then frozen and stored which can be used in the future to treat diseases.

6.3.6 Health and Safety Issue

Health and safety is a very relevant concern when working with medical implants. This system creates fibrin-based scaffolds with the goal of improving patient health and limiting the need for a highly invasive heart transplant. The scaffolds will need to be carefully sterilized so that it does not elicit an immune response while maintaining the integrity of the scaffold. The entire system has the capability to be used in an aseptic environment and therefore would eliminate much of the risks involved with contamination, risks that are commonly found in other alternatives used to control myocardial infarction such as a heart transplant. Fibrin is biocompatible with the body, in addition to the cells used are able to thrive and grow within the patient's body.

6.3.7 Manufacturability

The main objective of this project was to produce a scaffold that has reproducible characteristics. The current method of manufacturing these scaffolds is time and labor intensive

without reproducible results in the alignment and spacing. Challenges when working with microthreads include being lightweight, easily damaged from excess tension, affected by static electricity and difficult to visualize. The automated system is a method that increases the manufacturability of the scaffolds, by decreasing these difficulties that are experienced when manually aligning threads. Additionally the automated system fabricates scaffolds with consistent alignment with desired spacing of the fibrin microthreads. The process is intuitive and has limited steps to make it easy to manufacture when compared with the current manual process making it ideal for use by multiple users. Therefore future assays utilizing this reproducibly aligned scaffolds will produce data that clearly represents the effect of the aligned microthreads in various assays. This gives the user a powerful tool that will allow for the user to expedite the validation of this platform technology.

6.3.8 Sustainability

This system will be used in Pins's lab primarily to align fibrin microthreads in planar sheets. Therefore the most important aspect regarding sustainability would be the assessment of whether this system can be used in future years with multiple users. Multiple undergraduate student users have tested the device during the design process and given feedback on the system. Additionally the user has been involved in the design process for frequent feedback to ensure the final product is one that is best fit for its long term purpose. Regarding environmental sustainability, the acrylic used in this system should be disposed of properly because it is difficult to recycle and is not biodegradable.

7 Final Design and Validation

The challenge posed to the team was to develop a reproducible automated system to create fibrin microthread composite scaffolds that will facilitate the development of a multi-layered tissue construct. The current method of aligning fibrin threads is based on the manual placement of individual threads, which creates a lot of variance in the alignment of threads as well as it requires a lot of thread handling. Due to this unequal alignment and damaging thread handling, there was a need for a reproducible system to create to create fibrin microthread composite scaffolds.

Once the team had weighed alternative design options and reached a conclusion on the final system design, the team created a final automated system seen in schematics as well as actual pictures of the system below in Figure 82. The whole system consisted a platform that provided a secured thread alignment, followed by a transferable frame where the threads are placed to then be added in the composite frame that will allow for the gel casting to finally obtain the fibrin laminated composite.

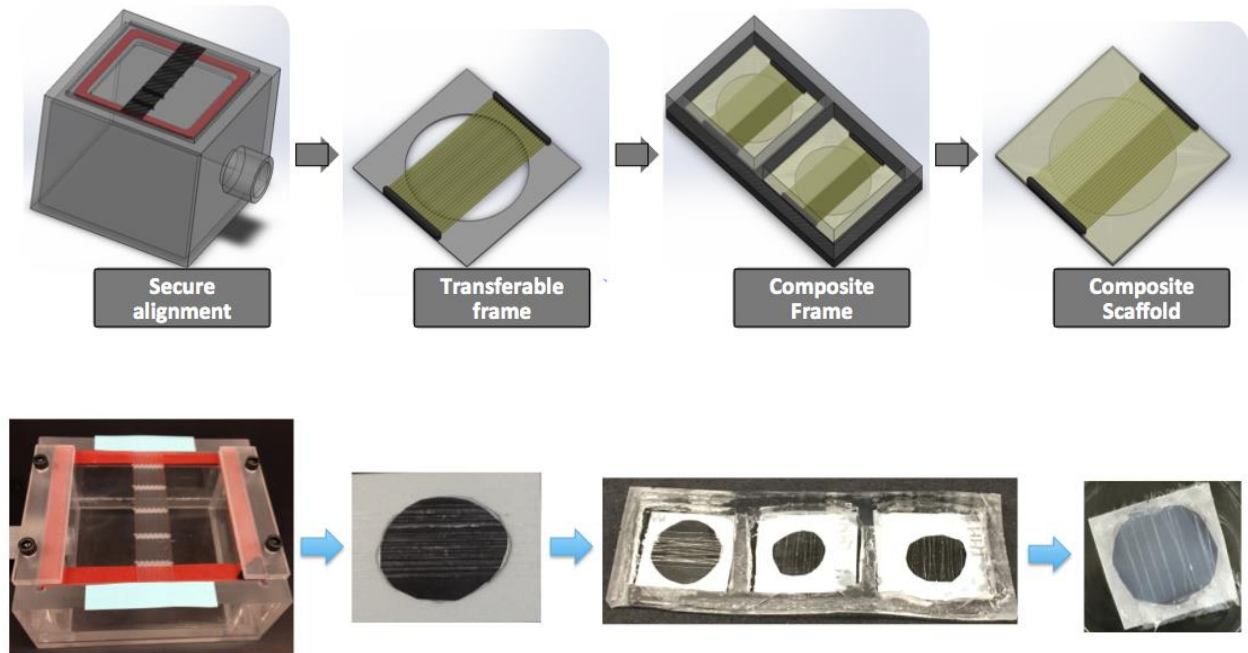


Figure 82: Schematic and pictures of automated system developed

7.1 System Validation

7.1.1 Secure Alignment: Suction Box

The first component of the final design is the secure alignment suction box. The suction box consists of a cast acrylic open topped box with a port for a vacuum to be attached onto one side. Beneath the top plate of the box is a square rubber gasket to ensure a secure seal of the box top, Figure 83 displays the design of the box. The top plate of the box consists of 21 grooves of 250 μm in diameter with 500 μm between each groove. In addition, each groove has five 150 μm diameter holes along their length to allow for the anchoring of threads during the alignment process.

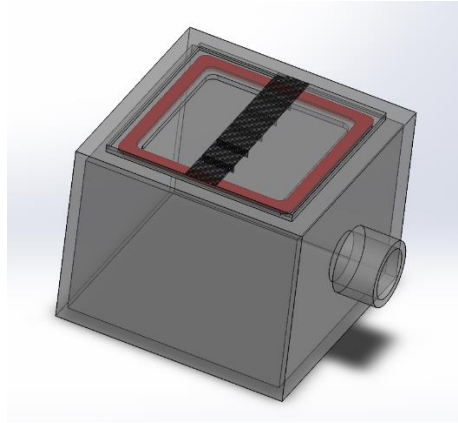


Figure 83: Suction Box with rubber gasket

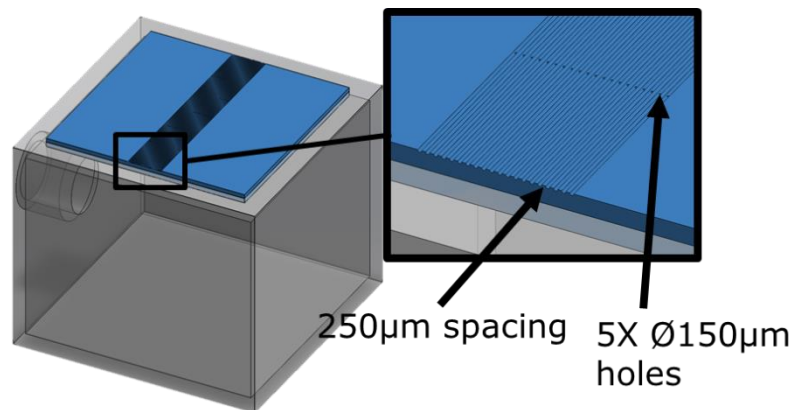


Figure 84: Suction box with zoomed in grooved platform

In order to correctly use the suction box, a bench top vacuum is turned on and attached to the vacuum port on the side of the box. Using forceps, fibrin microthreads are then placed into the grooves, of the top plate of the box, being secured by the suction of the vacuum through the holes within the grooves.

7.1.1 Transferable Frame: Adhesive Framing Mechanism and Vellum Frame

Adhesive Framing Mechanism

The second component of the final design is the framing mechanism that allows the scaffolds to be transferable. A combination of an adhesive and vellum frame are used to create this framing device that act as a mechanism to support the threads once they are aligned in the

grooved platform. The first component is the adhesive frame, which consists of an adhesive paper that sticks to the surface of the top plate of the suction box. This mechanism creates a smooth transition between the secured aligned threads for the addition of the framing of the vellum frame. The adhesive framing mechanism is represented in gray in the schematic picture Figure 85 and orange in the actual pictures of the device Figure 86.

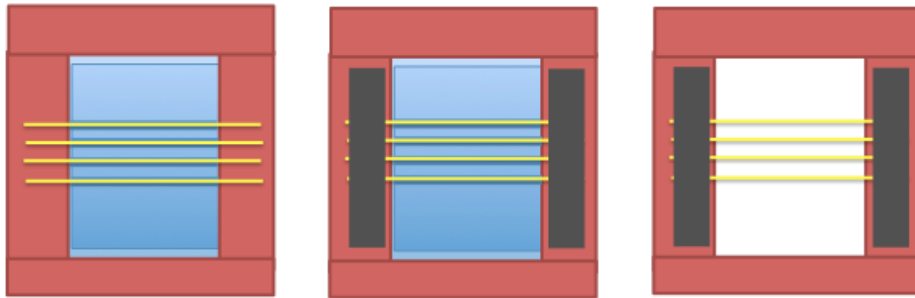


Figure 85: Adhesive Framing Mechanism

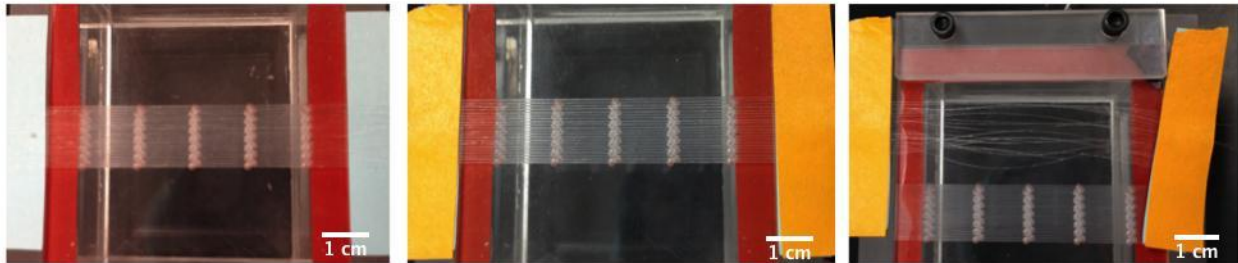


Figure 86: Picture of Adhesive Framing Mechanism

As shown in Figure 85 and Figure 86, this second part, to secure the threads, an adhesive strip of tape (grey in Figure 85 and orange in Figure 86) come into place on top of the threads to secure the alignment and allow for the threads to be transferred. Together, these two components make up the adhesive framing mechanism, in order to remove the aligned threads from the box and to move to the vellum frame.

Vellum Frame

The second part to this component is the vellum frame. Once the threads are and are attached with the adhesive framing system, they must be attached to a vellum paper frame using

silicone glue. This vellum paper frame allows for support of the threads and for the creation of the composite through the addition of the fibrinogen gel. The vellum frame is a circular hole with a diameter of 16 mm, which is cut out of a square of Vellum paper. For each set of aligned threads on the suction box, there are two scaffolds created (a simplified schematic of this is shown in Figure 87). The gray donut shape represents the vellum frame and the gray circles represent the silicon glue. After the glue is dried, the scaffold can be removed from the adhesive frame and then separated.

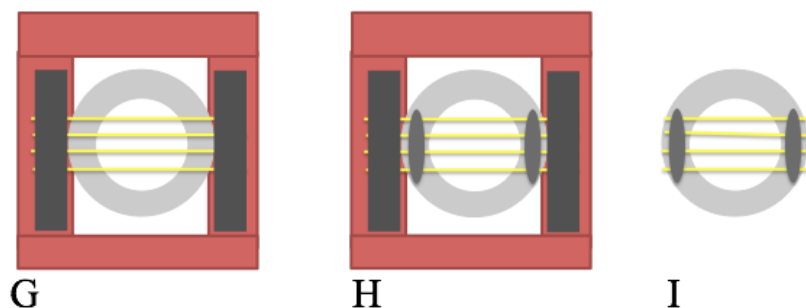


Figure 87: Vellum frame addition to the Adhesive Framing Mechanism

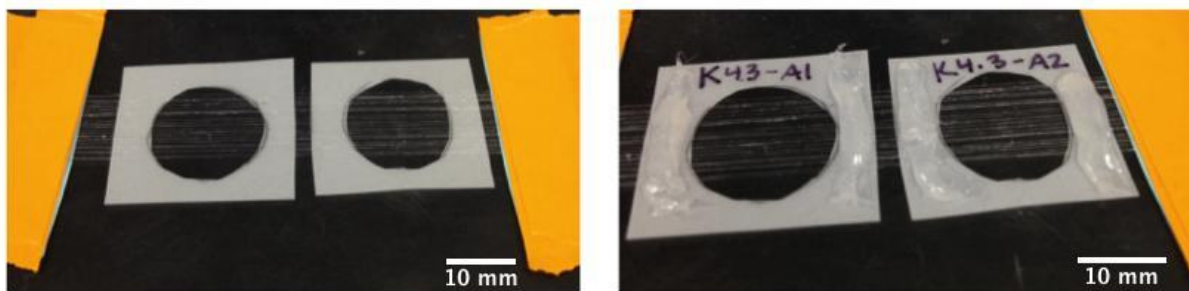


Figure 88: Picture of vellum frame process.

7.1.2 Composite Frame: Gel Casting

The next step is the addition of the fibrin gel to create a composite scaffold. The scaffolds are transferred to a black acetyl plastic and PDMS frame for the addition of the gel. The plastic measuring 74 mm x 24 mm rectangular with a thickness of 1mm (Figure 49) is placed underneath the newly created scaffolds.

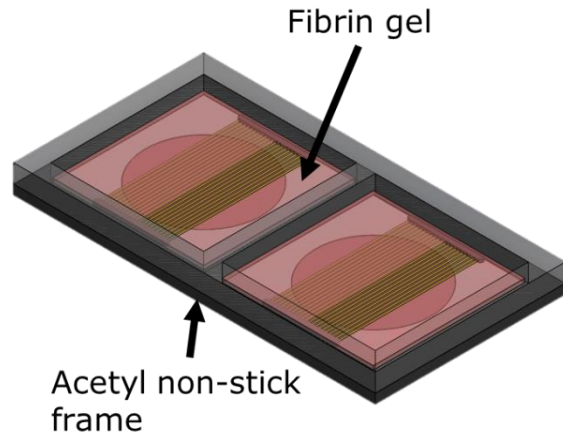


Figure 89: Frame for addition of fibrin gel



Figure 90: Picture of scaffolds in Composite Frame

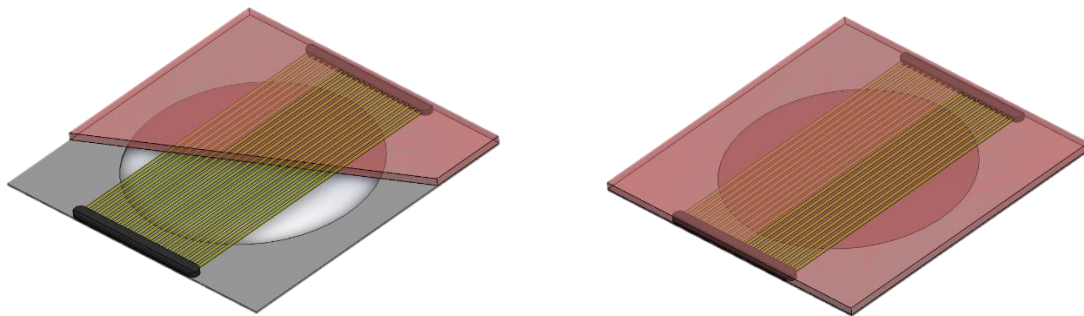


Figure 91: Final composite scaffold, with fibrin gel (red) and fibrin microthreads (yellow)

On top of the scaffolds, a polydimethylsiloxane (PDMS) framing wells are placed on top of them to form a “sandwich” (Figure 50). This creates a tight seal, to stop gel from spilling out when it is added. This also allows for defined wells to be created, so there may be the creation of multiple composite scaffolds on the same plastic framing system (Figure 91). Once the fibrin gel

has been cast, the composite stands for 30 minutes in order to guarantee the proper polymerization. Following this process, the composites are ready for testing.

In conclusion, with the use of all components of the automated fabrication system, the team successfully developed a reproducible system to create customizable fibrin microthread composite scaffolds.

8 Conclusions and Recommendations

The team was able to design, create and test an automated system that allows for the alignment of fibrin microthreads in order to create fibrin composite scaffolds. The system consists of 3 main parts; the secure alignment achieved through the suction box, a transferable vellum frame that allows for manipulation of the scaffolds and a composite scaffold frame that permits for gel casting. To validate the design the team assessed the reproducibility of the system quantitatively by measuring the thread alignment and conducting mechanical ball burst testing. Results show high reproducibility in the automated scaffolds compared to the manual ones. In conclusion, the automated final system created through this project was able to successfully create reproducible aligned fibrin microthread composite scaffolds.

8.1 Recommendations

Statistical Analysis

To more accurately statistically analyze the data a more robust method should be utilized. For instance, the data was analyzed as independent values to one another. However, due to the way that measurements were collected and the nature of fibrin threads, these data can be treated as either dependent or independent. Therefore, new methods for measuring and analyzing the thread separation should be developed to avoid these issues.

Top Plate Spacing Modification

Part of our objectives and device specifications, the team wanted to space the threads as close as possible in order to create a tighter scaffold. Due to machinery difficulties that closest threads could be aligned was 250 μm . Therefore, in order to control spacing the team suggests the modification of the top plate.

The suction box with alignment grooves for alignment allows for the customization of the top plate. Therefore, we recommend manufacturing new plates with multiple separations between threads so that scaffolds with customizable separations can be created. By modifying this plate to smaller separations and customizing the scaffolds we can generate more testing groups in order to analyze their structural and mechanical properties and seek for optimal conditions to mimic the complex myocardial structure.

Fiber Angle Orientation Modification

This method is based in simple trigonometric properties and it provides an alternative besides the superposition of threads. In order to bring the threads closer together, there is a need to decrease the space between the threads after they have been aligned. Threads are initially parallel to each other and perpendicular to the framing baseline as seen in Figure 92

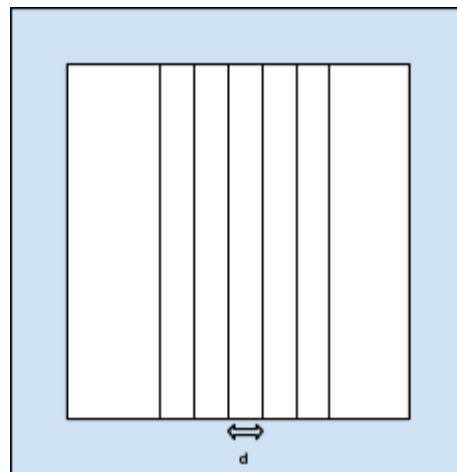


Figure 92: Aligned fibrin threads separated by distance 'd'

If one manipulates the angle at which threads are aligned with respect to the baseline, the final separation between threads will decrease. The threads are in a perpendicular orientation to the framing platform when they are aligned. As the angle between the thread and the framing platform decreases, the gap between threads shortens. Figure 93 shows a diagram that

demonstrates how angle manipulation works. In addition, Table 41 shows the estimated calculations of the distance between threads as the angle changes.

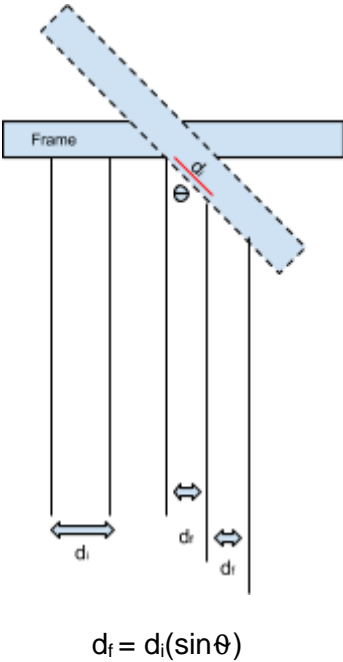


Figure 93: Angle manipulation diagram

Angle (degrees)	Gap (um)
90	250.00
75	241.48
70	234.92
65	226.58
60	216.51
50	191.51
45	176.78
30	125.00
20	85.51
15	64.70
10	43.41

Table 41: Gap calculation depending on the angle (θ)

As seen in the Figure 93 and Table 41 above, by moving the frame that holds the aligned threads towards a direction where the angle theta (θ) decreases, the separation between threads is reduced. Considering the initial separation between threads to be 250 μm as established in the aligning platform currently used, the distance between threads would reduce by a 50% if the angle of the frame changes by 30 degrees. Additional spacing can be selected with this process to alter the packing density in a customizable fashion.

On the other hand, there are certain limitations regarding this method. First, once the angle has been manipulated threads will not start or end at the same position. Therefore, these uneven regions, those at the ends, will go to waste. For instance, the closer the threads are placed the more angular manipulation needs to be performed and the more waste produced. Therefore, the client needs to consider if this is acceptable economically. Additionally, a new device should be constructed in order to verify the precision of the angle chosen. Nevertheless, this method presents a useful and easy mechanism that creates variability in the packing density of the scaffolds.

Mechanical Testing

In looking at the limitations of the mechanical ball burst testing outlined in section 0, there are several recommendations that should be taken into consideration for future work in this research area. Firstly, the use of a more precise load cell is recommended, as a 2000N load cell lacks precision below 2N. As this research progresses, it will be necessary to compare the loads sustained by the multi-layered composite scaffolds to physiologically relevant values that are experienced by the native fiber matrix in the heart. Therefore, accuracy in the load values obtained is essential

Cell Culture

With the addition of neonatal rat ventricular myocytes to the fibrin composite scaffolds, the creation of a functional contractile scaffold structures could be achieved. By seeing the scaffolds with cells, this would be able to see how the high alignment of the microthreads can impact the alignment of the cells to

create functional scaffolds. Also, as the alignment is reproducible, this would allow for a more predictable cellular behavior. Overall, the scaffold combined with healthy cardiomyocytes is a step closer to the ideal myocardial patch for myocardial tissue regeneration

Biaxial Composite Creation

By combining multiple scaffolds on top of one another at various angles, this creates a biaxial composite scaffold. These composites will more accurately mimic the tissue in the complex structure of the myocardium. In addition, the biaxially aligned scaffold of this composite could contain multiple cell and thread types. This would create a graft that can target multiple structures of tissue. The creation of the biaxial scaffold would allow for the complex structure of the tissue to be mimicked and thus able to function amongst the native tissue of the organ.

References

- AAMI. (2001). ISO 7198 - Cardiovascular implants--Tubular vascular prostheses.
- Arts, T., Costa, K. D., Covell, J. W., McCulloch, A. D., , , & (2001). Relating myocardial laminar architecture to shear strain and muscle fiber orientation. *American Journal of Physiology - Heart and Circulatory Physiology*, 280(5), 2222-2229.
- ASTM. (2011). D3787-07 Standard Test Method for Bursting Strength of Textiles--Constant-Rate-of-Traverse (CRT) Ball Burst Test.
- Ayres, C. E. (2008). Measuring fiber alignment in electrospun scaffolds: a user's guide to the 2D fast Fourier transform approach. *Journal of Biomaterials Science, Polymer Edition*, 19(5), 603-603. doi: 10.1163/156856208784089643
- Bosworth, L. A., Turner, L.-A., & Cartmell, S. H. (2013). State of the art composites comprising electrospun fibres coupled with hydrogels: a review. *Nanomedicine: Nanotechnology, Biology and Medicine*, 9(3), 322-335.
- Chan, B. P., & Leong, K. W. (2008). Scaffolding in tissue engineering: general approaches and tissue-specific considerations. *European spine journal*, 17(4), 467-479.
- Chen, Q.-Z., Bismarck, A., Hansen, U., Junaid, S., Tran, M. Q., Harding, S. E., . . . Boccaccini, A. R. (2008). Characterisation of a soft elastomer poly(glycerol sebacate) designed to match the mechanical properties of myocardial tissue. *Biomaterials*, 29(1), 47-57. doi: 10.1016/j.biomaterials.2007.09.010
- Christman, K. L., Vardanian, A. J., Fang, Q., Sievers, R. E., Fok, H. H., & Lee, R. J. (2004). Injectable Fibrin Scaffold Improves Cell Transplant Survival, Reduces Infarct Expansion, and Induces Neovasculture Formation in Ischemic Myocardium. *Journal of the American College of Cardiology*, 44(3), 654-660. doi: <http://dx.doi.org/10.1016/j.jacc.2004.04.040>
- Cloonan, O. D., Lee, Walsh, Barra, D., & McGloughlin. (2011). Spherical indentation of free-standing acellular extracellular matrix membranes. *Acta Biomaterialia*, 8, 262-273. doi: 10.1016/j.actbio.2011.08.003
- Coburn, J., Gibson, M., Bandalini, P. A., Laird, C., Mao, H.-Q., Moroni, L., . . . Elisseeff, J. (2011). Biomimetics of the extracellular matrix: an integrated three-dimensional fiber-hydrogel composite for cartilage tissue engineering. *Smart structures and systems*, 7(3), 213.
- Cornwell, K. G. (2007). *Collagen and fibrin biopolymer microthreads for bioengineered ligament regeneration*.
- Cornwell, K. G., & Pins, G. D. (2007). Discrete crosslinked fibrin microthread scaffolds for tissue regeneration. *Journal of biomedical materials research. Part A*, 82(1), 104-112. doi: 10.1002/jbm.a.31057
- Cornwell, K. G., & Pins, G. D. (2010). Enhanced proliferation and migration of fibroblasts on the surface of fibroblast growth factor-2-loaded fibrin microthreads. *Tissue engineering. Part A*, 16(12), 3669-3677. doi: 10.1089/ten.tea.2009.0600
- Costa, K. D., Holmes, J. W., & McCulloch, D. (2001). Modelling cardiac mechanical properties in three dimensions. *Philosophical Transactions of the Royal Society of London. Series A: Mathematical, Physical and Engineering Sciences*, 359(1783), 1233-1250. doi: 10.1098/rsta.2001.0828
- Dobaczewski, M., Gonzalez-Quesada C Fau - Frangogiannis, N. G., & Frangogiannis, N. G. (2010). The extracellular matrix as a modulator of the inflammatory and reparative response following myocardial infarction. (1095-8584 (Electronic)).
- Domb, A. J., Jain, J. P., & Ebrary Academic, C. (2011). *Biodegradable Polymers in Clinical Use and Clinical Development*. Hoboken, NJ: Wiley.
- EPA. (1994). *OPPT Chemical Fact Sheets*. Retrieved from <http://www.epa.gov/chemfact/methy-fs.txt>.
- Freytes, Badylak, Webster, Geddes, Rundell, a, . . . a. (2004). Biaxial strength of multilaminated extracellular matrix scaffolds. *Biomaterials*, 25, 2353-2361. doi: 10.1016/j.biomaterials.2003.09.015

- Froeling, M., Strijkers, G. J., Nederveen, A. J., Chamuleau, S. A., & Luijten, P. R. (2014). Diffusion Tensor MRI of the Heart – In Vivo Imaging of Myocardial Fibe. doi: 10.1007/s12410-014-9276-y
- Froeling, M., Strijkers, G. J., Nederveen, A. J., Chamuleau, S. A., Luijten, P. R., , & (2014). Diffusion Tensor MRI of the Heart – In Vivo Imaging of Myocardial Fibe. doi: 10.1007/s12410-014-9276-y
- Givertz, M. M. (2011). Ventricular Assist Devices.
- Glowacki, J., & Mizuno, S. (2008). Collagen scaffolds for tissue engineering. *Biopolymers*, 89(5), 338-344. doi: 10.1002/bip.20871
- Grasman, J. M., Page, R. L., Dominko, T., & Pins, G. D. (2012). Crosslinking strategies facilitate tunable structural properties of fibrin microthreads. *Acta biomaterialia*, 8(11), 4020-4030. doi: 10.1016/j.actbio.2012.07.018
- Grasman, J. M., Pumphrey, L. M., Dunphy, M., Perez-Rogers, J., & Pins, G. D. (2014). Static axial stretching enhances the mechanical properties and cellular responses of fibrin microthreads. *Acta biomaterialia*.
- Grover, C. N., Cameron, R. E., & Best, S. M. (2012). Investigating the morphological, mechanical and degradation properties of scaffolds comprising collagen, gelatin and elastin for use in soft tissue engineering. *Journal of the Mechanical Behavior of Biomedical Materials*, 10, 62-74. doi: 10.1016/j.jmbbm.2012.02.028
- Grover, C. N., Gwynne, J. H., Pugh, N., Hamaia, S., Farndale, R. W., Best, S. M., & Cameron, R. E. (2012). Crosslinking and composition influence the surface properties, mechanical stiffness and cell reactivity of collagen-based films. *Acta Biomaterialia*, 8(8), 3080-3090. doi: <http://dx.doi.org/10.1016/j.actbio.2012.05.006>
- Guyette, J. P., Fakharzadeh, M., Burford, E. J., Tao, Z. W., Pins, G. D., Rolle, M. W., & Gaudette, G. R. (2013). A novel suture-based method for efficient transplantation of stem cells. *Journal of Biomedical Materials Research Part A*, 101A(3), 809-818. doi: 10.1002/jbm.a.34386
- Hlatky, M. A., Flather, M., Hamm, C. W., Hueb, W. A., Kähler, J., Kelsey, S. F., . . . Danchin, N. (2009). Coronary artery bypass surgery compared with percutaneous coronary interventions for multivessel disease: a collaborative analysis of individual patient data from ten randomised trials. *The Lancet*, 373(9670), 1190-1197. doi: 10.1016/S0140-6736(09)60552-3
- Hollister, S. J., Maddox, R. D., & Taboas, J. M. (2002). Optimal design and fabrication of scaffolds to mimic tissue properties and satisfy biological constraints. *Biomaterials*, 23(20), 4095-4103.
- Kofidis, T., Akhyari P Fau - Wachsmann, B., Wachsmann B Fau - Boublik, J., Boublik J Fau - Mueller-Stahl, K., Mueller-Stahl K Fau - Leyh, R., Leyh R Fau - Fischer, S., . . . Haverich, A. (2002). A novel bioartificial myocardial tissue and its prospective use in cardiac surgery. (1010-7940 (Print)).
- Kofidis, T., Lenz A Fau - Boublik, J., Boublik J Fau - Akhyari, P., Akhyari P Fau - Wachsmann, B., Wachsmann B Fau - Stahl, K. M., Stahl Km Fau - Haverich, A., . . . Leyh, R. G. (2003). Bioartificial grafts for transmural myocardial restoration: a new cardiovascular tissue culture concept. (1010-7940 (Print)).
- Legrice, I., Hunter, P., Young, A., & Smaill, B. (2001). The architecture of the heart: a data-based model. *Philosophical Transactions of the Royal Society of London. Series A: Mathematical, Physical and Engineering Sciences*, 359(1783), 1217-1232. doi: 10.1098/rsta.2001.0827
- Lisi, A., Briganti, E., Ledda, M., Losi, P., Grimaldi, S., Marchese, R., & Soldani, G. (2012). A combined synthetic-fibrin scaffold supports growth and cardiomyogenic commitment of human placental derived stem cells. *PloS one*, 7(4), e34284. doi: 10.1371/journal.pone.0034284
- Lund, L. H., Yusen, R. D., Stehlik, J., Edwards, L. B., Kucheryavaya, A. Y., Dipchand, A. I., . . . Int Soc Heart Lung, T. (2013). The Registry of the International Society for Heart and Lung Transplantation: Thirtieth Official Adult Heart Transplant Report--2013; focus theme: age. *The Journal of heart and lung transplantation : the official publication of the International Society for Heart Transplantation*, 32(10), 951-964. doi: 10.1016/j.healun.2013.08.006

- Ma, P. X., Elisseeff, J. H., & CrcnetBase. (2006). *Scaffolding in tissue engineering*. Boca Raton: Taylor & Francis.
- Miller, L., Stewart, G. C., Stevenson, L. W., , , & (2011). Keeping Left Ventricular Assist Device Acceleration on Track. doi: 10.1161/CIRCULATIONAHA.110.982512
- Miyagi, Y., Zeng F Fau - Huang, X.-P., Huang Xp Fau - Foltz, W. D., Foltz Wd Fau - Wu, J., Wu J Fau - Mihic, A., Mihic A Fau - Yau, T. M., . . . Li, R. K. (2010). Surgical ventricular restoration with a cell- and cytokine-seeded biodegradable scaffold. (1878-5905 (Electronic)).
- Mohan, N. (2005). Novel porous, polysaccharide scaffolds for tissue engineering applications. *Trends in biomaterials & artificial organs*, 18(2), 219.
- Murphy, S. L., Xu, J., & Kochanek, K. D. (2012). National vital statistics reports. *National vital statistics reports*, 60(4), 1.
- National Institutes of Health. (2014). Heart Attack. doi: <http://www.nlm.nih.gov/medlineplus/heartattack.html>
- Nielsen, P. M., Le Grice, I. J., Smaill, B. H., & Hunter, P. J. (1991). Mathematical model of geometry and fibrous structure of the heart. *AJP - Heart and Circulatory Physiology*, 260(4), H1365-H1378.
- NIST/SEMATECH. (2012). Levene Test for Equality of Variances *e-Handbook of Statistical Methods*.
- Nordstokke, D. W., & Zumbo, B. D. (2010). A nonparametric Levene test for equal variances (Vol. 31, pp. 401-430). *Psicologica*.
- Page, R. L., Dominko, T., Malcuit, C., Vilner, L., Vojtic, I., Shaw, S., . . . Rolle, M. W. (2011). Restoration of skeletal muscle defects with adult human cells delivered on fibrin microthreads. *Tissue engineering. Part A*, 17(21-22), 2629-2640. doi: 10.1089/ten.tea.2011.0024
- Pins, G. D., Christiansen, D. L., Patel, R., & Silver, F. H. (1997). Self-assembly of collagen fibers. Influence of fibrillar alignment and decorin on mechanical properties. *Biophysical Journal*, 73(4), 2164-2172.
- Proulx, M. K., Pins, G. D., Gaudette, G. R., Carey, S. P., DiTroia, L. M., Jones, C. M., . . . Rolle, M. W. (2011). Fibrin microthreads support mesenchymal stem cell growth while maintaining differentiation potential. *Journal of Biomedical Materials Research Part A*, 96A(2), 301-312. doi: 10.1002/jbm.a.32978
- Sakai, T., Li, R.-K., Weisel, R. D., Mickle, D. A. G., Kim, E. T. J., Jia, Z.-Q., & Yau, T. M. (2001). The fate of a tissue-engineered cardiac graft in the right ventricular outflow tract of the rat. *The Journal of Thoracic and Cardiovascular Surgery*, 121(5), 932-942. doi: 10.1067/mtc.2001.113600
- Sapir, Y., Kryukov, O., & Cohen, S. (2011). Integration of multiple cell-matrix interactions into alginate scaffolds for promoting cardiac tissue regeneration. *Biomaterials*, 32(7), 1838-1847. doi: <http://dx.doi.org/10.1016/j.biomaterials.2010.11.008>
- Severs, N. J., Bruce, A. F., Dupont, E., & Rothery, S. (2008). Remodelling of gap junctions and connexin expression in diseased myocardium. *Cardiovascular Research*, 80(1), 9-19. doi: 10.1093/cvr/cvn133
- Shapiro, J. M., & Oyen, M. L. (2013). Hydrogel Composite Materials for Tissue Engineering Scaffolds. *JOM*, 65(4), 505-516. doi: 10.1007/s11837-013-0575-6
- Silvestri, A., Boffito M Fau - Sartori, S., Sartori S Fau - Ciardelli, G., & Ciardelli, G. (2013). Biomimetic materials and scaffolds for myocardial tissue regeneration. (1616-5195 (Electronic)).
- Smaill, B. H., LeGrice, I. J., Hooks, D. A., Pullan, A. J., Caldwell, B. J., & Hunter, P. J. (2004). Cardiac structure and electrical activation: Models and measurement. *Clinical and Experimental Pharmacology and Physiology*, 31(12), 913-919. doi: 10.1111/j.1440-1681.2004.04131.x
- Stroncek, J. D., & Reichert, M. W. (2008). Overview of Wound Healing in Different Tissue Types. doi: <http://www.ncbi.nlm.nih.gov/books/NBK3938/>
- Thygesen, K., Alpert, J. S., Jaffe, A. S., Simoons, M. L., Chaitman, B. R., & White, H. D. (2012). Third Universal Definition of Myocardial Infarction. doi: 10.1161/CIR.0b013e31826e1058
- U.S. Department of Health and Human Services. (2014). OPTN: Organ Procurement and Transplantation Network. from <http://optn.transplant.hrsa.gov/data/>

- UNOS Transplant Living. (2015). Transplant Living | Financing A Transplant | Costs.
- Wainwright, Czajka, Patel, Freytes, Tobita, Gilbert, & Badylak. (2010). Preparation of Cardiac Extracellular Matrix from an Intact Porcine Heart. *Tissue Engineering: Part C*, 16, 525-532. doi: 10.1089=ten.tec.2009.0392
- Washington University School of Medicine in St. Louis. Biomaterials Lab: Research Capabilities.
- Watanabe, S., Paredes, O. L., Yokoyama, M., Shite, J., Takaoka, H., Shinke, T., . . . Ogasawara, D. (2006). Myocardial stiffness is an important determinant of the plasma brain natriuretic peptide concentration in patients with both diastolic and systolic heart failure. *European heart journal*, 27(7), 832-838. doi: 10.1093/eurheartj/ehi772
- Wei-Ning, L., Pernot, M., Couade, M., Messas, E., Bruneval, P., Bel, A., . . . Tanter, M. (2012). Mapping Myocardial Fiber Orientation Using Echocardiography-Based Shear Wave Imaging. *IEEE Transactions on Medical Imaging*, 32(3), 554-562. doi: 10.1109/TMI.2011.2172690
- Xin, M., Olson, E. N., Bassel-Duby, R., , , , & (2013). Mending broken hearts: cardiac development as a basis for adult heart regeneration and repair. *Nature reviews Molecular cell biology*, 14(8), 529-541.
- Yang, Y., Wimpenny, I., & Ahearne, M. (2011). Portable nanofiber meshes dictate cell orientation throughout three-dimensional hydrogels. *Nanomedicine: Nanotechnology, Biology and Medicine*, 7(2), 131-136.
- Zijlstra, F. (2001). Acute myocardial infarction: primary angioplasty. *Heart*, 85(6), 705-709. doi: 10.1136/heart.85.6.705
- Zimmermann, W. H., Melnychenko I Fau - Eschenhagen, T., & Eschenhagen, T. (2004). Engineered heart tissue for regeneration of diseased hearts. (0142-9612 (Print)).
- Zong, X., Bien, H., Chung, C.-Y., Yin, L., Fang, D., Hsiao, B. S., . . . Entcheva, E. (2005). Electrospun fine-textured scaffolds for heart tissue constructs. *Biomaterials*, 26(26), 5330-5338.

Appendix A - Metrics Rubric

This appendix shows the rubric used to rate the elements described in detail in chapter 4. Each objective and sub-objective was considered and below the specifications of each are shown:

Objectives

1. Reproducible – 0.4

a. Accuracy: Thread separation

Units: The ability to align threads with a specific separation

- 0- threads are separated with a distance more than 150 um
- 1- threads are separated with a distance more than 100 um
- 2- threads are separated with a distance that ranges between 50 - 100um

b. Precision: Consistent layer properties

Units: The ability to create scaffold layers with similar properties

- 0- Scaffolds present completely different properties
- 1- Some characteristics of scaffolds are similar
- 2- Most/ all characteristics of scaffolds are similar

c. Reusable

Units: The ability to reuse the device

- 0- It is not reusable
- 1- Allows for the use of 2-5 times
- 2- Allows for the use of 6-10 times

d. High scaffold production rate

Units: The ability to assemble a scaffold in a specific period of time

- 0- The scaffold assembly takes 4 hours or more
- 1- The scaffold assembly takes between 1-4 hours
- 2- The scaffold assembly takes less than 1 hour

e. Able to be scaled up

Units: The design allows for a process that can be scaled to a bigger magnitude

- 0- It doesn't allow for scaling

- 1- It allows some scaling
- 2- It allows for several scaling up possibilities

f. Sterilizable device

Units: Ability of the design to allow for sterilization without affecting the structure, performance of device itself

- 0- affects both the structure or performance of the device
- 1- affects either the structure or performance of the device
- 2- allows for sterilization with no negative effect

2. Easy to use – 0.1

a. Automated or limited number of steps

Units: Ability of the design to be automated

- 0- Constant manual steps
- 1- Limited steps
- 2- Automated

b. Intuitive

Units: Ability to prevent the user from breaking the device and intuitively use the device

- 0- Ability to use the device damaging it
- 1- Ability to use the device with instructions without breaking it
- 2- Ability to use the device with no instructions without breaking it

c. Reliable

Units: The ability of the device to function continuously

- 0- The device has potential of breaking down and stops working
- 1- The device has potential of breaking down but continue working
- 2- The device presents prevention mechanisms against malfunction

d. Easily maintained

- i. Easy to clean
- ii. Easy to repair

Units: The ability of the design to be user friendly

- 0- Not easy to use
- 1- Easy to use with instructions
- 2- Easy to use

3. Transferable – 0.2

Units: The ability of the scaffold to be transferred bench to bench

- 0- The transfer mechanism destroys the scaffold
- 1- The transfer mechanism affects the scaffold properties
- 2- The transfer mechanism does not affect the scaffold mechanical and structural properties

4. Mimic Myocardium Fiber Alignment– 0.2

a. Maintain thread mechanical integrity

Units: The ability of the design to maintain intact the structural and mechanical properties of the thread

- 0- the mechanical/structural integrity of the thread is destroyed
- 1- Either mechanical/ structural integrity is somehow affected
- 2- Mechanical integrity is kept intact

b. Minimize thread handling

Unit: The ability of the design to avoid unnecessary handling

- 0- Grab and touch the threads constantly
- 1- Grab and touch the threads a couple of times
- 2- Grab and touch the threads once

c. Stackable layers

Unit: The design allows for each layer of fibrin sheets to be stacked upon each other

- 0- The design is not stackable
- 1- The design allows for 2 stackable layers
- 2- the design allows for 3 or more stackable layers

d. Alignment

Unit: The ability of the scaffold to present threads that mimic aligned myocardial tissue

- 0- The scaffold threads are not aligned
- 1- The scaffold threads are somewhat aligned
- 2- The scaffold is completely aligned

e. Efficient degradation

Unit: The scaffold has the ability to degrade

- 0- The scaffold doesn't degrade
- 1- The scaffold degrades too fast/slow
- 2- The scaffold has optimal degradation rate

f. Mechanical strength

Unit: The scaffold presents similar mechanical strength to the myocardium

- 0- The scaffold has no mechanical strength at all
- 1- The scaffold mimics some myocardial mechanical properties
- 2- The scaffold mimics all myocardial mechanical properties

g. Planar orientation

Unit: The planar sheets of the scaffold are oriented in multiple directions

- 0- The planar sheets are oriented in 1 direction
- 1- The planar sheets are oriented in multiple orientations, however it doesn't mimic the myocardial fiber alignment
- 2- The planar sheets are oriented in multiple orientations and these mimic the myocardial tissue fiber alignment

h. Customizable number of threads

Units: The number of threads in each scaffold is customizable

- 0- Doesn't grab any threads
- 1- Ability to gather 2 – 25 threads
- 2- Ability to gather 26+ threads

i. Customizable types of threads

Unit: the device allows for the assembly of scaffolds using multiple kinds of threads

- 0- Doesn't allow for assembly of more than 1 type of thread
- 1- Allows for assembly of more than 1 type of thread similar to fibrin threads
- 2- Allows for assembly of more than 1 type of thread

5. Able to be manipulated – 0.1

Unit: The ability of the scaffold to be tested

- 0- The manipulations destroys the scaffold

- 1- The manipulations deteriorates the scaffold
- 2- The manipulation doesn't affect the scaffold at all

Appendix B – Decision Matrices

This appendix displays the decision matrices for each of the four functions that the device needs to accomplish. Each element scored is shown at the top of the tables. Three types of scores are shown: the regular scores which were based on a scale from 0 (lowest score) to 2 (highest score), the normalized score and the weighted sum according to each objective.

Function: Gathering Threads														
C/O	Weight (%)	Attribute	Spool Storage			Box Remover			Rolling Grabber			Lint roller		
			Score	Normalized Score	Weighted Sum	Score	Normalized Score	Weighted Sum	Score	Normalized Score	Weighted Sum	Score	Normalized Score	Weighted Sum
C		Time		Y			Y			Y			Y	
C		Budget		Y			Y			Y			Y	
C		Safe for user		Y			Y			Y			Y	
C		Supplies		Y			Y			Y			Y	
C		Limited Team members		Y			Y			Y			Y	
Obj 1	40	Reproducible		3	100		3	120		3	120		1	20
O		Reusable	0	0		2	1		2	1		0	0	
O		High Scaffold production rate	1	1		1	1		1	1		0	0	
O		Sterilizable device	2	1		2	1		2	1		0	0	
O		Able to be scaled up	2	1		1	1		1	1		1	1	
Obj 2	10	Easy to use		1	10		4	35		2	20		2	15
O		Automated	1	1		1	1		1	1		0	0	
O		Intuitive	0	0		2	1		1	1		2	1	
O		Reliable	1	1		2	1		1	1		0	0	
O		Easily maintained	0	0		2	1		1	1		1	1	
Obj 4	20	Mimic Myocardium Structure		3	60		4	80		4	80		3	50
O		Maintain thread mechanical integrity	1	1		2	1		2	1		1	1	
O		Minimize thread handling	1	1		2	1		2	1		1	1	
O		Customizable number of threads	2	1		2	1		2	1		1	1	
O		Customizable types of threads	2	1		2	1		2	1		2	1	
		TOTALS	13		170	21		355	18		340	9		85

Figure 1 – Decision Matrix for Gathering Threads

Function: Aligning Threads																										
C/O	Weight (%)	Attribute	Threaded rod			Hinge device			Clips on a rail			Grooved device			Pot holder			Roller			Shaker			Funnel		
			Score	Normalized Score	Weighted Sum	Score	Normalized Score	Weighted Sum	Score	Normalized Score	Weighted Sum	Score	Normalized Score	Weighted Sum	Score	Normalized Score	Weighted Sum	Score	Normalized Score	Weighted Sum	Score	Normalized Score	Weighted Sum	Score	Normalized Score	Weighted Sum
C		Time	Y			Y			Y			Y			Y			Y			Y			Y		
C		Budget	Y			Y			Y			Y			Y			Y			Y			Y		
C		Safe for user	Y			Y			Y			Y			Y			Y			Y			Y		
C		Supplies	Y			Y			Y			Y			Y			Y			Y			Y		
C		Limited Team members	Y			Y			Y			Y			Y			Y			Y			Y		
Obj 1	40	Reproducible		4	140		3	120		4	160		5	180		2	60		5	180		4	160		4	160
O		Accuracy - thread separation	1	1		1	1		1	1		2	1		1	1		1	1		1	1		0		
O		Reusable	2	1		1	1		2	1		2	1		1	1		2	1		2	1		2	1	
O		High Scaffold production rate	1	1		1	1		1	1		2	1		0	0		2	1		2	1		2	1	
O		Sterilizable device	2	1		2	1		2	1		2	1		1	1		2	1		1	1		2	1	
O		Able to be scaled up	1	1		1	1		1	1		1	1		0	0		2	1		2	1		2	1	
Obj 2	10	Easy to use		3	25		2	15		2	20		4	35		2	20		3	25		3	30		3	25
O		Automated	1	1		1	1		1	1		2	1		0	0		2	1		2	1		1	1	
O		Intuitive	1	1		0	0		1	1		2	1		2	1		1	1		1	1		2	1	
O		Reliable	1	1		1	1		1	1		1	1		0	0		1	1		1	1		1	1	
O		Easily maintained	2	1		1	1		1	1		2	1		2	1		1	1		2	1		1	1	
Obj 4	20	Mimic Myocardium Structure		2	30		3	50		2	30		3	60		2	30		3	50		3	60		3	50
O		Maintain thread mechanical integrity	1	1		2	1		1	1		2	1		2	1		1	1		2	1		2	1	
O		Minimize thread handling	0	0		2	1		1	1		2	1		0	0		2	1		2	1		2	1	
O		Customizable number of threads	2	1		1	1		1	1		2	1		1	1		2	1		2	1		1	1	
		TOTALS	15		195	14		185	14		210	22		275	10		110	19		255	20		250	18		235

Figure 2 – Decision Matrix for Aligning Threads

Function: Anchoring Threads																	
C/O	Weight (%)	Attribute	Suction			Saran wrap			PDMS sandwich			Clips			Glue/Tape		
			Score	Normalized Score	Weighted Sum	Score	Normalized Score	Weighted Sum	Score	Normalized Score	Weighted Sum	Score	Normalized Score	Weighted Sum	Score	Normalized Score	Weighted Sum
C		Time		Y			Y			Y			Y			Y	
C		Budget		Y			Y			Y			Y			Y	
C		Safe for user		Y			Y			Y			Y			Y	
C		Supplies		Y			Y			Y			Y			Y	
C		Limited Team members		Y			Y			Y			Y			Y	
Obj 1	40	Reproducible		3	120		0	0		3	120		3	100		0	0
O		Reusable	2	1		0	0		2	1		2	1		0	0	
O		High Scaffold production rate	2	1		0	0		1	1		1	1		0	0	
O		Sterilizable device	1	1		0	0		2	1		1	1		0	0	
O		Able to be scaled up	1	1		0	0		1	1		1	1		0	0	
Obj 2	10	Easy to use		4	35		3	30		3	25		3	25		2	15
O		Automated	2	1		1	1		1	1		1	1		0	0	
O		Intuitive	2	1		2	1		2	1		2	1		2	1	
O		Reliable	2	1		1	1		1	1		1	1		1	1	
O		Easily maintained	1	1		2	1		1	1		1	1		0	0	
Obj 4	20	Mimic Myocardium Structure		4	70		2	40		4	80		4	80		3	60
O		Maintain thread mechanical integrity	2	1		1	1		2	1		2	1		1	1	
O		Minimize thread handling	2	1		1	1		2	1		2	1		1	1	
O		Customizable number of threads	1	1		1	1		2	1		2	1		2	1	
O		Customizable types of threads	2	1		1	1		2	1		2	1		2	1	
		TOTALS	20		225	10		70	19		225	18		205	9		75

Figure 3 – Decision Matrix for Anchoring Threads

Function: Frame to hold threads											
C/O	Weight (%)	Attribute	Washer and Peg			Square platform/PDMS			Loom Platform		
			Score	Normalized Score	Weighted Sum	Score	Normalized Score	Weighted Sum	Score	Normalized Score	Weighted Sum
C		Time		Y			Y			Y	
C		Budget		Y			Y			Y	
C		Safe for user		Y			Y			Y	
C		Supplies		Y			Y			Y	
C		Limited Team members		Y			Y			Y	
Obj 1	40	Reproducible		3	120		2.5	100		4	140
O		Reusable	1	1		1	0.5		2	1	
O		High Scaffold production rate	1	1		1	0.5		1	1	
O		Sterilizable device	2	1		2	1		2	1	
O		Able to be scaled up	2	1		1	0.5		2	1	
Obj 2	10	Easy to use		4	35		2.5	25		2	15
O		Automated	1	1		1	0.5		0	0	
O		Intuitive	2	1		1	0.5		1	1	
O		Reliable	2	1		1	0.5		1	1	
O		Easily maintained	2	1		2	1		1	1	
Obj 4	20	Mimic Myocardium Structure		5	100		5	100		3	50
O		Maintain thread mechanical integrity	2	1		2	1		1	1	
O		Minimize thread handling	2	1		2	1		0	0	
O		Stackable layers	2	1		2	1		0	0	
O		Customizable number of threads	2	1		2	1		2	1	
O		Customizable types of threads	2	1		2	1		2	1	
		TOTALS	23		255	20		225	15		205

Figure 4 – Decision Matrix for Framing and Holding Threads

Appendix C – Automated Composite Scaffold Production

Materials List

- Fibrin microthreads
- Vellum paper
- Forceps
- Tape
- Suction box
- Composite mold (black acetyl platform, PDMS molds, vacuum grease)
- Fibrinogen aliquots (70mg/mL)
- Thrombin aliquots (40u/mL)
- Calcium Chloride CaCl₂ (40 mM)
- 200µm micropipette
- Micropipette tips

Methods

Suction box thread alignment

1. Place one piece of tape on either side of the grooves on the suction box starting at the edge of the grooves.

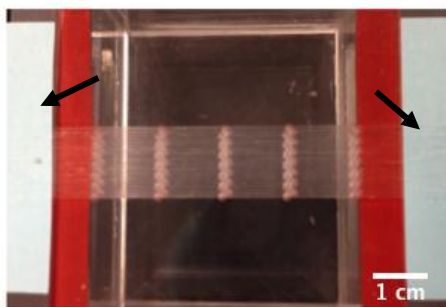


Figure 94: Suction box with tape on either side of grooves (indicated by arrows).

2. Attach hose to aspirator to the connector on the suction box, and turn on the aspiration.
3. Using forceps, grab one thread and place onto suction box above grooves and cut to the length of the box.
4. Using forceps grasp thread at end and place into individual groove
 - a. Ensure that thread is only in desired groove before moving to next thread
5. Be careful not to grasp thread in the center portion of the thread as this will damage its structural integrity. Figure 95 shows four dyed threads aligned in the suction box.

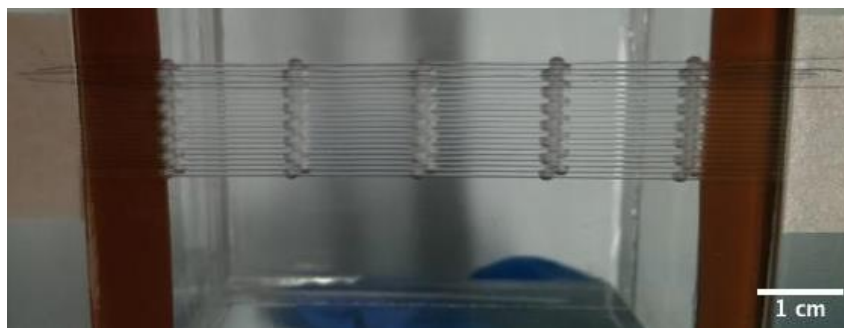


Figure 95: Dyed microthreads within four grooves of the suction box.

6. Repeat until the number of desired threads are placed within individual grooves.
7. To secure the threads in place, adhere one piece of tape on either side of the threads on top of the initial pieces.



Figure 96: Tape placed on top of threads to secure in alignment.

8. Carefully remove the tape from the box, being careful to not apply stress to the aligned threads.



Figure 97: Removal of threads from aligned grooves.

Adherence to vellum frame

9. Transfer aligned threads secured with tape to a clear transfer paper.



Figure 98: Transfer of aligned threads to transfer paper.

10. Secure tape onto transfer paper, placing each side at the same distance as the suction box so that the threads are pulled in tension.

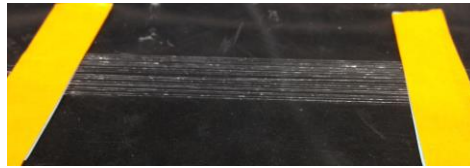


Figure 99: Threads pulled in tension on transfer paper.

11. Fold transfer paper to allow for forceps to be gently placed under all threads.
12. Place two vellum frames under threads, lifting the threads carefully with the forceps.
13. Position frames so that the aligned threads are in the center of the circular opening.

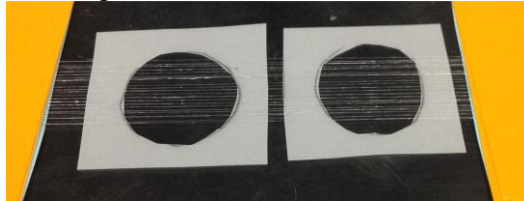


Figure 100: Two vellum frames positioned under aligned threads.

14. Extrude silicone glue onto either side of the threads, ensuring that the glue adheres to the frame and the threads. Do not apply excess force to the threads to avoid changing the alignment of the threads.

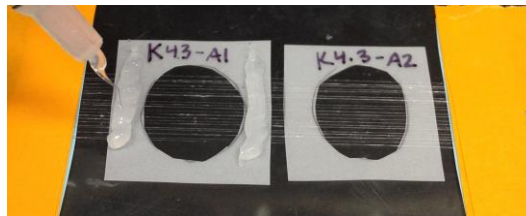


Figure 101: Addition of silicone glue to vellum frame and aligned threads.

15. Allow the silicone glue to dry for 24 hours.

- Using a razor blade, cut the threads on the outside of the vellum frames to the remove excess threads.

Addition of fibrin gel

- Place a small amount of vacuum grease between the PDMS mold and the black acetyl platform to ensure a tight seal.
- Place aligned threads on vellum scaffold in molds using forceps.



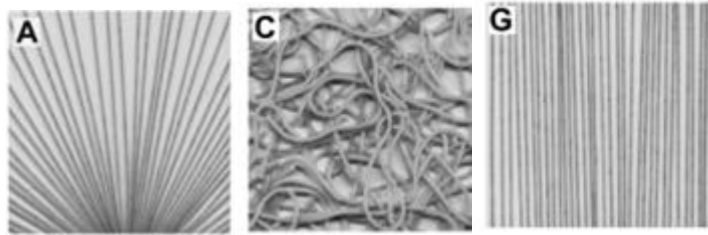
Figure 102: Composite mold with three scaffolds.

- Prepare 1 ml of fibrin hydrogel that will allow for 5 gel castings using the following protocol:
 - In a small conical tube dilute 137.8 μl of fibrinogen in 862.2 μl of HBS (Diluted fibrinogen)
 - In a small conical tube dilute 58.75 μl of thrombin in 941.25 μl of HBS (Diluted thrombin)
 - In a new small conical tube add 100 μl of the diluted thrombin
 - To the diluted thrombin, add 80 μl of CaCl_2 and mix
 - To the mix, add 150 μl of PBS and mix
 - Add 670 μl of the diluted fibrinogen and mix
- Add 200 μl of fibrin hydrogel to each well immediately after the gel preparation is completed in order to prevent polymerization
- Let it stand for 20-30 minutes
- Using forceps, take the composite out of the mold and store it in 2 ml of PBS
- Refrigerate

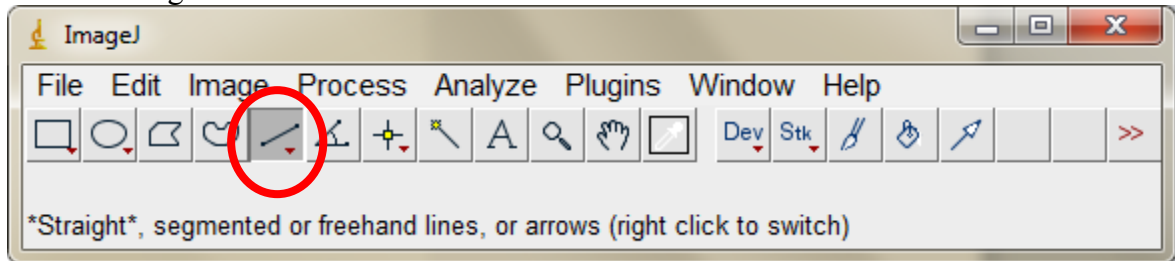
Appendix D – Alignment Testing Method Validation Procedure

This procedure was based in the data by (Ayres, 2008). Pictures published in his study are used in this validation test. More specific Figure 58 of this report is used for validation explained below.

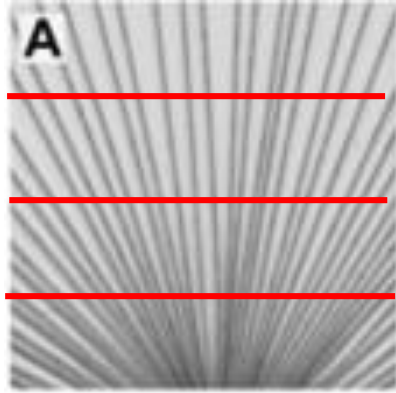
1. Crop the pictures to separate the published figure into three different images. Three images are needed in order to analyze each sample individually.



2. Upload picture A to the NIH software Image J.
3. Select “Straight”



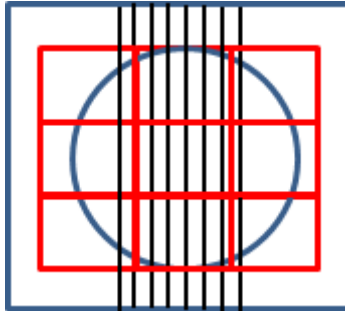
4. Drag a line across the spacing between two fibers.
5. Press the keyboard letter ‘M’. This will create a list that contains the distance measurements.
6. Repeat 4 and 5 until all distances in each picture are measured in three parallel regions, as seen below.



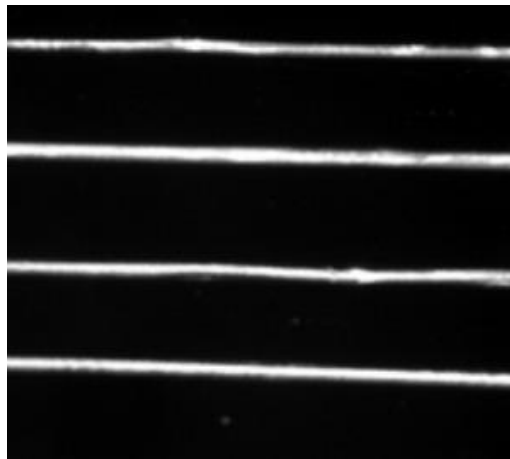
7. Repeat for picture "C" and "G".
8. Perform statistical analysis including mean, standard deviation calculations, etc.

Appendix E – Alignment Testing Protocol

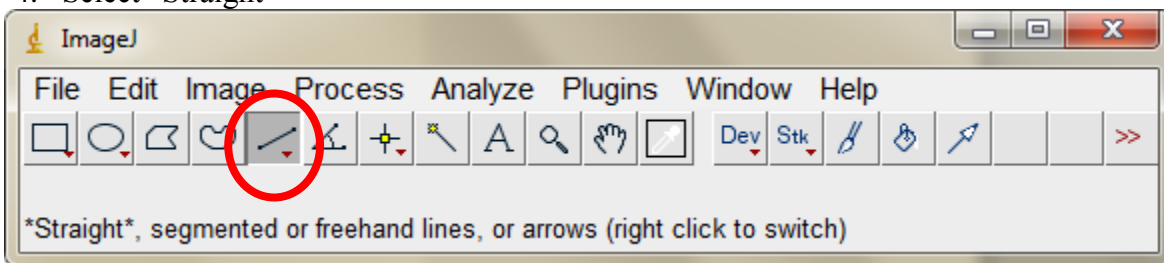
1. Visually, divide the scaffold in 9 equally spaced regions as seen below. Each region is outlined in red for visual purposes.



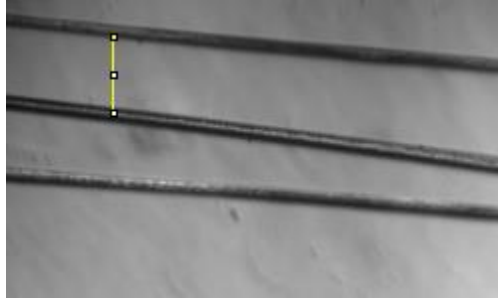
2. Using a brightfield microscope with 2X magnification take a picture of each region and save it in JPEG format.
3. Open the NIH software Image J and upload the scaffold pictures. A sample zoomed-in picture is shown below.



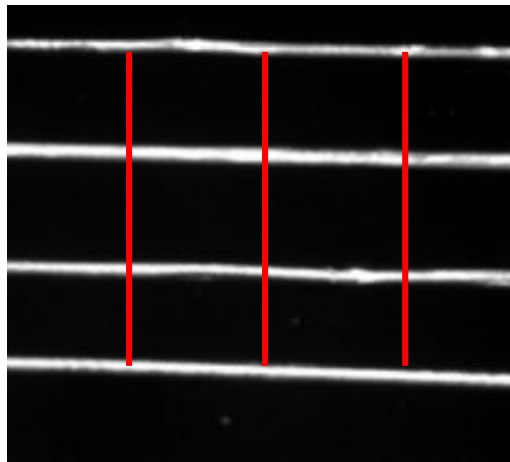
4. Select “Straight”



5. Drag a line across the spacing between two threads as seen in the figure below.



6. Press the keyboard letter 'M'. This will create a list that contains the distance measurements.
7. Repeat 5 and 6 until all distances in each frame are measured in three parallel regions, as seen below. For instance, in the figure shown below, we measure 3 distances in 3 regions having a total of 9 measurements.



8. Perform statistical analysis including mean, standard deviation calculations, etc.


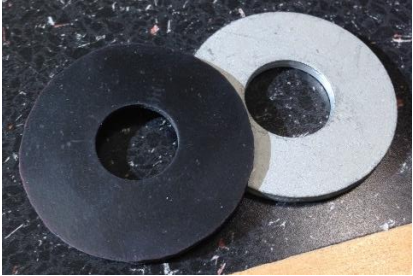

Appendix F – Ball Burst Testing Method Validation Procedure

1. Mix gelatin powder with boiling water to create the one of the specified concentrations:
 - b. Concentrated – 1.25 grams gelatin powder/10mL water.
 - c. Regular – 0.625 grams of gelatin powder/10mL water.
2. Once the powder is fully dissolved, pour mixture into a vessel/container (the team created tin foil vessels which can be seen below, but these leaked and didn't maintain gelatin thickness, therefore the use of plastic containers is highly recommended).
3. After the gels have set for a short period of time and are slightly more congealed (test with a toothpick to determine extent of solidification) add a small square of tissue paper or vellum paper (4.5x4.5cm) with a circle (diameter = 2.5cm) cut out of the middle to the concentrated samples to reinforce the gels for testing. The gelatin should be viscous enough so that the paper does sink to the bottom, but not so much so that the paper cannot be slightly submerged into the gelatin.
 - a. For the gels of regular concentration, place one piece of tissue paper at the bottom of the vessel/container prior to pouring of the gel and a second on top, again after solidification had begun to occur (slightly submerged).
4. Place the fridge groups in the fridge and the others outside at ambient temperature and let set for 24-48 hours.
5. Cut along borders of sample frames in the vessels/containers with a sharp blade/scalpel.
6. Gently remove cut samples out of vessels/containers with forceps, being careful not to tear the gelatin.



Appendix G - Ball Burst Compression Testing Procedure

Materials List

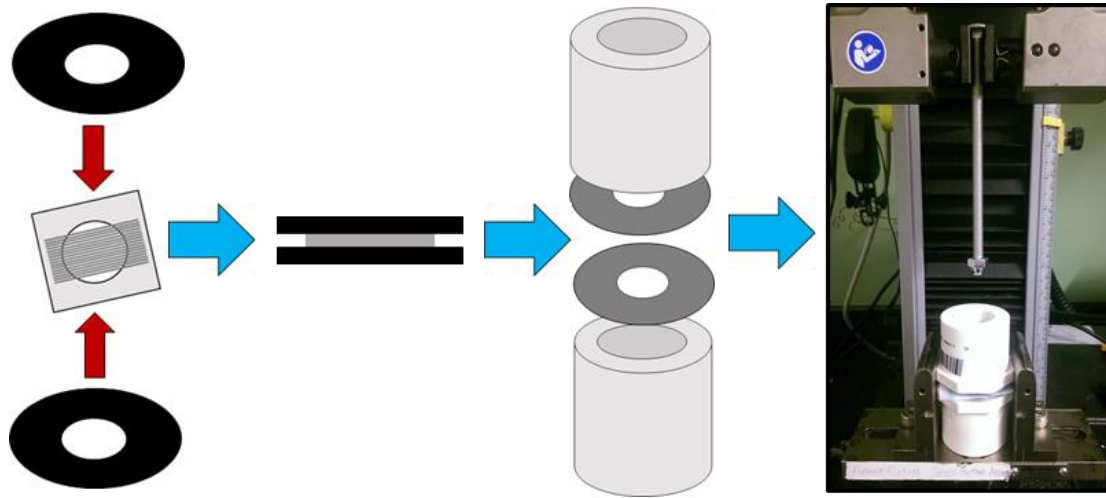
Height: 37.0mm	
Outer Cylindrical Diameter: 42.0mm Inner Cylindrical Diameter: 28.0mm	
Width (top surface): 47.0mm	
Quantity: 2	
Outer Diameter (metal): 44.0mm Inner Diameter (metal): 18.0mm	
Outer Diameter (nylon): 44.0mm Inner Diameter (nylon): 16.0mm	
Thickness (metal): 2.00mm Thickness (nylon): 1.50mm	
Quantity: 2 of each	
Bolt Diameter: 6.35mm Bolt Length (with cap nut): 130mm	
Hex Width of Cap Nut: 11.0mm Sphere Width of Cap Nut: 9.00mm	
Quantity: 1 of each	

1-1/4" x 3/4" PVC Bushing

**Everbilt 5/8" x 2" Nylon Washer
3/4" Cut Metal Washer**

**1/4" x 5" Carriage Bolt
Everbilt 1/4" Zinc Cap Nut**

Methods – Using Instron 5544 Mechanical Testing Frame



1. Remove composite scaffold from PBS, allowing excess liquid to drip off before placing in testing fixture. Ensure that scaffold remains hydrated until transferred for testing.
2. Position composite scaffold sample in between two nylon washers ensuring inner circles of both washers and scaffold frame are relatively concentric.
3. Place one PVC pipe fitting onto bending platform with one metal washer on top.
4. Place nylon washers with sample on top of metal washer and PVC pipe fitting.
5. Fit bolt with cap nut into upper tensile grip and lower it slowly to make sure it is centered above the testing components below.
6. Bring the grip down until the cap nut is just touching the surface of the sample to set the testing height (30.7cm, but will vary depending on sample type) and set safety stops approximately 3.00cm below this.
7. Raise the grip back up and place a second washer and PVC pipe fitting on top of the already placed components.
8. Slide the edges of the bending platform inward and tighten them to secure the testing components in place to ensure they don't shift during testing.
9. Lower the upper grip back down to the testing height measured above (for example, 30.7cm).
10. Run a standard compression test utilizing BlueHill 3 software with the following parameters:
 - a. Rate of extension: 9.00mm/min*

- b. End of test: extension of 2.50cm
- c. Data capture interval: 100ms

11. Following the end of testing, raise grip above the PVC fixture and discard the tested scaffold. Dry nylon and metal washers as needed between samples.

**It should be noted that a rate of 9.00mm/min was not referenced in the literature mentioned in Section 0, nor was a ring clamp of diameter 16mm. However, the literature in that section seemed to indicate that rate of extension was a reflection of the sphere diameter and specifically the ratio of this to the ring clamp diameter (Cloonan et al., 2011; Freytes et al., 2004; Wainwright et al., 2010). Since that the sphere used for the team's testing was 9.00mm, they altered their rate to 9mm/min. As for the ring clamp diameter, the ratio between the sphere diameter and ring diameter in the above referenced literature was 0.5714 (25.4mm diameter sphere, 44.45mm internal ring clamp diameter) (Cloonan et al., 2011). For the team's testing set up this ratio was 0.5625 (9mm sphere diameter, 16mm internal ring clamp diameter (nylon washer)). Because the team's samples would be much smaller than 25.4mm across, it was necessary for them to utilize a smaller sphere and therefore smaller ring clamp. This being said, they believed that the ratio between the two, however, should be maintained. Since the difference between the literature ratio and their own testing set up was only 0.006, the team determined that their modification to the testing set-up was acceptable.*